

Review

Synthesis of Arginase Inhibitors: An Overview

Maria Cristina Molaro ¹, Chiara Battisegola ¹, Marica Erminia Schiano ¹, Mariacristina Failla ²,
Maria Grazia Rimoli ¹, Loretta Lazzarato ², Konstantin Chegaev ² and Federica Sodano ^{1,*}

¹ Department of Pharmacy, “Federico II” University of Naples, 80131 Naples, Italy; mariacristina.molaro@unina.it (M.C.M.); chiara.battisegola@unina.it (C.B.); maricaerminia.schiano@unina.it (M.E.S.); rimoli@unina.it (M.G.R.)

² Department of Drug Science and Technology, University of Turin, 10125 Turin, Italy; mariacristina.failla@unito.it (M.F.); loretta.lazzarato@unito.it (L.L.); konstantin.chegaev@unito.it (K.C.)

* Correspondence: federica.sodano@unina.it; Tel.: +39-081678604

Abstract: Arginase (ARG) is a binuclear manganese-containing metalloenzyme that can convert L-arginine to L-ornithine and urea and plays a key role in the urea cycle. It also mediates different cellular functions and processes such as proliferation, senescence, apoptosis, autophagy, and inflammatory responses in various cell types. In mammals, there are two isoenzymes, ARG-1 and ARG-2; they are functionally similar, but their coding genes, tissue distribution, subcellular localization, and molecular regulation are distinct. In recent decades, the abnormal expression of ARG-1 or ARG-2 has been reported to be increasingly linked to a variety of diseases, including cardiovascular disease, inflammatory bowel disease, Alzheimer’s disease, and cancer. Therefore, considering the current relevance of this topic and the need to address the growing demand for new and more potent ARG inhibitors in the context of various diseases, this review was conceived. We will provide an overview of all classes of ARG inhibitors developed so far including compounds of synthetic, natural, and semisynthetic origin. For the first time, the synthesis protocol and optimized reaction conditions of each molecule, including those reported in patent applications, will be described. For each molecule, its inhibitory activity in terms of IC₅₀ towards ARG-1 and ARG-2 will be reported specifying the type of assay conducted.



Academic Editor: Anna Carbone

Received: 17 December 2024

Revised: 12 January 2025

Accepted: 14 January 2025

Published: 16 January 2025

Citation: Molaro, M.C.; Battisegola, C.; Schiano, M.E.; Failla, M.; Rimoli, M.G.; Lazzarato, L.; Chegaev, K.; Sodano, F. Synthesis of Arginase Inhibitors: An Overview.

Pharmaceutics **2025**, *17*, 117.

<https://doi.org/10.3390/pharmaceutics17010117>

Copyright: © 2025 by the authors. Licensee MDPI, Basel, Switzerland. This article is an open access article distributed under the terms and conditions of the Creative Commons Attribution (CC BY) license (<https://creativecommons.org/licenses/by/4.0/>).

Keywords: Arginase; Arginase inhibitors; synthetic protocols

1. Introduction

Arginase (ARG) has roots in early life forms. It is a manganese-containing binuclear metalloenzyme capable of converting L-arginine to urea and L-ornithine. Urea provides protection against ammonia (NH₃), while L-ornithine serves to stimulate cell growth and other physiological functions. This interconnection with various metabolic pathways, such as polyamine synthesis and energy metabolism regulation, underscores the importance of ARG in maintaining metabolic homeostasis [1]. L-arginine is one of the most versatile amino acids in animal cells, serving as a precursor not only for the protein synthesis but also for the production of nitric oxide, urea, polyamines, proline, glutamate, creatine, and agmatine [2]. In mammals, there are two isoenzymes: arginase-1 (ARG-1) and arginase-2 (ARG-2). They are functionally similar, but the coding genes, tissue distribution, subcellular localization, and molecular regulation are distinctive. ARG-1 is localized in the cytoplasm and mainly expressed in the liver, where it is responsible for the detoxification of ammonia in the urea cycle [1]. In contrast, ARG-2 is predominantly found in the mitochondria and is primarily involved in polyamine generation [3]. Both enzymes metabolize L-arginine, which is severely depleted in the immunosuppressive tumour microenvironment (TME),

where it is crucial for proliferating cells. This positions them at the forefront of immune escape through various mechanisms.

Within the TME, ARG-1 plays a crucial role in immune evasion by activating immunosuppressive cells, such as myeloid-derived suppressor cells (MDSCs), a heterogeneous population of bone marrow-derived cells that suppress immune responses and facilitate tumour progression [4]. In addition to high expression in MDSCs, ARG-1 is also upregulated in tumour-associated macrophages (TAMs) and activated neutrophils within the TME [5,6]. In these cells, it depletes L-arginine, impairing T-cell activation and proliferation, ultimately enabling cancer cells to evade immune surveillance.

Recently, ARG-2 has received special attention. It has been reported that the ARG-2 pathway is a means by which regulatory T cells (Tregs), also called CD_4^+ cells, regulate inflammation in tissues. Compared to psoriatic Tregs, healthy Tregs express almost 4-fold more ARG-2; similarly, Tregs in metastatic melanoma lesions express high levels of ARG-2 protein, with these levels being higher in tumour-infiltrating Tregs than in Tregs isolated from healthy skin [7]. ARG-2 reduces the survival and proliferation of effector T cells (CD_8^+), thereby impacting antitumour immune responses. Thus, L-arginine metabolism via ARG-2 is an immunoregulatory pathway used by Tregs in human tissues, with significant implications for both autoimmunity and cancer.

The disturbance in the expression of ARG can lead to a range of vascular, neurological, immunological, and inflammatory disorders, as the isoforms ARG-1 and ARG-2 are involved in the regulation of nitric oxide (NO), polyamines, proline, and, particularly in the immune system, endothelial cells, and neuronal cells [8–10].

Regarding the involvement of ARG in the immune system, in the presence of an inflammatory stimulus, the enzyme nitric oxide synthase (NOS) produces NO. This NO interacts with reactive oxygen species (ROS), creating a cytotoxic nitrosative stress environment that inhibits both cellular replication and pathogenic activity [11]. On the other hand, the enzyme ARG metabolizes L-arginine, regulating defence mechanisms and downregulating NO production. This helps prevent uncontrolled cellular apoptosis triggered by $ONOO^-$ species generated from excess NO reacting with superoxide radicals (O_2^-) [12].

An altered balance in the expression of these two enzymes can cause serious issues for the immune system. Additionally, the dysregulated release of ARG from cells and tissues into extracellular fluids can further compromise the defence mechanisms of macrophages against pathogens by limiting the bioavailability of L-arginine, reducing NO levels, and disrupting cytokine production pathways. It has been shown that ARG is implicated in disorders such as multiple sclerosis, as the increased regulation of the enzyme ARG-2 stimulates the production of cytokines that differentiate T helper 17 cells, thus inducing inflammation [13]. In studies on obesity-induced vasculopathy, it has been observed that high levels of fats and sucrose activate Rho-associated kinases, increasing the expression of ARG-1. The increased synthesis of polyamines mediated by ARG-1 promotes cellular proliferation and fibrosis; additionally, the rise in ROS levels contributes to dysfunction [14].

The enzyme ARG, particularly its isoform ARG-2, plays a crucial role in maintaining the balance of the cardiovascular system by regulating the levels of NO [15]. This helps reduce oxidative damage to the endothelium, promotes blood vessel dilation, and prevents the adhesion and aggregation of leukocytes and platelets. An imbalance between the enzymes that degrade L-arginine (ARG and NOS) can contribute to many age-related cardiovascular complications, such as vascular stiffness, ventricular hypertrophy, hypertension, inflammation, and disorders caused by oxidative stress [16]. Studies have shown that a high-fat, high-cholesterol diet causes liver damage in mice, leading to the overexpression of ARG-1, a consequent reduction in circulating L-arginine levels, and cardioprotective effects mediated by NO [17]. In contrast, a glucose-free diet in mice results in increased

expression of ARG-2, triggering signalling pathways that protect hepatocytes from fat accumulation, inflammatory responses, insulin resistance, and glucose intolerance [18].

ARG and NOS are present in both the peripheral and central nervous systems, but their interaction is complicated by the complexity of the brain. ARG is essential for the detoxification of ammonia and the synthesis of polyamines, which are necessary for neuronal development and regeneration. NO, on the other hand, is a neurotransmitter that contributes to synaptic plasticity and cerebral blood flow. During development, high levels of cAMP stimulate ARG-1 to promote neuronal survival. However, with ageing, an imbalance between ARG and NOS can reduce NO production, contributing to neurodegenerative diseases [19].

One neurodegenerative disease associated with the alteration of ARG enzyme expression is Alzheimer's disease. It has been observed that microglial activation leads to the production of cytokines, which induce increased expression of ARG-1 and ARG-2 in the brain. However, the accumulation of ARG-2 at sites of β -amyloid deposition causes the uncoupling of NOS, generating O_2^- and neurodegenerative oxidative stress [20]. This may be an attractive molecular imaging target for the evaluation of Alzheimer's disease progression [21]. In certain contexts, an excess of NO can cause neuronal damage and brain trauma due to excitotoxicity. Notably, the role of ARG-2 is completely reversed in neurodegenerative diseases compared to cardiovascular disorders, highlighting the importance of understanding the distinct contributions of each isoform in different disease contexts. This underscores the need for selective molecules tailored to each isoform.

In line with the significant role of ARG-1 and ARG-2 in numerous diseases, there has been growing interest in developing inhibitors for these enzymes. In particular, identifying the ARG enzymes as critical metabolic checkpoints in the TME has spurred the design of novel ARG inhibitors. Both natural and synthetic compounds have been evaluated in various *in vitro*, *ex vivo*, and *in vivo* models [22,23]. Natural compounds like chlorogenic acid and picetannol, as well as synthetic compounds such as L-arginine-like derivatives and boronic acid derivatives, have been studied. These boronic acids are α -amino acids with a lateral boronic group capable of chelating the two manganese ions required for enzymatic activity. However, their inhibitory activity (IC_{50}) was in the micromolar range, indicating the need for further improvement. The initial approach taken by Van Zandt et al., later upgraded by others, focused on expanding 2-(S)-amino-6-borono-hexanoic acid (ABH) with moieties capable of additional interactions with residues Asp181, Asp183, and Asp202 [24–26]. Further improvements in the pharmacological profile were achieved by limiting the conformational flexibility of ABH. Notable examples include CB-1158 (numidargistat) and OATD-02 [27,28]. In a recent study, OATD-02 demonstrated superior *in vivo* antitumor capacity compared to CB-1158, as it inhibited both extracellular ARG-1 within the TME and cellular ARG-2 overexpressed in the TME [29]. By inhibiting ARG-2, OATD-02 was found to regulate the activity of $CD8^+$ cells and Tregs, thus controlling a key player responsible for the metabolic adaptation typical of hypoxic tumours.

This review aims to provide a comprehensive overview of ARG inhibitors, focusing on the ongoing search for these molecules involved in multiple key pathophysiological processes. We categorize these inhibitors into generations and classes, as illustrated in Figure 1. For each molecule, its inhibitory activity (IC_{50}) against ARG-1 and ARG-2 will be reported, with colorimetric assays used for all compounds unless otherwise specified.

Three reviews have previously addressed this topic, each from a different perspective. Borek et al. focused on the SAR and pharmacokinetic properties of each inhibitor [22]; Niu et al. discussed the underlying mechanism of ARG in tumour cell growth and summarized recent clinical research on ARG targeting for cancer therapy [30]. Clemente et al. explored the potential of ARG as a molecular imaging biomarker, stimulating the development of

high-affinity, specific ARG imaging probes [16]. Failla et al. analysed the structural characteristics and plasticity of ARG-1 and ARG-2 binding sites, aiming to design inhibitors with new binding patterns [31]. However, none of these reviews have addressed the synthetic procedures of ARG inhibitors, a critical aspect from a medicinal chemistry perspective.

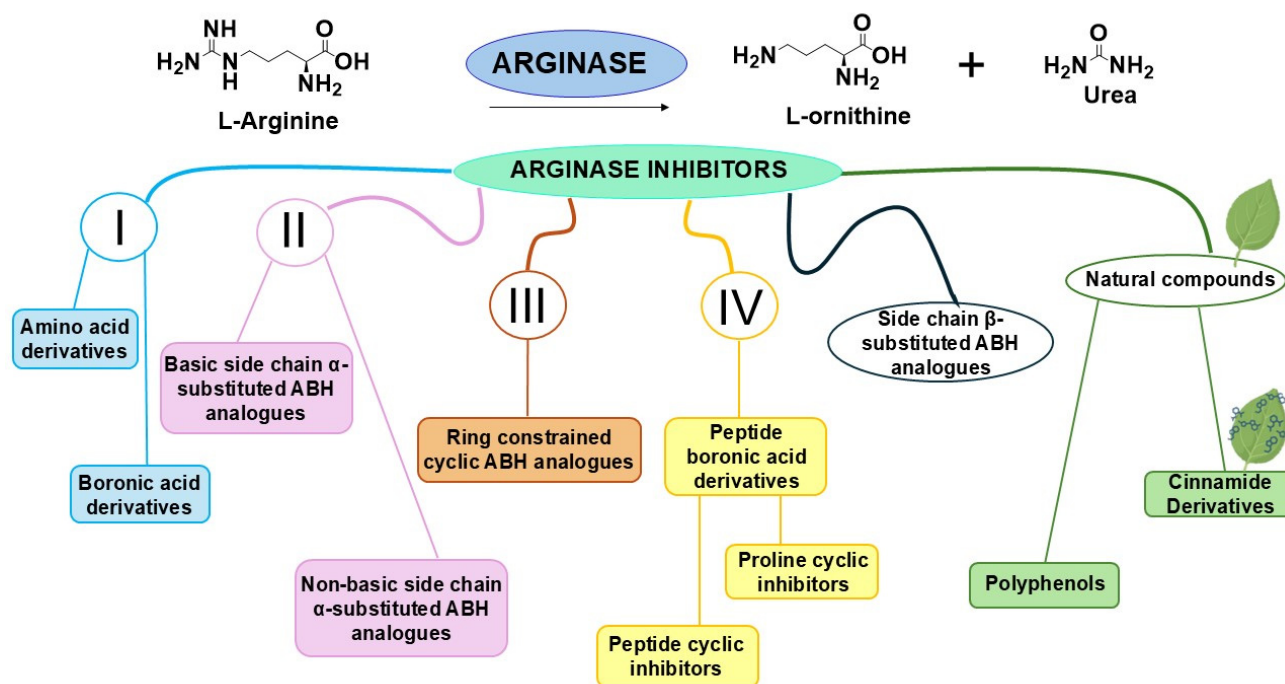


Figure 1. Schematic representation of all ARG inhibitor classes.

The chemical synthesis of these inhibitors presents numerous challenges, primarily due to their inherent chemical complexity. For instance, replacing the guanidine group with a boronic acid residue has proven effective. This modification preserves the geometry and electrophilicity of the original group while improving the compound's physicochemical properties, such as reduced polarity and non-basicity. However, synthesizing a boronic acid derivative is challenging due to the reactivity of the functional group, necessitating the use of a protected ester form. Although using a protecting group can simplify the synthetic process, this is not always the case with amino acid derivatives, such as ARG inhibitors. These derivatives must mimic the amino acid L-arginine, requiring both amino and carboxylic groups. Given that these functional groups are as reactive as boronic acid, selecting the optimal protecting group and synthetic strategy is challenging. The inherent chemical complexity of these procedures presents scalability issues and challenges with reproducibility, further complicated by the presence of chiral centres and the need for stereoselective syntheses.

In this review, we provide a complete overview of all classes of ARG inhibitors, including molecules of synthetic and natural origins. For the first time, we also present the synthetic protocols and the optimized reaction conditions for each molecule. Many structures and syntheses of ARG inhibitors have been reported in patents that are often difficult to access and interpret. This review aims to be a comprehensive guide to the synthesis of ARG inhibitors, addressing critical issues from a synthetic chemical perspective and suggesting how these can be overcome through medicinal chemistry strategies.

2. First-Generation Inhibitors

The first ARG inhibitors were developed by analysing the chemical structure of the enzyme's natural substrates, such as L-arginine and other structurally similar amino acids.

The enzyme's small and highly polar active site favours the accommodation of amino acids with a natural L-configuration (such as L-arginine analogues), which is also the configuration responsible for the enzyme's activity.

The subsequent inclusion of a boronic group into the inhibitor structures was crucial for two main reasons. First, during the binding mechanism with the ARG enzyme, the boronic group forms a tetrahedral boronate anion by incorporating an OH group, effectively mimicking the transition state of the hydrolysis of the trigonal planar guanidine group in L-arginine by ARG. Second, the boron atom's electron deficiency facilitates nucleophilic attack by the hydroxide ion, enhancing the activity of the inhibitor. Boronic acid also serves as an excellent guanidine substitute due to its similar geometry and electrophilicity, while offering better physicochemical properties—it is less polar, non-basic, and has fewer hydrogen bond donors [32]. In addition to incorporating the boronic moiety, other structural modifications included varying the length of the alkyl side chain, introducing a sulphur atom along the carbon chain, and adding a phenyl ring to the side chain to create a conformationally restricted analogues. These modifications led to the development of ARG inhibitors, which, divided into α -amino acid derivatives and boronic acid-containing compounds, constitute the class of first-generation inhibitors [22].

2.1. α -Amino Acid Derivatives

ARG inhibitors derived from amino acids include L-homoarginine (1), L-ornithine (2), and L-citrulline (3) categorized as “natural amino acids compounds” (Figure 2). L-homoarginine interacts slowly with ARG, as the enzyme's hydrolytic efficiency depends on the side chain of the α -amino acid substrate. It inhibits human hARG-1 with IC_{50} and K_i values of 8.14 ± 0.52 mM and 6.1 ± 0.50 mM, respectively, and hARG-2 with IC_{50} and K_i values of 2.52 ± 0.01 mM and 1.73 ± 0.10 mM, respectively. ARG activity was assessed by measuring L-ornithine formation in HEK293T cell lysates [33]. L-ornithine shows a significant inhibition of rat ARG, achieving 85.9% inhibition at 10 mM. Similarly, L-citrulline exhibits inhibition levels comparable to L-ornithine, with a bovine liver ARG inhibition of 60% at 20 mM for L-ornithine and 53% at 20 mM for L-Citrulline, as measured by a [^{14}C] urea assay [34,35]. The IC_{50} values, in the millimolar range, obtained with the aforementioned α -amino acid derivatives in in vitro models indicated that they were weak ARG inhibitors, predicting an even weaker therapeutic potential in vivo.

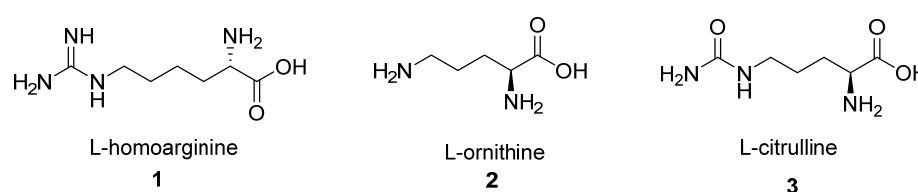
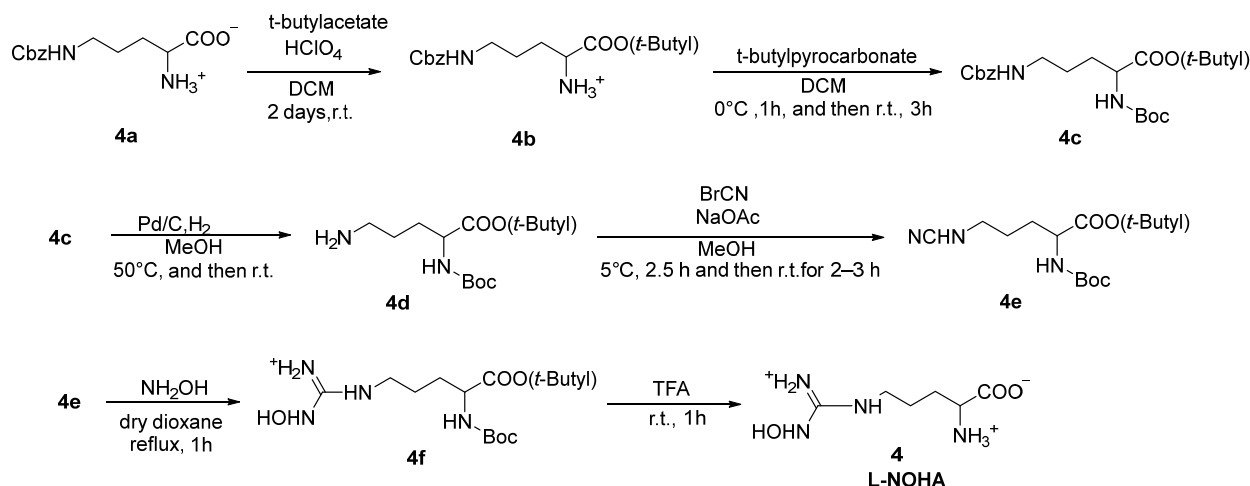


Figure 2. Chemical structures of compounds 1–3.

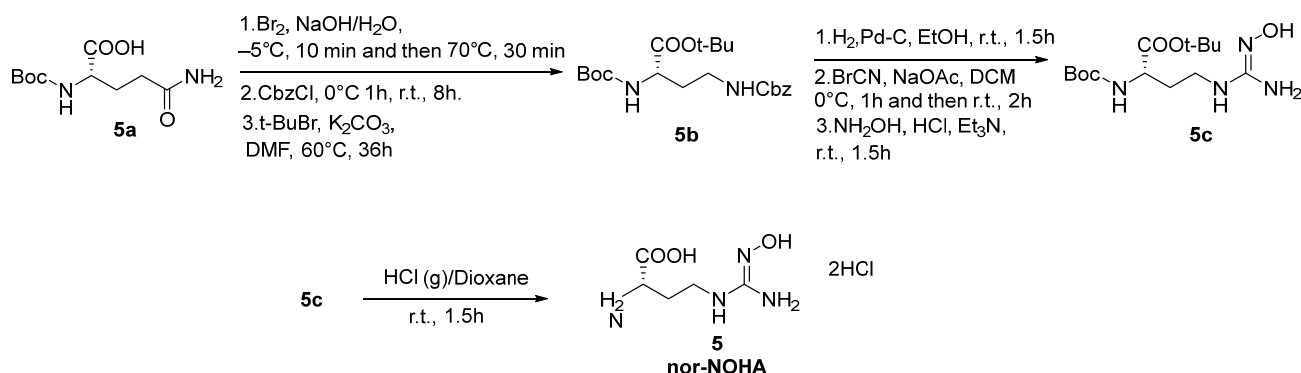
N^{ω} -hydroxyarginine (L-NOHA, 4), is a hydroxylated derivative of L-arginine and a potent ARG inhibitor. It demonstrated the following activity against hARG with the following results: hARG-1 with a K_d of 3.6 μ M (pH 8.5, surface plasmon resonance, SPR) and hARG-2 with K_i values of 1.6 μ M, (pH 7.5) and 2 μ M (pH 9.5, radioactive assay) [36,37]. For the synthesis of L-NOHA, Wallace et al. adopted Bodanszky's method (Scheme 1) [38,39]. Starting with N^{δ} -(benzyloxycarbonyl)-L-ornithine (4a), the carboxylic acid group was protected using *tert*-butylacetate and $HClO_4$, yielding the corresponding *tert*-butyl ester (4b). Compound 4b was treated with *tert*-butyl pyrocarbonate in dichloromethane (DCM) at 0 $^{\circ}C$ and then at room temperature (r.t.) to protect the amine group, producing compound 4c. Next, hydrogenation with H_2 and Pd/C removed the benzyloxycarbonyl group, generating the N^{α} -(*tert*-butyroxycarbonyl)-L-ornithine *tert*-butyl ester (4d) [39]. To form

the cyanamide derivative **4e**, the reaction of **4d** with BrCN in MeOH using NaOAc as a base (Bailey's method) was performed [40]. The subsequent reaction of **4e** with NH₂OH in dry dioxane under reflux produced the *N*^α-(*tert*-butyloxycarbonyl)-*N*^ω-hydroxy-L-arginine *tert*-butyl ester (**4f**). Finally, deprotection of **4f** with trifluoroacetic acid (TFA) yielded *N*^ω-hydroxyarginine (**4**) [39].



Scheme 1. Synthesis of L-NOHA (**4**).

Nor-NOHA (5), a hydroxyguanidine derivative with a shorter alkyl chain, is another compound that effectively inhibits the enzyme ARG [41]. It was tested on hARG with the following results: on hARG-1 (pH 8.5) it showed a *K*_d of 0.517 μM (SPR) and 0.047 μM (isothermal titration calorimetry determination, ITC), while on hARG-2 it exhibited a *K*_i of 51 nM (pH 7.5). As shown by the data from the ARG inhibition tests, the smaller derivative nor-NOHA demonstrated higher affinity compared to L-NOHA and also exhibited a better pharmacokinetic profile, including improved bioavailability and faster elimination. The synthesis of nor-NOHA, which is very similar to that of L-NOHA, is outlined in Scheme 2 [36,37].



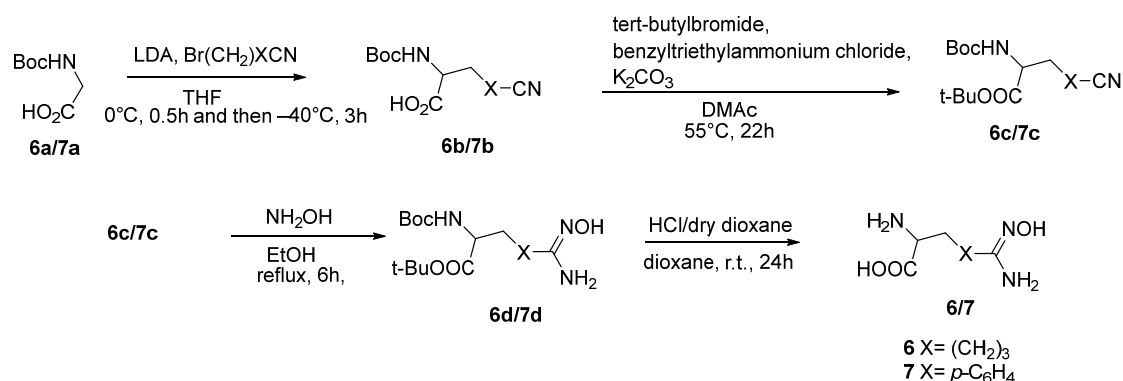
Scheme 2. Synthesis of compound **5**.

The synthesis of nor-NOHA (**5**), began with *N*^α-*tert*(butyloxycarbonyl)-L-glutamine (**5a**) as the starting material [42]. After the Hofmann degradation of the carboxamide, the amine group was protected using benzyl chloroformate (CbzCl), followed by the protection of the carboxyl group with a *tert*-butyl ester, yielding *N*^α-*tert*(butyloxycarbonyl)-*N*^γ-benzyloxycarbonyl-L-2,4-*tert*-butyl-diaminobutyrate (**5b**). This intermediate **5b** underwent further reactions, including catalytic hydrogenation to selectively deprotect the amine group, followed by treatment with BrCN and NH₂OH-HCl to introduce the hydroxygani-

dine group, forming N^α -*tert*(butyloxycarbonyl)- N^ω -hydroxy-nor-L-*tert*-butyl arginine (**5c**). These steps were streamlined into two stages. Finally, dry HCl removed all protecting groups, yielding the target compound, nor-NOHA·2HCl (**5**) [43].

Two additional first-generation inhibitors, N^ω -hydroxy-indospicin (**6**) and 4-hydroxy-amino-D,L-phenylalanine (**7**), are analogues of L-NOHA in which the hydroxyguanidine group is replaced by hydroxyamidine. Both have shown micromolar activity against bovine liver ARG ([14 C] urea assay) with IC_{50} values of $50 \pm 10 \mu\text{M}$ for compound **6** and $230 \pm 5 \mu\text{M}$ for compound **7** [41].

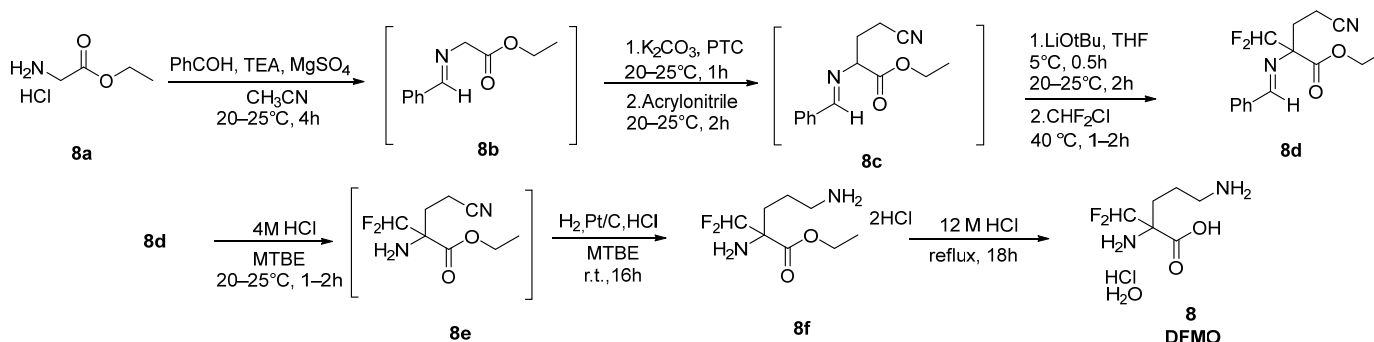
The synthesis of compounds **6** and **7** (see Scheme 3) has been described by Vadon et al. Briefly, *N*-BOC-glycine was alkylated using 5-bromopentanenitrile (for compound **6**) or 4-(bromomethyl)benzonitrile (for compound **7**) in dry tetrahydrofuran (THF) using lithium diisopropylamide (LDA). The resulting products, N^α -*tert*-butoxycarbonyl-6-cyano-D,L-norleucine (**6b**) and N^α -*tert*-butoxycarbonyl-*p*-cyano-D,L-phenylalanine (**7b**) had their carboxyl groups protected as a *tert*-butyl ester using benzyltriethylammonium chloride, K_2CO_3 , and *tert*-butyl bromide in dimethylacetamide (DMAc). The intermediates N^α -*tert*-butoxycarbonyl-6-cyano-D,L-norleucine-*tert*-butylester (**6c**) and N^α -*tert*-butoxycarbonyl-*p*-cyano-D,L-phenylalanine-*tert*-butylester (**7c**) were refluxed with ethanolic hydroxylamine for 6 h to form the hydroxiimidine derivatives N^α -*tert*-butoxycarbonyl- N^ω -hydroxy-D,L-indospicine-*tert*-butylester (**6d**) and N^α -*tert*-butoxycarbonyl-*p*-hydroxyamidino-D,L-phenylalanine-*tert*-butylester (**7d**). In the final synthetic step, treatment with HCl in dry dioxane at r.t. for 24 h removed the protecting groups, producing the final compounds N^ω -hydroxy-D,L-indospicine (**6**) and 4-hydroxy-amino-D,L-phenylalanine (**7**), respectively [44].



Scheme 3. Synthesis of compounds **6** and **7**.

α -Difluoromethylornithine (**DFMO**, **8**) is an irreversible inhibitor of ornithine decarboxylase (ODC), the enzyme involved in polyamines biosynthesis [34,45]. It also exhibited weak inhibitory activity against intestinal ARG, with a K_i of $3.9 \pm 1.0 \text{ mM}$ in intact HT-29 cells and $80 \pm 3\%$ inhibition at 10 mM on bovine liver arginase [46]. The synthesis of DFMO is shown in Scheme 4 [47]. The process began with glycine ethyl ester hydrochloride salt (**8a**) reacting with benzaldehyde in the presence of magnesium sulphate, acetonitrile (ACN), and triethylamine (TEA) to form the 2-benzylideneamino glycine ethyl ester (**8b**). This intermediate was then treated with acrylonitrile in the presence of K_2CO_3 and triethylbenzylammonium chloride, yielding ethyl 2-benzylideneamino-4-cyanobutyrate (**8c**). Next, **8c** reacted with chlorodifluoromethane and lithium *tert*-butoxide in THF at 40°C producing ethyl-2-benzylideneamino-2-difluoromethyl-4-cyanobutyrate (**8d**). Compound **8d** was then deprotected with 4 M HCl in methyl-*tert*-butyl ether (MTBE) to give ethyl-2-amino-2-difluoromethyl-4-cyanobutyrate (**8e**), which underwent catalytic hydrogenation in MTBE and 12 M HCl to form ethyl 2,5-diamino-2-difluoromethylpentanoate dihydrochloride (**8f**).

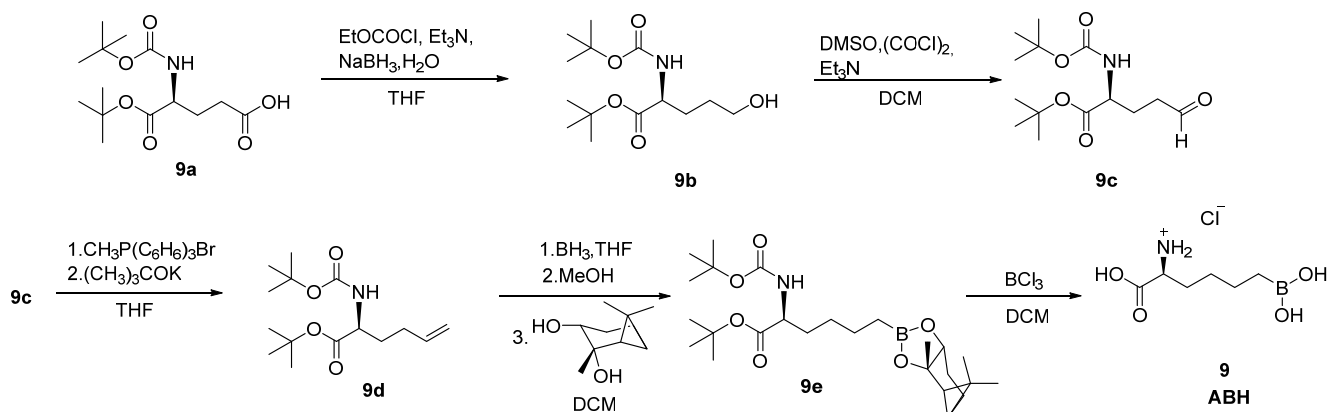
In the final step, **8f** was deprotected with 12 M HCl, yielding DFMO monohydrochloride monohydrate (**8**).



Scheme 4. Synthesis of compound **8**.

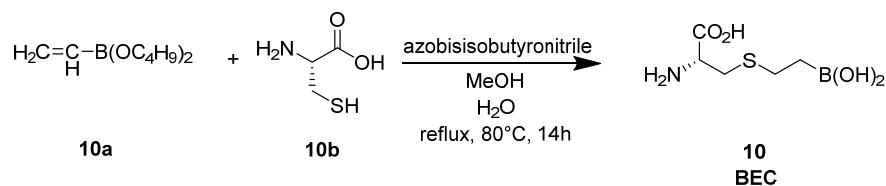
2.2. Boronic Acid Derivatives

Another class of first-generation ARG inhibitors consists of boronic acid derivatives. The compound 2(S)-amino-6-boronoheptanoic acid (**ABH**, **9**) is the first boronic acid-based arginine isostere [48]. **ABH** exhibited strong activity, with a K_d of 5 nM for hARG-1, a K_i of 8.5 nM for hARG-2, and an IC_{50} of 0.8 μ M for rat liver ARG-1 [22]. The synthesis of **ABH** is outlined in Scheme 5 [48,49]. First, (R)-5-(tert-butoxy)-4-((tert-butoxycarbonyl)amino)-5-oxopentanoic acid (**9a**) was reduced using sodium borohydride and ethyl chloroformate to produce a primary alcohol derivative (**9b**). In the next step, **9b** underwent Swern oxidation to form an aldehyde **9c**, which was used directly in a Wittig reaction with triphenylphosphonium methylilide, yielding olefin (**9d**). The hydroboration of **9d**, followed by treatment with MeOH and protection with (1S,2S,3R,5S)-(+)-pinanediol, yields intermediate **9e**. The final step involved complete deprotection using BCl_3 , yielding **ABH** (**9**) as a white semi-crystalline solid.



Scheme 5. Synthesis of compound **9**.

2-Boronoethyl-L-cysteine (**BEC**, **10**) is an analogue of **ABH**, where a sulphur atom replaces carbon in the main chain. **BEC** exhibited activity with a K_d of 270 nM for hARG-1 (ITC) and a K_i of 30 nM for hARG-2 (radioactive assay) [22]. The synthesis of **BEC** (Scheme 6) involved a single-step reaction [50]. A solution of cysteine (**10b**) and dibutylboronate (**10a**) in MeOH and H_2O was refluxed at 80 °C under N_2 for 14 h. Afterward, azobisisobutyronitrile was added, yielding the desired compound **10**.



Scheme 6. Synthesis of compound 10.

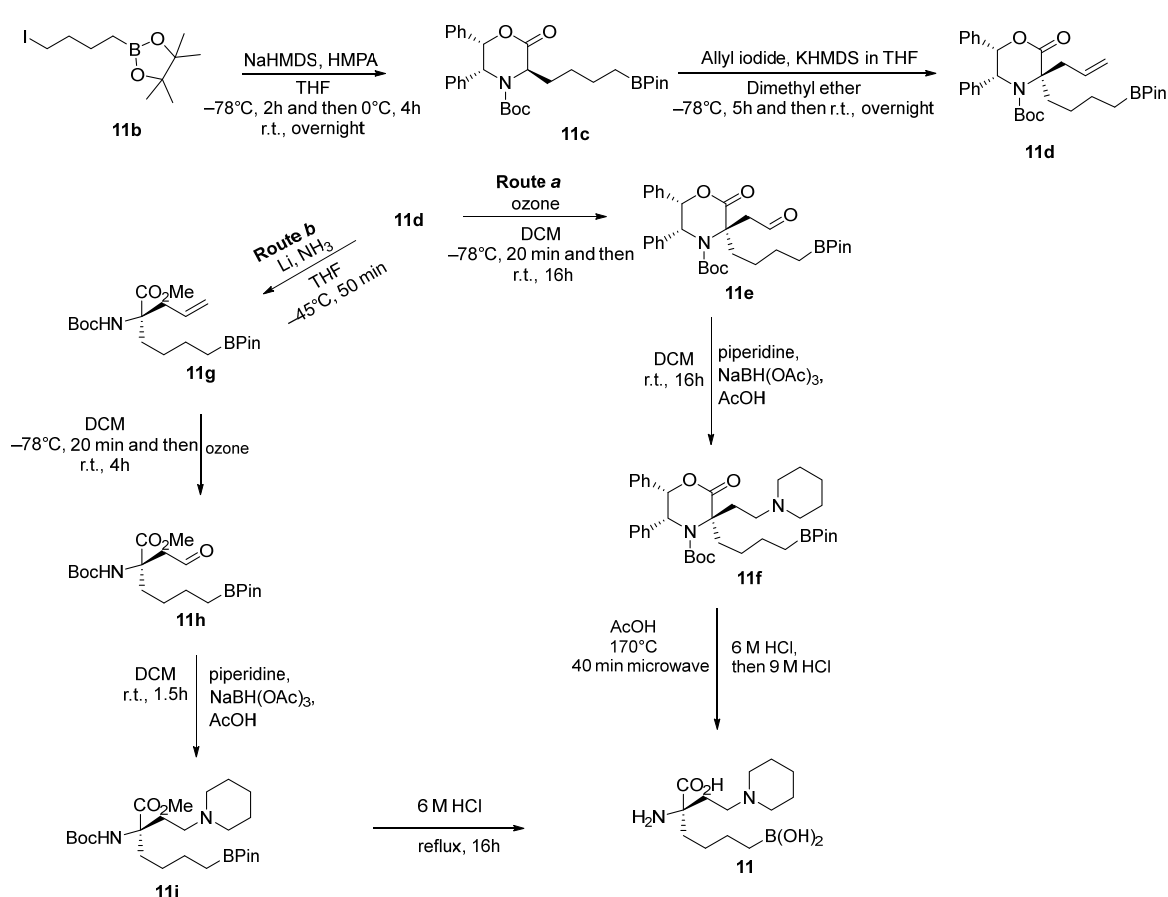
ABH and BEC exhibited higher affinity for ARG than α -amino acid derivatives. However, their bioavailability was relatively low, with undetectable plasma levels, likely due to their limited ability to cross biological membranes. Additionally, their unacceptable toxicity to normal cells, stemming from their chemical reactivity and instability, rendered them unsuitable for clinical use in cancer treatment. As a result, a structural optimization study, along with the exploration of medicinal chemistry strategies—such as drug delivery systems—became crucial. Approaches aimed at enhancing the permeability and stability of these ARG inhibitors, potentially through carrier or bioprecursor prodrug strategies, are urgently needed.

3. Second-Generation Inhibitors

Second-generation inhibitors include α -substituted ABH analogues, which have shown promising and potent ARG inhibitors. These inhibitors are further divided into two subclasses: basic side chain α -substituted ABH analogues (see Section 3.1) and non-basic side chain α -substituted ABH analogues (see Section 3.2) [16].

3.1. Basic Side Chain α -Substituted ABH Analogues

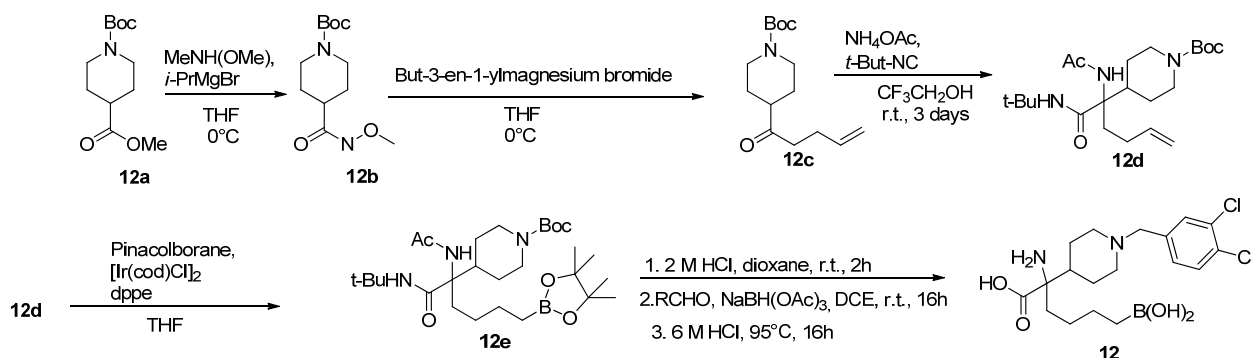
The first second-generation molecule discussed in this review is (R)-2-amino-6-borono-2-(2-piperidin-1-yl) ethyl) hexanoic acid (**11**), which demonstrated inhibition activity against hARG-1 and hARG-2 with IC_{50} values of 223 nM and 509 nM, respectively [24]. Its cellular activity against hARG-1 in CHO cells was also confirmed (IC_{50} = 509 nM) [22]. The patented synthesis of compound **11** (Scheme 7) began with (4S,5S)-tert-butyl-6-oxo-4,5-diphenyl-1,3-oxazinane-3-carboxylate (**11a**), which was alkylated with 2-(4-iodobutyl)-4,4,5,5-tetramethyl-1,3,2-dioxaborolane (**11b**) using NaHMDS and HMPA in THF at -78°C , forming boronate (**11c**). A second alkylation with allyl iodide, using potassium bis(trimethylsilyl)amide (KHMDs) as the base and DME (dimethoxyethane) as the solvent, yielded oxazinone **11d**, which followed two possible synthetic routes a or b. In route a, **11d** underwent ozonolysis in DCM at -78°C (**11e**) followed by reductive amination with piperidine, $\text{NaBH}(\text{OAc})_3$, and AcOH in DCM to produce amine **11f** in a 95% yield. The auxiliary oxazinone was then removed by treatment with 6 M HCl in a microwave reactor at 170°C for 40 min, yielding compound **11** in a 87% yield. For route b, the steps were reversed. First **11d** was treated with Li in liquid ammonia to produce (R)-methyl 2-allyl-2-(tert-butoxycarbonylamino)-6-(4,4,5,5-tetramethyl-1,3,2-dioxaborolan-2-yl)hexanoate (**11g**) as a colourless oil. This intermediate was then subjected to ozonolysis in DCM at -78°C (**11h**), followed by reductive amination with piperidine, $\text{NaBH}(\text{OAc})_3$, and AcOH forming amine **11i** in 67% yield. The deprotection of **11i** with 6 M HCl under reflux for 16 h produced the final compound **11** as a dihydrochloride salt [51]. The two synthetic procedures for compound **11** (route a and route b) were developed to facilitate large-scale synthesis. Route a required fewer synthetic steps and provided a higher overall yield compared to route b. The need to optimize the synthesis of compound **11**, addressed by the same authors who designed this inhibitor, was driven by the need for a precise configuration of the target inhibitor and the requirement to start with a flexible intermediate, such as the aldehyde, which could be prepared on a large scale and with high enantioselectivity.



Scheme 7. Synthesis of compound 11.

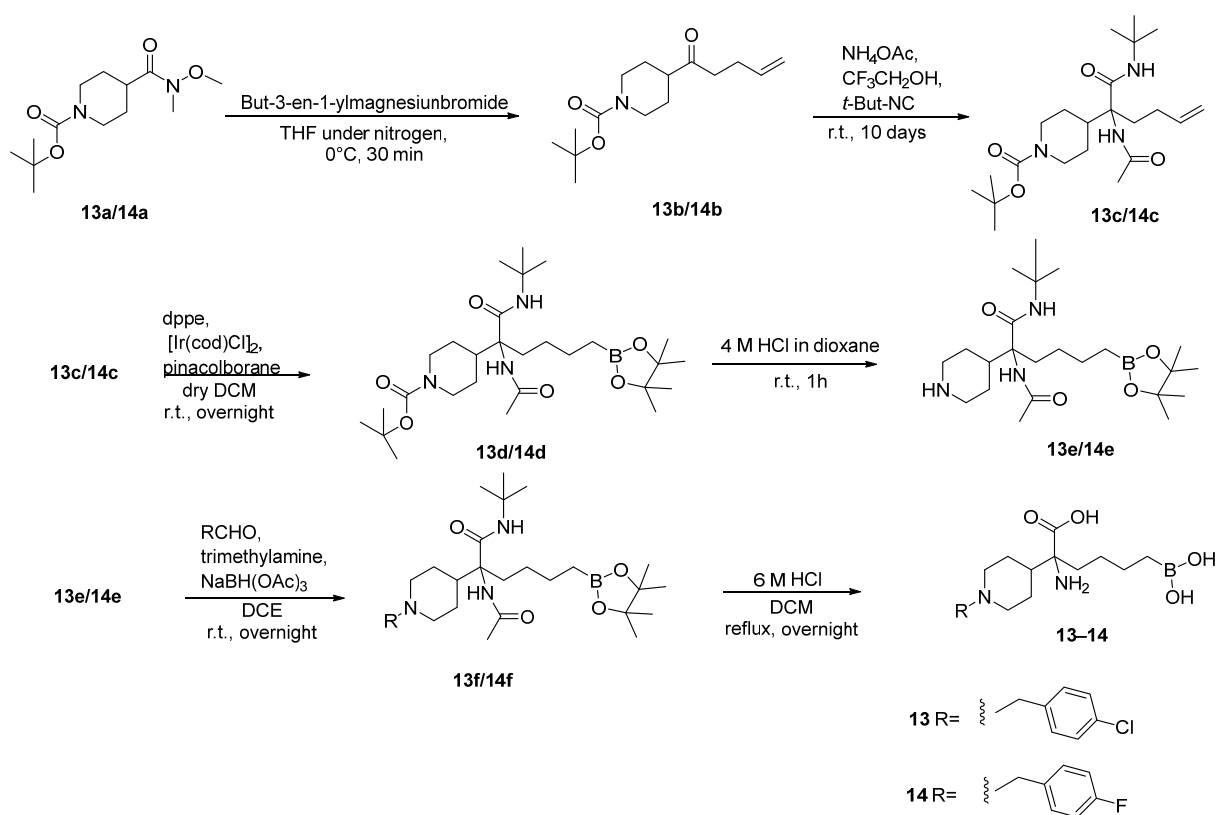
Among α , α -disubstituted amino acid-based ARG inhibitors, compound 2-amino-6-borono-2-(1-(3,4-dichlorobenzyl) piperidin-4-yl) hexanoic acid (**12**), stands out. This derivative, featuring a piperidine ring linked to a quaternary amino acid centre, was synthesized by Golebiowski et al. (Scheme 8) [26]. It demonstrated potent inhibitory activity with IC_{50} values of 200 nM for hARG-1 and 290 nM for hARG-2 [16]. The synthesis of compound **12** began with the reaction of 1-tert-butyl-4-methyl piperidine-1,4-dicarboxylate (**12a**) with N,O-dimethylhydroxylamine and i-PrMgBr in THF, forming Weinreb amide **12b**. Next, **12b** underwent substitution with but-3-en-1-yl-magnesiumbromide in THF at 0°C under N_2 yielding tert-butyl 4-(pent-4-enoyl) piperidine-1-carboxylate (**12c**) in a 91% yield. In the third step, an Ugi reaction was performed by treating ketone **12c** with tert-butyl isocyanide and ammonium acetate (NH_4OAc) in 2,2,2-trifluoroethanol, producing intermediate tert-butyl-4-(2-acetamido-1-(tert-butylamino)-1-oxohex-5-en-2-yl) piperidine-1-carboxylate (**12d**). This was followed by a hydroboration reaction using pinacolborane, chloro-1,5-cyclooctadiene iridium (I) dimer ($[\text{Ir}(\text{cod})\text{Cl}]_2$), and 1,2-bis(diphenylphosphino)ethane (dppe) in THF, to yield derivative **12e**. A subsequent step included the deprotection of the piperidine ring with 2 M HCl in dioxane at r.t. for 2 h. The deprotected piperidine was then N-alkylated with 3,4-dichlorobenzaldehyde and $\text{NaBH}(\text{OAc})_3$ in 1,2 dichloroethane (DCE) at r.t. for 16 h. Final acid deprotection with 6 M HCl yielded the target compound **12** [26,51]. This synthetic procedure was optimized by the authors and involved seven steps, each achieving notably high yields. The optimization process incorporated a multi-component reaction strategy, specifically the Ugi reaction, using a ketone derivative (**12c**) as a model substrate and tert-butyl isocyanide. Optimal conditions were achieved by using ammonium acetate as both the amino and acid component, along with replacing methanol with

trifluoroethanol as the solvent. This adjustment effectively suppressed the competitive Passerini reaction.



Scheme 8. Synthesis of compound **12**.

Two additional N-alkylated piperidine derivatives are 2-amino-6-borono-2-(1-(4-chlorobenzyl) piperidin-4-yl)-hexanoic acid (**MARS**, **13**) and 2-amino-6-borono-2-(1-(4-fluorobenzyl)piperidin-4-yl)hexanoic acid (**FMARS**, **14**), which differ in the halogen substituent. MARS exhibited IC_{50} values of 0.9 μ M for hARG-1 and 0.7 μ M for hARG-2, while FMARS showed IC_{50} values of 1.1 μ M for hARG-1 and 0.4 μ M for hARG-2 [52]. The synthesis of both compounds (Scheme 9), reported by Clemente et al., followed the patented protocol established by Adam Golebiowski et al. [51,52]. The strategy was similar to that used for compound **12**, with the key difference being the use of a reductive amination step (4-chloro and 4-fluoro benzaldehydes for MARS and FMARS, respectively).

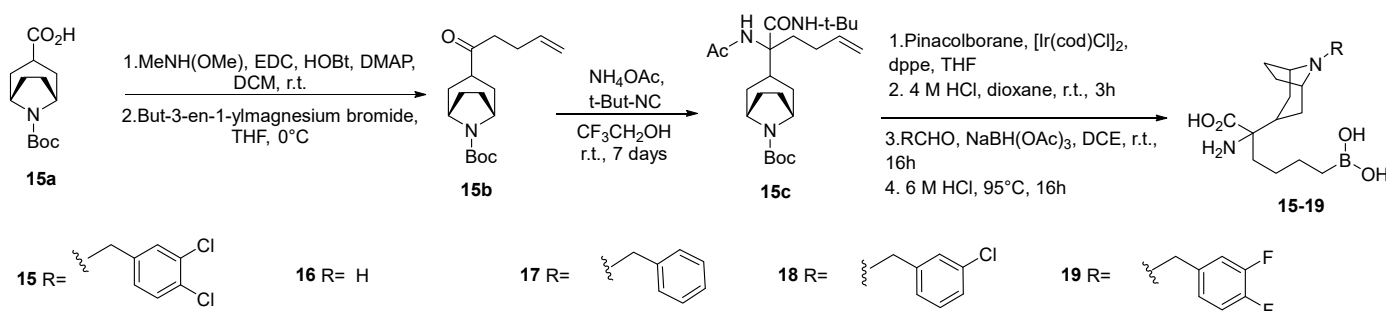


Scheme 9. Synthesis of compounds **13** and **14**.

Another class of ARG inhibitors includes tropane derivatives (**15–19**), characterized by a two-carbon bridge within the piperidine ring, which enhances their activity. These

compounds demonstrated significant inhibition of hARG-1 and hARG-2, with IC₅₀ values ranging from nanomolar to micromolar levels [22,24,26,52–54]. The increased potency of tropane derivatives **15–19** compared to the simpler piperidine derivatives **12–14** has been thoroughly investigated. For derivatives **12–14**, the piperidine ring adopts a chair conformation, with the nitrogen atom interacting with two aspartate residues in the binding pocket of ARG-1 and ARG-2 through a water molecule. In contrast, for derivatives **15–19**, the two-carbon bridge of the tropane forces the piperidine ring into a boat conformation, enabling the nitrogen atom to establish direct contact with one of the aspartate residues in the pocket of interest. The other aspartate residue is still contacted via the water molecule. Thus, the tropane derivatives benefit from two key advantages that explain their enhanced potency: the fixed ring geometry positions the nitrogen atom optimally (resulting in an entropy gain) and the nitrogen establishes direct contact with one aspartate residue, bypassing the need for water-mediated interaction. Furthermore, this significant improvement in in vitro activity was accompanied by reduced polarity and an improved pharmacokinetic profile.

The synthesis of the derivatives **15–19** involved a seven-step protocol (Scheme 10) [55]. The initial four steps were consistent across all compounds. For the synthesis of compound 2-amino-2-(8-azabicyclo [3.2.1]octan-3-yl)-6-boronohexanoic acid (**16**), the fifth and sixth steps were omitted, proceeding directly to the final stage. For compounds 2-((1R,5S)-8-(3,4-dichlorobenzyl)-8-azabicyclo[3.2.1]octan-3-yl)hexanoic acid (**ABHtrop**, **15**), 2-amino-2-(8-benzyl-8-azabicyclo[3.2.1]octan-3-yl)-6-boronohexanoic acid (**17**), 2-amino-6-borono-2-(8-(3-chlorobenzyl)-8-azabicyclo[3.2.1]octan-3-yl) hexanoic acid (**18**), and 2-amino-6-borono-2-(8-(3,4-difluorobenzyl)-8-azabicyclo [3.2.1]octan-3-yl) hexanoic acid (**19**), the sixth step varied depending on the aldehyde reagent used.

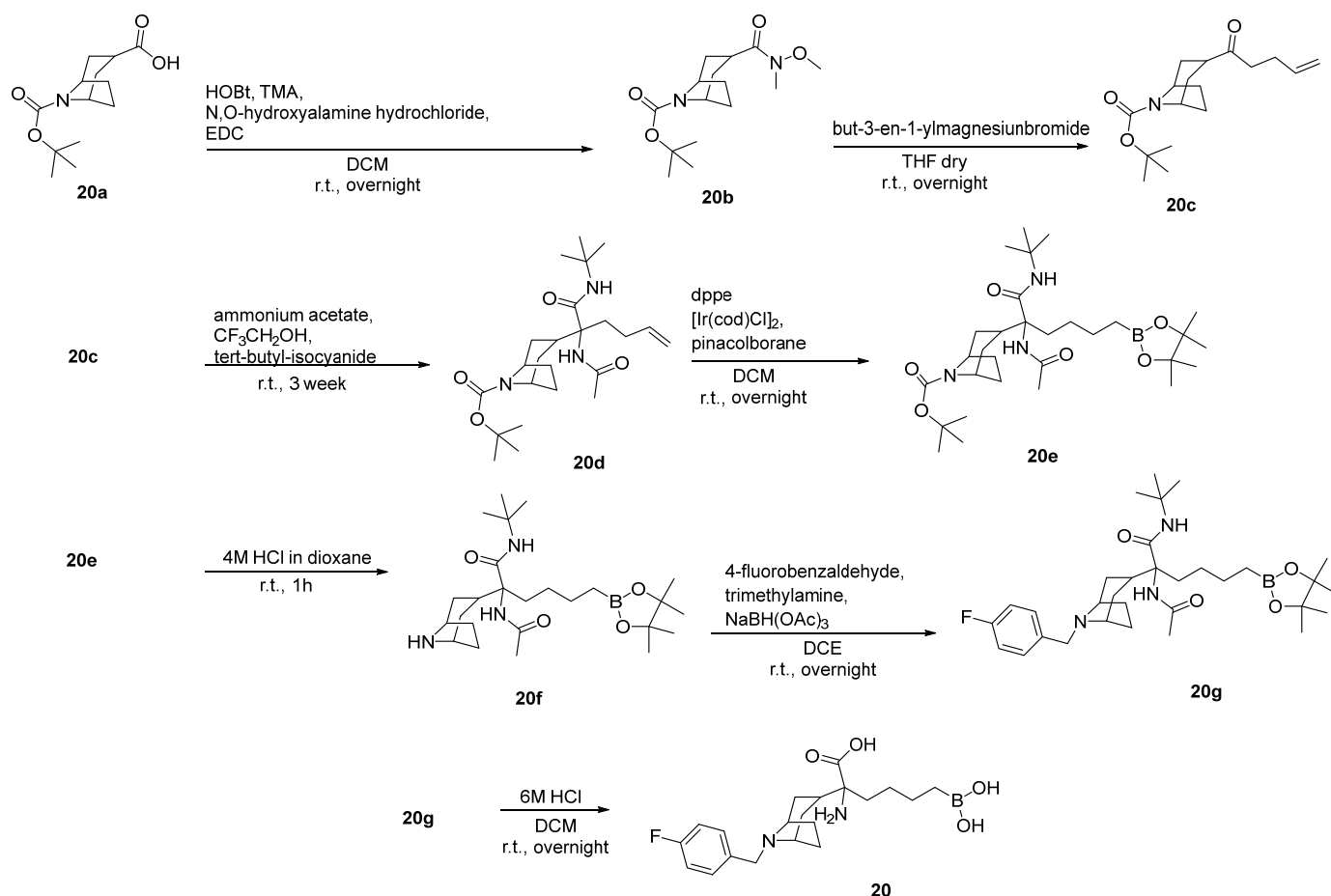


Scheme 10. Synthesis of compounds **15–19**.

The synthetic strategy for these tropane ring analogues closely resembles that developed by the same authors for compound **12**. In this case, the intermediate **15b** was used as the model substrate in the Ugi reaction. Both this intermediate and the subsequent Ugi product, **15c**, were thermodynamically favoured. Notably, the use of the trans isomer of derivative **15b** as a substrate for the Ugi reaction resulted in the same relative stereochemistry for **15c**. Starting with (1R,5S)-8-(tert-butoxycarbonyl)-8-azabicyclo[3.2.1]octane-3-carboxylic acid (**15a**), the first step was the coupling with N-methyl-N-methoxyamide using MeNH(OMe), 1-ethyl-3-(3-dimethylaminopropyl)carbodiimide (EDC), hydroxybenzotriazole (HOBT), and 4-dimethylaminopyridine (DMAP) in DCM at r.t. The intermediate underwent substitution with but-3-en-1-yl-magnesium bromide in THF at 0 °C, forming (1R,5S)-tert-butyl 3-(pent-4-enoyl)-8-azabicyclo[3.2.1]octane-8-carboxylate (**15b**). In the next step, **15b** participated in an Ugi reaction with NH₄OAc, tert-butyl-isocyanide, and 2,2,2-trifluoroethanol at r.t. for 7 days, yielding (1R,3s,5S)-tert-butyl 3-(2-acetamido-1-(tert-butylamino)-1-oxohex-5-en-2-yl)-8-azabicyclo[3.2.1]octane-8-carboxylate (**15c**). Notably, both ketone **15b** and Ugi product **15c** were thermodynamically favoured, with the trans isomer of **15b** yielding the same stereochemistry in **15c**. Next, **15c** underwent hydrobora-

tion reaction with pinacolborane, $[\text{Ir}(\text{cod})\text{Cl}]_2$, and dppe in THF, producing a hydroborate intermediate. This was treated with 4 M HCl in dioxane at r.t. for 3 h to selectively deprotect the tropane nitrogen. N-alkylation for compounds **15** and **17–19** was carried out using $\text{NaBH}(\text{OAc})_3$ and various aldehydes (3,4-dichlorobenzaldehyde for compound **15**, benzaldehyde for **17**, 3-chlorobenzaldehyde for **18**, and 3,4-difluorobenzaldehyde for **19**) in DCE. The intermediates were finally deprotected with 6 M HCl at 95 °C for 16 h, producing the desired compounds.

The same strategy was applied to synthesize **FBMARS** (**20**, Scheme 11). Starting from amino acid **20a**, a coupling reaction with N,O-dimethylhydroxylamine hydrochloride in the presence of EDC, HOBt, and trimethylamine (TMA) in DCM yielded the Weinreb amide **20b**. This intermediate was substituted with but-3-en-1-yl-magnesiumbromide in dry THF, forming ketone **20c**. Ketone (**20c**) underwent an Ugi reaction with NH_4OAc , 2,2,2-trifluoroethanol, and tert-butyl-isocyanide, yielding **20d** after 3 weeks. Hydroboration with dppe, $[\text{Ir}(\text{cod})\text{Cl}]_2$, DCM and 4,4,5,5-tetramethyl-1,3,2-dioxaborolane produced **20e**. Subsequent treatment with 4 M HCl in dioxane for 1 h removed the tert-butyloxycarbonyl group, yielding **20f** as a salt. This salt was N-alkylated with 4-fluorobenzaldehyde in DCE using TMA and sodium triacetoxyborohydride, forming intermediate **20g**. Finally, deprotection with 6 M HCl in DCM gave **FBMARS** (**20**) [52].



Scheme 11. Synthesis of compound **20**.

The same research group detailed the synthesis of the ^{18}F -fluoroanalogues of **FMARS** (**14**) and **FBMARS** (**20**) using copper-mediated late-stage radiofluorination. These radioactive compounds are highly valuable for ARG imaging, which has proven effective

in detecting and monitoring ARG-related diseases. The structures of ^{18}F -FMARS and ^{18}F -FBMARS are shown in Figure 3.

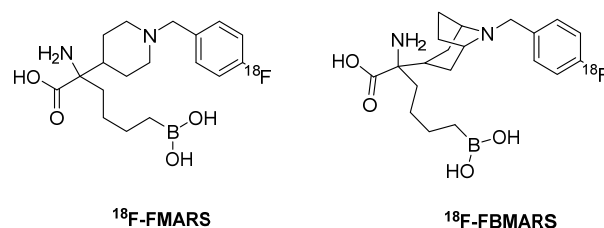


Figure 3. Chemical structures of compounds ^{18}F -FMARS and ^{18}F -FBMARS.

Another class of ARG inhibitors includes *N*-alkylcyclobutylamine derivatives, featuring a nitrogen atom substituted with diverse functional groups such as phenyl and biphenyl moieties, which can be further modified. As summarized in Table 1, these compounds (21–46) exhibited activity against hARG-1 and hARG-2, with potency ranging from 0.1 nM to 100 nM.

Table 1. Chemical structures of compounds 21–46.

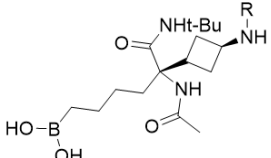
		
Compound	R	IC ₅₀
21 (S)-2-amino-6-borono-2-((1S,3R)-3-(3-phenylpropylamino)cyclobutyl)hexanoic acid		0.1–25 nM (hARG-1) 26–100 nM (hARG-2)
22 (S)-2-amino-6-borono-2-((1S,3R)-3-(3-(3-chloro-5-fluorophenyl)propylamino)cyclobutyl)hexanoic acid		26–100 nM (hARG-1) 0.1–25 nM (hARG-2)
23 (S)-2-amino-6-borono-2-((1S,3R)-3-(3-(3,4-difluorophenyl)propylamino)cyclobutyl)hexanoic acid		26–100 nM (hARG-1) 26–100 nM (hARG-2)
24 (S)-2-amino-6-borono-2-((1S,3R)-3-(3-(2,4-dichlorophenyl)propylamino)cyclobutyl)hexanoic acid		26–100 nM (hARG-1) 26–100 nM (hARG-2)
25 (S)-2-amino-6-borono-2-((1S,3R)-3-(2,3-dihydro-1H-inden-2-ylamino)cyclobutyl)hexanoic acid		0.1–25 nM (hARG-1) 26–100 nM (hARG-2)
26 (S)-2-amino-6-borono-2-((1S,3R)-3-(4-tert-butylbenzylamino)cyclobutyl)hexanoic acid		26–100 nM (hARG-1) 26–100 nM (hARG-2)
27 (S)-2-amino-2-((1S,3R)-3-(biphenyl-3-ylmethylamino)cyclobutyl)-6-borohexanoic acid		0.1–25 nM (hARG-1) 26–100 nM (hARG-2)
28 (S)-2-amino-6-borono-2-((1S,3R)-3-((4'-(trifluoromethyl)biphenyl-3-yl)methylamino)cyclobutyl)hexanoic acid		26–100 nM (hARG-1) 26–100 nM (hARG-2)

Table 1. Cont.

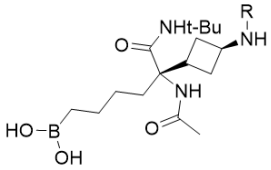
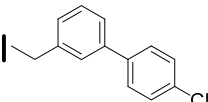
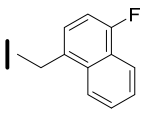
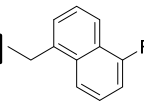
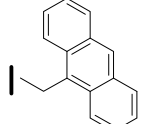
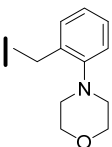
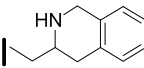
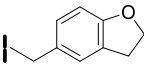
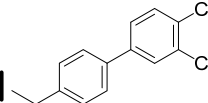
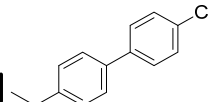
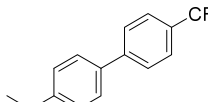
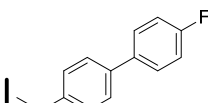
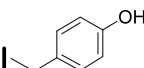
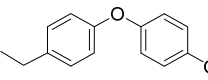
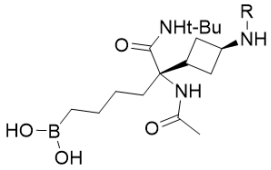
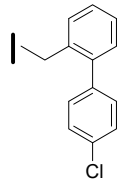
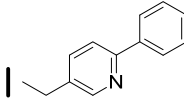
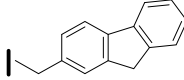
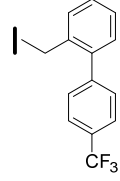
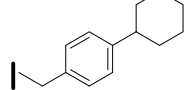
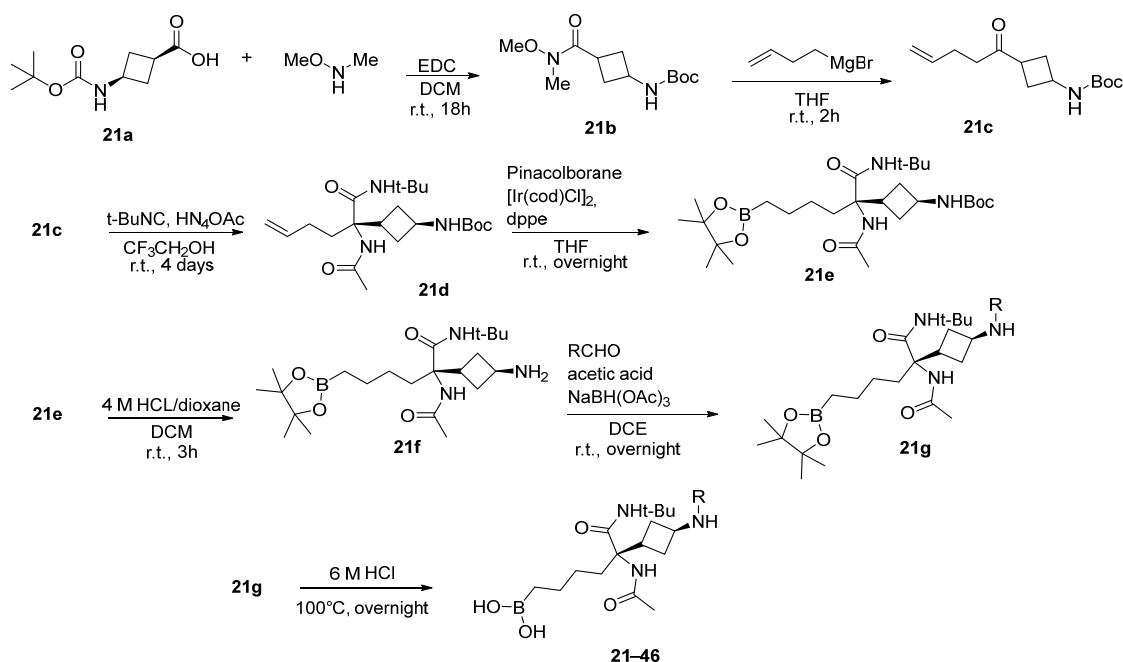
		
Compound	R	IC ₅₀
29 (S)-2-amino-6-borono-2-((1S,3R)-3-((4'-chlorobiphenyl-3-yl)methylamino)cyclobutyl)hexanoic acid		0.1–25 nM (hARG-1) 0.1–25 nM (hARG-2)
30 (S)-2-amino-6-borono-2-((1S,3R)-3-((4-fluoronaphthalen-1-yl)methylamino)cyclobutyl)hexanoic acid		0.1–25 nM (hARG-1) 0.1–25 nM (hARG-2)
31 (S)-2-amino-6-borono-2-((1S,3R)-3-((5-fluoronaphthalen-1-yl)methylaminocyclobutyl)hexanoic acid		0.1–25 nM (hARG-1) 26–100 nM (hARG-2)
32 (S)-2-amino-2-(1S,3R)-3-(anthracen-9-ylmethylamino)cyclobutyl)-6-borono hexanoic acid		26–100 nM (hARG-1) 0.1–25 nM (hARG-2)
33 (S)-2-amino-6-borono-2-((1S,3R)-3-(2-morpholinobenzylamino)cyclobutyl)hexanoic acid		26–100 nM (hARG-1) 26–100 nM (hARG-2)
34 (S)-2-amino-6-borono-2-((1R,3R)-3-(((S)-1,2,3,4-tetrahydroisoquinolin-3-yl)methylamino)cyclobutyl)hexanoic acid		26–100 nM (hARG-1) 26–100 nM (hARG-2)
35 (S)-2-amino-6-borono-2-((1S,3R)-3-((2,3-dihydrobenzofuran-5-yl)methylamino)cyclobutyl)hexanoic acid		26–100 nM (hARG-1) 26–100 nM (hARG-2)
36 (S)-2-amino-6-borono-2-((1S,3R)-3-((3',4'-dichlorobiphenyl-4-yl)methylamino)cyclobutyl)hexanoic acid		0.1–25 nM (hARG-1) 0.1–25 nM (hARG-2)
37 (S)-2-amino-6-borono-2-((1S,3R)-3-((4'-chlorobiphenyl-4-yl)methylamino)cyclobutyl)hexanoic acid		0.1–25 nM (hARG-1) 0.1–25 nM (hARG-2)
38 (S)-2-amino-6-borono-2-((1S,3R)-3-((4'-(trifluoromethyl)biphenyl-4-yl)methylamino)cyclobutyl)hexanoic acid		0.1–25 nM (hARG-1) 0.1–25 nM (hARG-2)
39 (S)-2-amino-6-borono-2-((1S,3R)-3-((4'-fluorobiphenyl-4-yl)methylamino)cyclobutyl)hexanoic acid		0.1–25 nM (hARG-1) 26–100 nM (hARG-2)
40 (S)-2-amino-6-borono-2-((1S,3R)-3-(4-hydroxybenzylamino)cyclobutyl)hexanoic acid		26–100 nM (hARG-1) 26–100 nM (hARG-2)
41 (S)-2-amino-6-borono-2-((1S,3R)-3-(4-(4-chlorophenoxy)benzylamino)cyclobutyl)hexanoic acid		0.1–25 nM (hARG-1) 0.1–25 nM (hARG-2)

Table 1. Cont.

		
Compound	R	IC ₅₀
42 (S)-2-amino-6-borono-2-((1S,3R)-3-((4'-chlorobiphenyl-2-yl)methylamino)cyclobutyl)hexanoic acid		26–100 nM (hARG-1) 26–100 nM (hARG-2)
43 (S)-2-amino-6-borono-2-((1S,3R)-3-((6-phenylpyridin-3-yl)methylamino)cyclobutyl)hexanoic acid		26–100 nM (hARG-1) 0.1–25 nM (hARG-2)
44 (S)-2-((1S,3R)-3-((9h-fluoren-2-yl)methylamino)cyclobutyl)-2-amino-6-borono-hexanoic acid		0.1–25 nM (hARG-1) 0.1–25 nM (hARG-2)
45 (S)-2-amino-6-borono-2-((1S,3R)-3-((4'-(trifluoromethyl)biphenyl-2-yl)methylamino)cyclobutyl)hexanoic acid		26–100 nM (hARG-1) 26–100 nM (hARG-2)
46 (S)-2-amino-6-borono-2-((1S,3R)-3-(4-cyclohexylbenzylamino)cyclobutyl)hexanoic acid		0.1–25 nM (hARG-1) 26–100 nM (hARG-2)

The synthesis of compounds **21–46**, patented by Van Zandt et al. and illustrated in Scheme 12, closely resembles previously described methods. The process involved seven steps differing only in the reagent used during the sixth step [55]. The first step was a coupling reaction involving (1S,3S)-3-(*tert*-butoxycarbonylamino)cyclobutanecarboxylic acid (**21a**), N,O-dimethylhydroxylamine hydrochloride, *N*-methyl-morpholine, and EDC in DCM. This reaction, carried out at r.t. over 18 h, produced *tert*-butyl(1S,3S)-3-(methoxy(methyl)carbamoyl)cyclobutylcarbamate (**21b**). The second step involved the substitution of **21b** with 3-butenylmagnesium bromide in THF for 2 h at r.t., yielding *tert*-butyl(1S,3S)-3-pent-4-enoylcyclobutylcarbamate (**21c**). In the third step, an Ugi reaction with **21c** in 2,2,2-trifluoroethanol, NH₄OAc and *tert*-butyl isocyanide over 4 days produced *tert*-butyl(1S,3S)-3-(R-2-acetamido-1-(*tert*-butylamino)-1-oxohex-5-en-2-yl)cyclobutylcarbamate (**21d**). Next, **21d** underwent hydroboration with pinacolborane in the presence of [Ir(cod)Cl]₂ and dppe in DCM, forming *tert*-butyl(1S,3S)-3-((R)-2-acetamido-1-(*tert*-butylamino)-1-oxo-6-(4,4,5,5-tetramethyl-1,3,2-dioxaborolan-2-yl)hexan-2-yl)cyclobutylcarbamate (**21e**). In the fifth step, **21e** was treated with 4 M HCl in dioxane for 3 h to remove the *tert*-butyloxycarbonyl group, yielding (S)-2-acetamido-2-((1S,3R)-3-aminocyclobutyl)-*N*-*tert*-butyl-6-(4,4,5,5-tetramethyl-1,3,2-dioxaborolan-2-yl)hexanamide (**21f**) as a hydrochloride salt. For the sixth step, **21f** was reacted overnight with acetic acid, NaBH(OAc)₃, and various aldehydes (depending on the desired derivative) in DCE, producing the respective *N*-alkylated intermediates (**21g**). In the final step, these intermedi-

ates were treated with 6 M HCl and heated to 100 °C overnight, yielding the final products **21–46**, whose names are provided in Table 1.

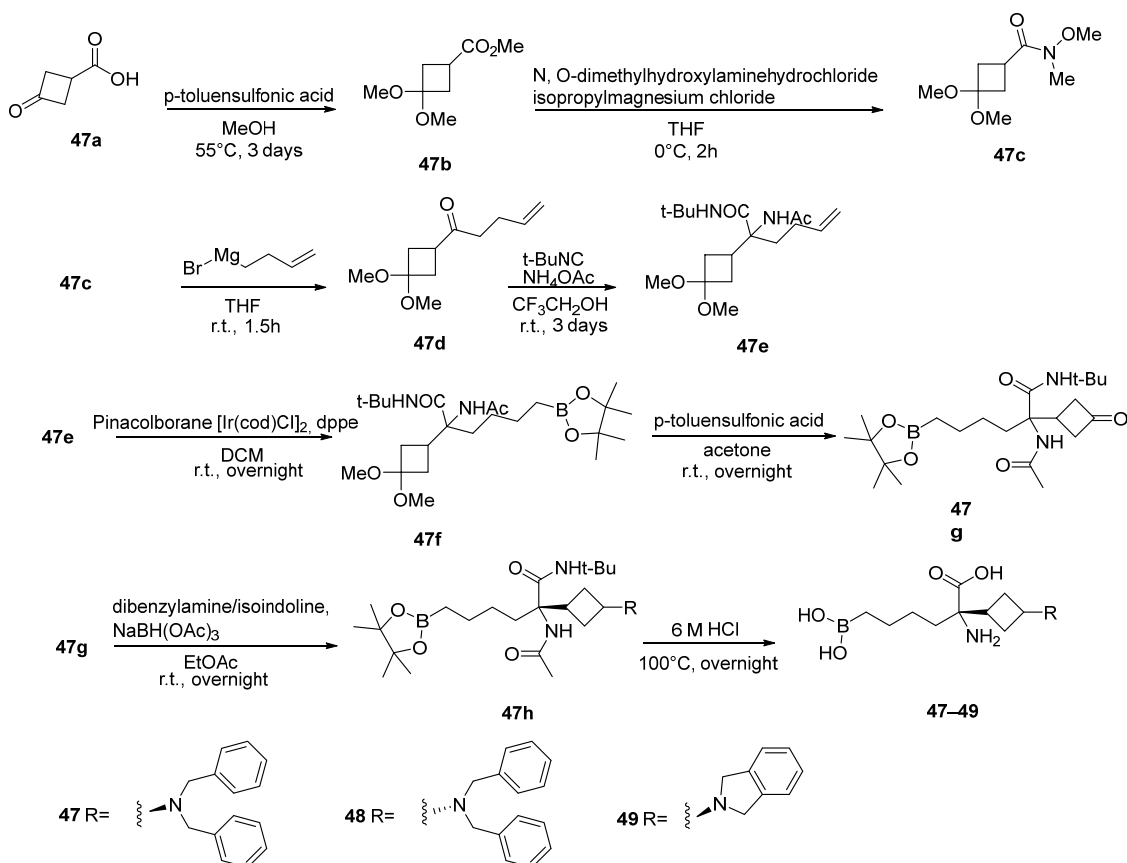


Scheme 12. Synthesis of compounds **21–46**.

Further investigations into the *N*-alkylcyclobutylamine scaffold led to the development of tertiary amine derivatives (compounds **47–49**). However, these derivatives displayed lower potency compared to the parent compounds **21–46**. Their syntheses and structures are shown in Scheme 13.

The synthesis of compounds **47–49** followed an eight-step protocol starting with the reaction of 3-oxocyclobutanecarboxylic acid (**47a**) in MeOH and *p*-toluenesulfonic acid at 55 °C for 3 days to yield methyl-3,3-dimethoxycyclobutanecarboxylate (**47b**). This intermediate underwent coupling with *N,O*-dimethylhydroxylaminehydrochloride and isopropylmagnesium chloride in THF to produce **47c**. Next, substitution with 3-butenylmagnesium bromide yielded 1-(3,3-dimethoxycyclobutyl)pent-4-en-1-one (**47d**), which was subjected to an Ugi reaction with ammonium acetate, *tert*-butyl-isocyanide, and 2,2,2-trifluoroethanol, producing 2-acetamido-*N*-*tert*-butyl-2-(3,3-dimethoxycyclobutyl)hex-5-enamide (**47e**). The hydroboration of **47e** with pinacolborane, [Ir(cod)Cl]₂ and dppe generated 2-acetamido-*N*-*tert*-butyl-2-(3,3-dimethoxycyclobutyl)-6-(4,4,5,5-tetramethyl-1,3,2-dioxaborolan-2-yl)hexanamide (**47f**), which was then treated with *p*-toluenesulfonic acid overnight in acetone to form 2-acetamido-*N*-*tert*-butyl-2-(3-oxocyclobutyl)-6-(4,4,5,5-tetramethyl-1,3,2-dioxaborolan-2-yl) hexanamide (**47g**), containing an oxidized cyclobutyl ring. In the penultimate step, **47g** was reacted with either dibenzylamine (for compound **47**), its *trans* isomer (for **48**), or isoindoline (for **49**), followed by NaBH(OAc)₃ reduction to form intermediates **47h**. Finally, global deprotection using 6 M HCl at 100 °C yielded the desired compounds **47–49** [47].

The basic side chain α -substituted ABH analogues (compounds **50–51**) also emerged as potent ARG inhibitors. Compound **50**, i.e., 2-amino-6-borono-2-(3-(4-(4-chlorophenyl)-4-hydroxypiperidin-1-yl)propyl)hexanoic acid, with a cyclic amine side chain, showed strong inhibitory activity ($K_i < 10$ nM) against both hARG-1 and 2 [22]. Compound **51**, featuring a linear amine side chain, exhibited comparable potency.

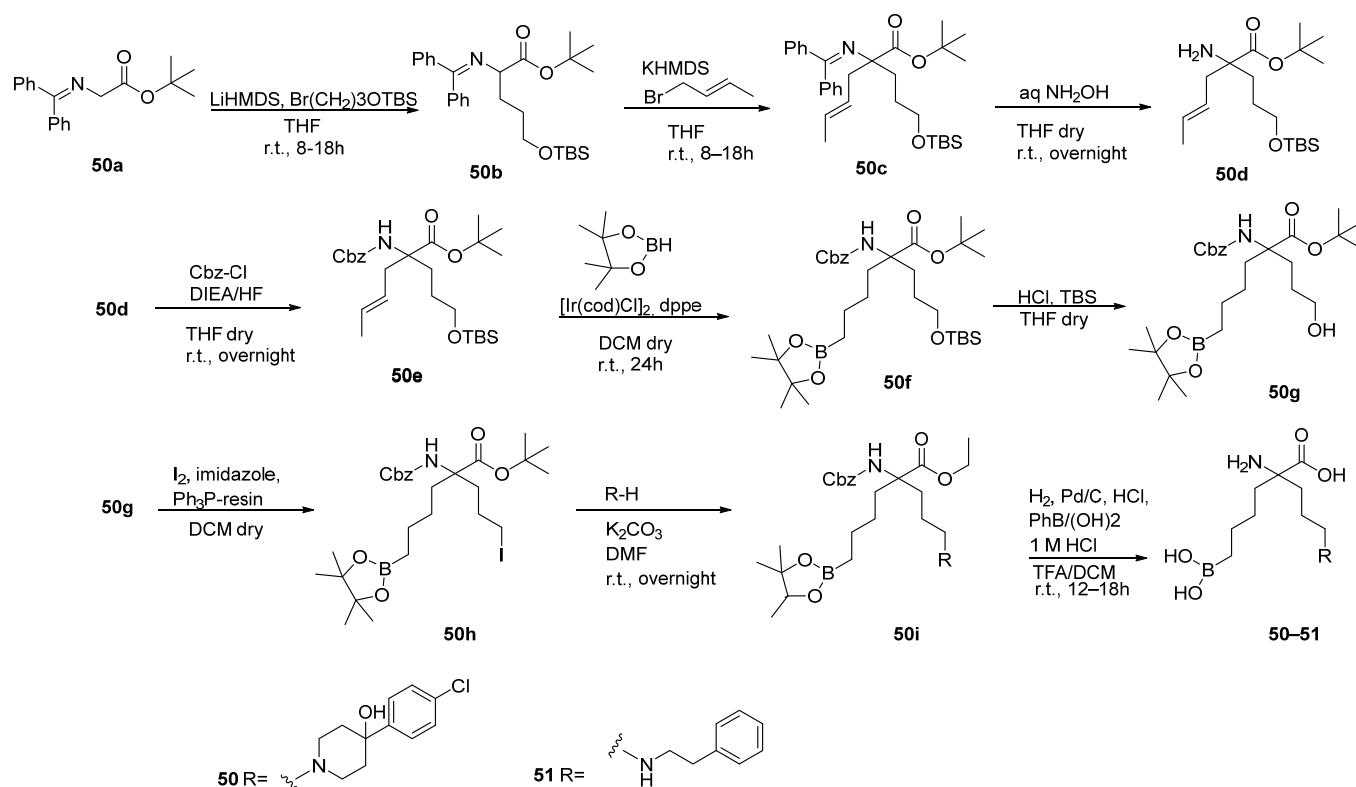


Scheme 13. Synthesis of compounds 47–49.

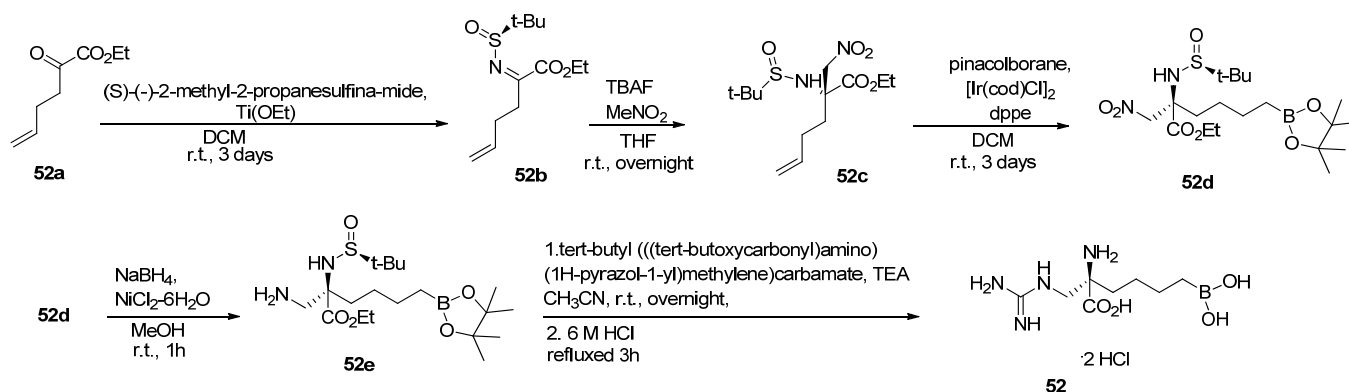
Their synthesis involved a nine-step protocol (Scheme 14) [56]. The initial steps consisted of sequential alkylations starting from tert-butyl-2-((diphenylmethylene)amino)acetate (**50a**) generating tert-butyl-5-(tert-butyldimethylsiloxy)-2-(diphenylmethylenamino)pentanoate (**50b**) and then tert-butyl-2-(3-tert-butyldimethylsiloxy)propyl-2-(diphenylmethylenamino)hex-4-enoate (**50c**). After amine deprotection with hydroxylamine hydrochloride, the amino group was re-protected with benzyl chloroformate to yield tert-butyl-2-(benzyloxycarbonylamino)-2-(3-(tert-butyldimethylsiloxy)propyl)hex-4-enoate (**50e**). The hydroboration of **50e** with pinacolborane in the presence of $[\text{Ir}(\text{cod})\text{Cl}]_2$ and dppe in dry DCM gave tert-butyl-2-(benzyloxycarbonylamino)-2-(3-(tert-butyldimethylsiloxy)propyl)-6-(4,4,5,5-tetramethyl-1,3,2-dioxaborolan-2-yl)hexanoate (**50f**), followed by the removal of the tert-butyldimethylsilyl (TBDMS) group under acid conditions to form **50g**. The alcohol group in **50g** was iodinated to produce tert-butyl-2-(benzyloxycarbonylamino)-2-(3-iodopropyl)-6-(4,4,5,5-tetramethyl-1,3,2-dioxaborolan-2-yl)hexanoate (**50h**). In the eighth step, N nucleophilic substitution was carried out using 4-(4-chlorophenyl)piperidin-4-ol hydrochloride (for compound **50**) or 2-phenylethanamine (for compound **51**), yielding tert-butyl-2-(benzyloxycarbonylamino)-2-(3-(3-phenylpiperidin-1-yl)propyl)-6-(4,4,5,5-tetramethyl-1,3,2-dioxaborolan-2-yl)hexanoate (**50i**). Finally, global deprotection using 1 M HCl, Pd/C, TFA and DCM under argon, followed by the addition of phenyl boronic acid, afforded final products **50–51**.

OncoArendi Therapeutics (now Molecule) has developed (R)-2-amino-6-borono-2-(guanidinomethyl)hexanoic acid (**52**), a compound featuring a methylguanidine side chain at the α position relative to the amino acid group. The pure (R)-enantiomer demonstrated potent ARG inhibition, with an IC_{50} of 32 nM against hARG-1. The synthesis protocol of this compound is shown in Scheme 15 and is patented. The starting compound was ethyl-2-oxohex-5-enoate (**52a**), which was treated with (S)-(-)-2-methyl-2-propanesulfonamide,

Ti(OEt)₄ in DCM to form imine (**52b**), which was reacted in turn with TBAF and MeNO₂ undergoing a nitro methylene addition on the α-carbon atom. The asymmetric, diastereoselective aza-Henry reaction led to the formation of the nitro amine ester (**52c**), which was subjected to hydroboration using pinacolborane, [Ir(cod)Cl]₂, dppe, DCM, and the subsequent reduction of the nitro group with NaBH₄ and NiCl₂·6H₂O in MeOH to obtain boronate (**52e**). The amine (**52e**) was then guanylated using *tert*-butyl(((*tert*-butoxycarbonyl)amino)(1H-pyrazol-1-yl)methylene) carbamate, TEA, and ACN and was deprotected with a solution of 6 M HCl to obtain the desired compound (**52**) [25,57].



Scheme 14. Synthesis of compounds 50–51.

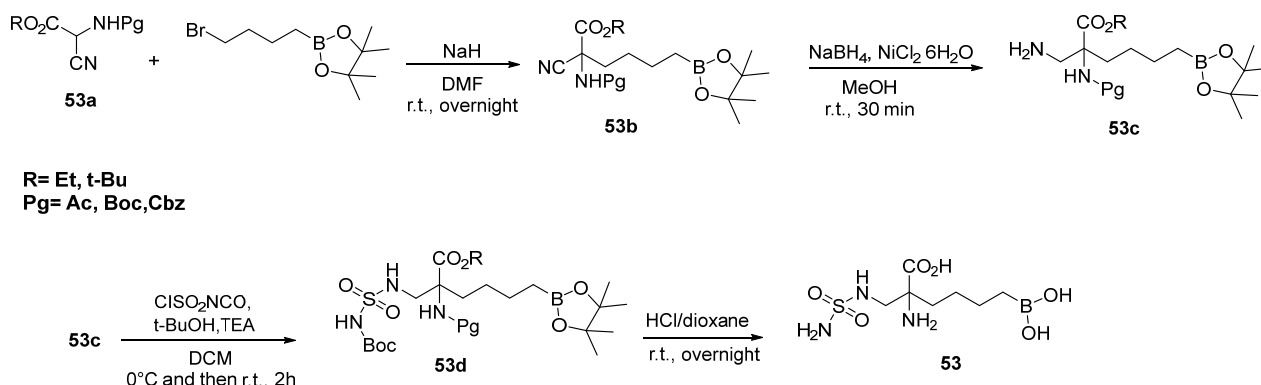


Scheme 15. Synthesis of compound 52.

3.2. Non-Basic Side Chain α-Substituted ABH Analogues

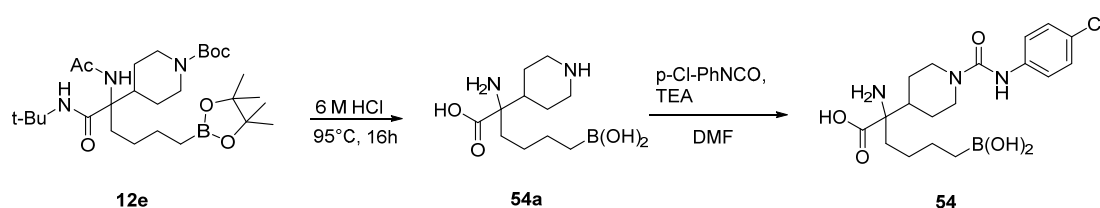
To this subclass belong sulphamide derivatives such as 2-amino-6-borono-2-((sulfamoylamino)methyl)hexanoic acid (**53**), which exhibited an inhibition activity against hARG-1 with an IC₅₀ of 330 nM [25]. The synthesis of **53** (see Scheme 16) consisted of an alkylation reaction of compound **53a** with pinacol-4-bromobutylboronate and sodium hydride (NaH)

in *N,N*-dimethylformamide (DMF) to obtain a quaternary boronic cyanoaminoester (**53b**), which was then reduced with sodium borohydride (NaBH_4) to form the intermediate **53c**. Compound **53c** was subsequently subjected to sulphamoylation with chlorosulfonyl isocyanate (ClSO_2NCO) in the presence of *tert*-butanol in TEA and DCM at 0°C . The final step involved acid hydrolysis with HCl /dioxane, yielding the desired boronic acid (**53**).



Scheme 16. Synthesis of compound **53**.

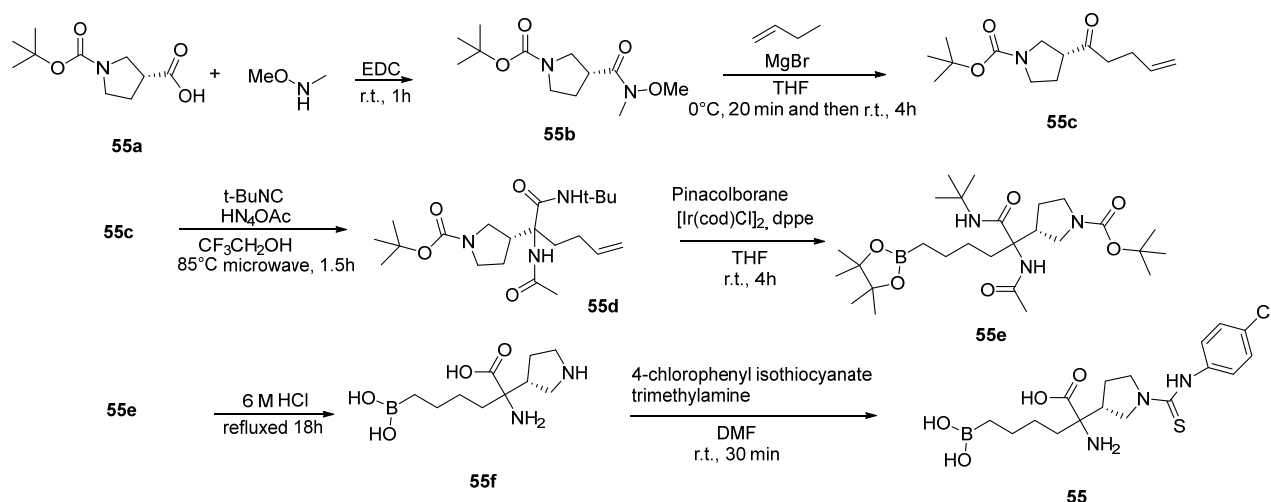
Other compounds designed as ARG inhibitors with a non-basic side chain included derivatives **54–55**, which contained urea and thiourea moieties, respectively. Both **54** (2-amino-6-borono-2-(1-((4-chlorophenyl)carbamoyl)piperidin-4-yl)hexanoic acid) and **55** (2-amino-6-borono-2-(1-((4-chlorophenyl)carbamothioyl)pyrrolidin-3-yl)hexanoic acid) were capable of inhibiting hARG-1 and -2 in the range of 251 to 1000 nM. Despite their similar activities, the synthesis pathways for these compounds differed [22,51]. For compound **54** (Scheme 17), the first four-steps of its synthesis were identical to those for compound **12**, as shown in Scheme 8. Starting from intermediate **12e**, the fifth step involved an acid deprotection reaction using 6 M HCl solution at 95°C for 16 h, giving intermediate **54a**. This intermediate was then selectively carbamylated at the piperidine nitrogen using 4-chlorophenyl isocyanate (*p*-Cl-PhNCO) in the presence of TEA and DMF, producing the target compound **54** [26].



Scheme 17. Synthesis of compound **54**.

For the synthesis of compound **55**, as shown in Scheme 18, Van Zandt et al. used **55a** as the starting material [51]. This compound underwent a coupling reaction with *N,O*-dimethylhydroxylamine hydrochloride and EDC, yielding intermediate **55b**, which in turn was then subjected to a substitution with 3-butenylmagnesium bromide in THF producing compound **55c**. Next, an Ugi reaction was performed with NH_4OAc and *tert*-butyl isocyanide in 2,2,2-trifluoroethanol, generating derivative **55d**. This was followed by a hydroboration reaction using pinacolborane, $[\text{Ir}(\text{cod})\text{Cl}]_2$ and *dppe* to give *tert*-butyl-(3*R*)-3-[1-acetamido-1-(*tert*-butyl-carbamoyl)-5-(4,4,5,5-tetramethyl-1,3,2-dioxaborolan-2-yl)pentyl]pyrrolidine-1-carboxylate (**55e**). In the fifth step, a solution of 6 M HCl in 1,4-dioxane was added to **55e**, yielding intermediate **55f**, which was then treated with 4-chlorophenyl-isothiocyanate in TEA and DMF to obtain the desired compound

55. In addition to the inhibitors mentioned, several other compounds featuring different substituents in their side chains were synthesized, through their activities were found to be comparatively lower [58].



Scheme 18. Synthesis of compound 55.

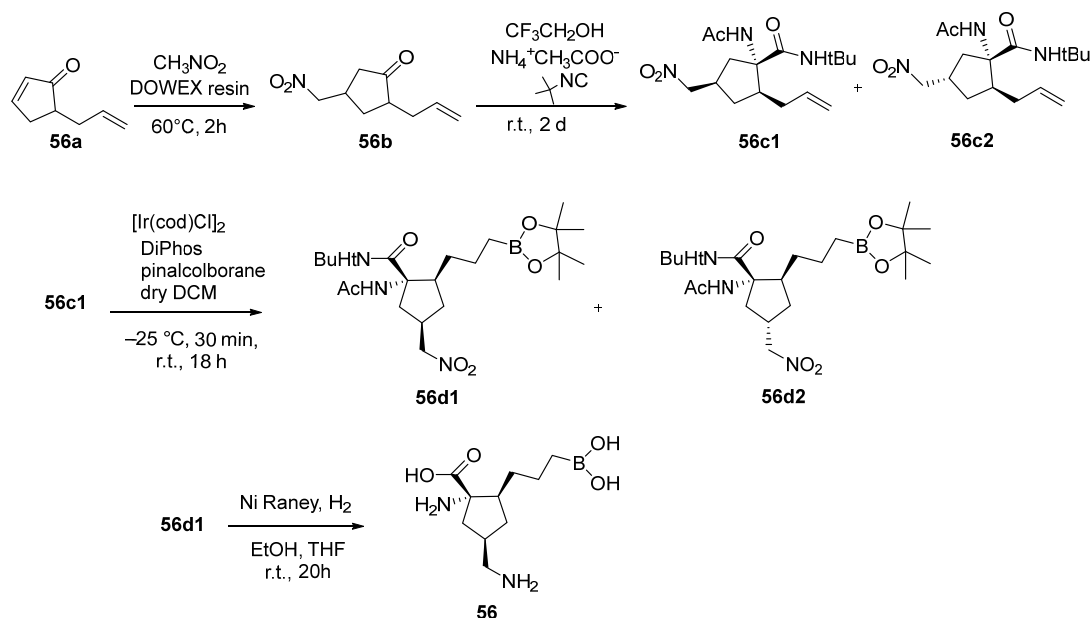
Comparing the two subclasses of second-generation ARG inhibitors, it was observed that the presence of a basic side chain in the α -substituted ABH derivatives led to a notable improvement not only in activity but also in selectivity against both ARG-1 and ARG-2, compared to their non-basic counterparts. This enhancement was attributed to the formation of an additional hydrogen bond, mediated by a water molecule, between the basic centre in the side chain of the ARG inhibitor and an aspartate residue in the pocket of both ARG-1 and ARG-2—a feature absent in non-basic side chain α -substituted ABH analogues. However, despite the improved selectivity and activity, the presence of a basic side chain did not result in significant improvements in bioavailability compared to non-basic analogues, and the pharmacokinetic profile still required optimization.

4. Third-Generation Inhibitors

The third generation of inhibitors features ring-constrained cyclic ABH analogues, including compounds based on modified cyclopentyl and pyrrolidine structures. These compounds have an alkyl linker with a boronic acid group inserted at ring position 2. One example is (1*S*,2*S*,4*R*)-1-amino-4-(aminomethyl)-2-(3-boronopropyl)cyclopentanecarboxylic acid (**56**), which showed an IC_{50} of 0.1–0.250 nM for both hARG-1 and hARG-2 in a colorimetric assay. While the cited patent describes many analogues of **56**, the lack of its further development is likely due to its unsatisfactory pharmacokinetic properties. These issues could potentially be addressed through strategies such as the prodrug approach or the design of nanodelivery systems, which, as demonstrated in thousands of studies, have been shown to overcome various pharmacokinetic and related limitations. Compound **56** was synthesized by Van Zandt et al. according to the Scheme 19 [59].

The synthesis began with commercially available 5-(propene-3-yl)cyclopent-2-enone (**56a**), which was treated in nitromethane with the DOWEX[®] 550A-OH resin at 60 °C to obtain the nitroderivative (**56b**). This was then dissolved in 2,2,2-trifluoroethanol and reacted with NH_4OAc and tert-butylisocyanide under N_2 for 2 days, affording two isomers, **56c1** and **56c2**, with acetamido and allyl substituents in the syn-relative position. Isomer **56c1** was stirred in DCM and treated with pinacolborane, $[Ir(cod)Cl]_2$ and Diphos[®] at −25 °C, yielding **56d** (isomers **56d1** and **56d2**). For the final step, a solution of (1*S*,2*S*,4*R*)-1-acetamido-N-tert-butyl-4-(nitromethyl)-2-(3-(4,4,5,5-tetramethyl-1,3,2-dioxaborolan-2-

yl)propyl)cyclopentanecarboxamide (isomer **56d1**) in ethanol and THF under N₂ was treated with Raney nickel. The mixture was purged with H₂ and stirred for 20 h. After purging with nitrogen, the mixture was filtered through Celite[®], and the filtrate concentrated under reduced pressure. The crude product was dissolved in HCl/acetic acid/H₂O in a pressure bottle and stirred for 2 h at 60 °C, then capped and heated for 18 h at 130 °C. After cooling to r.t. and uncapping, the desired compound **56** was obtained after chromatography purification as a white foam.



Scheme 19. Synthesis of compound **56**.

A wide range of pyrrolidine-derived compounds has been developed through further optimization. The ring-constrained pyrrolidines help reduce entropy by positioning the quaternary amino acid moiety in an optimal orientation for binding. Notably, the presence of a cyclopentane derivative forces the amino group and boronic acid side chain into an anti orientation, preventing van der Waals interactions with active site residues. Furthermore, the atoms within the ring act as scaffolds for incorporating additional substituents that can form hydrogen bonds with the aspartate residues in the ARG-1 and ARG-2 pockets. These structural features collectively contribute to the enhanced potency of these compounds. The most effective compound in this series was **NED-3228** (**57**, Figure 4), which showed IC₅₀ values for hARG-1 and hARG-2 of 1.3 and 8.1 nM, respectively. Another notable compound, **58** (see Figure 4), features an N-(piperidin-2-yl-methyl) substituent in place of the N-(2-amino-3-phenylpropyl) group in **57**. This compound exhibited IC₅₀ values for hARG-1 and hARG-2 of 2.6 and 14 nM, respectively.

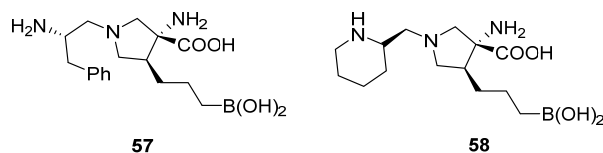
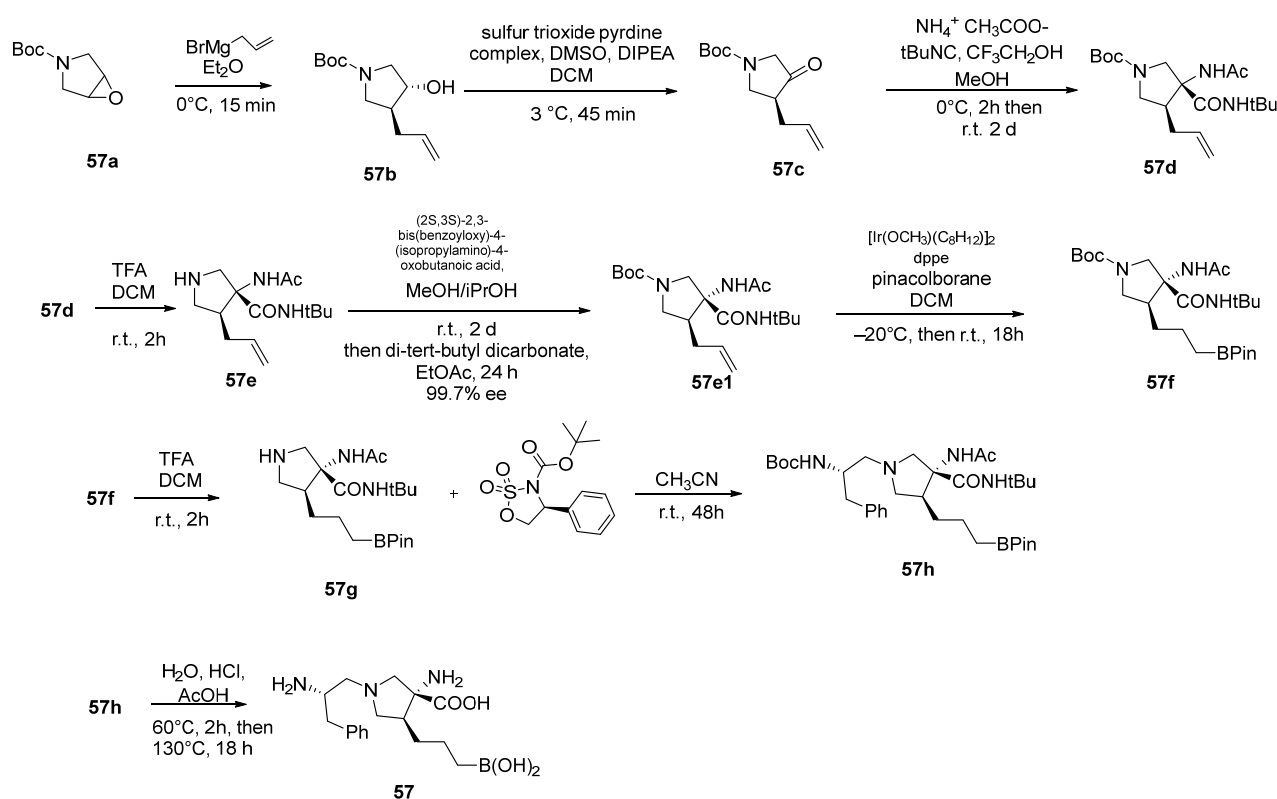


Figure 4. Chemical structures of compounds **57–58**.

Compound **57** was synthesized by Van Zandt et al. through a nine-step process, as outlined in Scheme 20 [60]. The synthesis began by reacting a solution of tert-butyl-6-oxa-3-azabicyclo[3.1.0]hexane-3-carboxylate (**57a**) in dry Et₂O with allyl magnesium

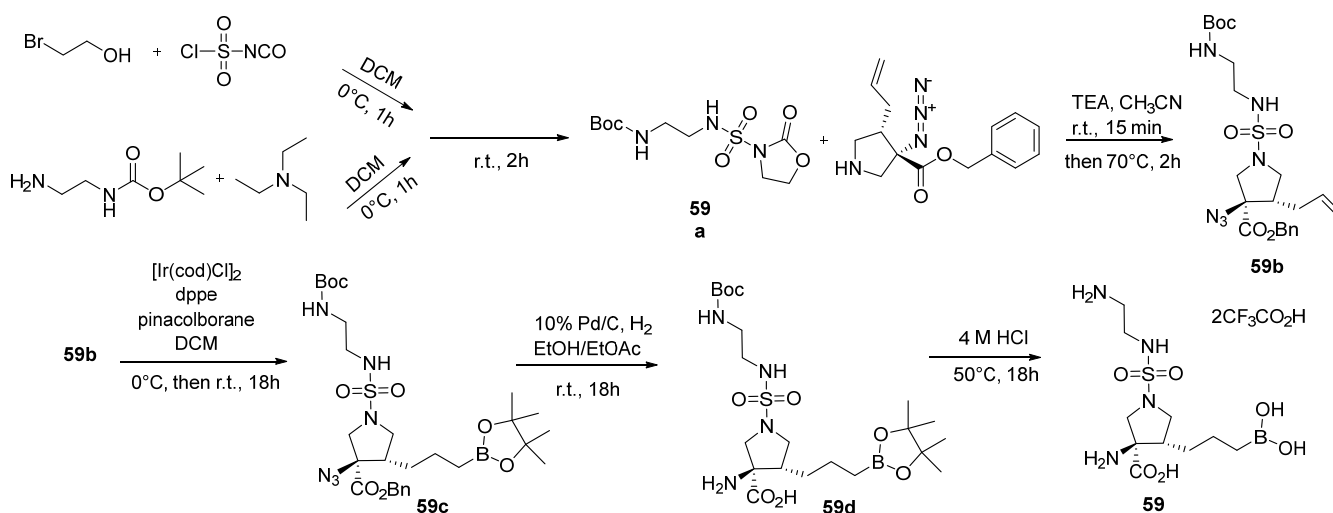
bromide at 0 °C. After stirring for 15 min, the reaction produced tert-butyl-trans-3-allyl-4-hydroxypyrrolidine-1-carboxylate (**57b**). This was then treated with sulphur trioxide pyridine complex in DMSO under nitrogen, yielding ketone intermediate **57c**. Compound **57c** was reacted with tert-butyliocyanide and ammonium acetate, resulting in a mixture of anti- and syn-isomers of **57d**. Next, the BOC group was removed using DCM and TFA giving racemic **57e**. To obtain the pure enantiomer **57e1**, racemic **57e** was treated with (2S,3S)-2,3-bis(benzoyloxy)-4-(isopropylamino)-4-oxobutanoic acid in warm MeOH/i-PrOH. After cooling, the desired salt crystallized out, and the crystals were filtered, washed, and dried to give **57e1** with 99.7% ee. In the following step, **57e1** was reacted with pinacolborane in the presence of [Ir(cod)Cl]₂ and dppe in DCM to afford **57f** as a white solid. A BOC deprotection with an excess of TFA in dry DCM under N₂ yielded **57g**. This was then reacted with tert-butyl-(S)-4-phenyl-1,2,3-oxathiazolidine-3-carboxylate 2,2-dioxide in ACN at r.t. for 2 days, producing **57h**, which was used directly without further purification. Finally, **57h** was deprotected in glacial acetic acid, water, and concentrated hydrochloric acid in a pressure bottle. After stirring at 60 °C for 2 h, the mixture was capped and heated to 130 °C for 18 h to yield NED-3228 (compound **57**) as a white solid.



Scheme 20. Synthesis of compound **57**.

Compound (3R,4S)-3-amino-1-(N-(2-aminoethyl)sulfamoyl)-4-(3-boronopropyl)pyrrolidine-3-carboxylic acid (**59**) also demonstrated strong activity against hARG-1 and hARG-2, with IC₅₀ values ranging from 0.1 to 100 nM for both enzymes. Compound **59** was synthesized by Wan et al. in 2018, following the procedure outlined in Scheme 21 [61]. The synthesis began with the reaction between sulfurisocyanatidic chloride and 2-bromoethan-1-ol in DCM, followed by the addition of tert-butyl-(2-aminoethyl)carbamate and TEA in DCM. The intermediate (tert-butyl (2-((2-oxooxazolidine)-3-sulfonamido)ethyl)carbamate) **59a** was reacted with a solution of (rac)benzyl trans-4-allyl-3-azidopyrrolidine-3-carboxylate in ACN and TEA, resulting in **59b** ((rac)(benzyl trans-(4-allyl-3-azido-1-(N-(2-((tert-butoxycarbonyl)amino)ethyl)sulfamoyl)pyrrolidine-3-carboxylate)). Next, **59b** was hydrob-

orated with pinacolborane, $[\text{Ir}(\text{cod})\text{Cl}]_2$ and dppe in DCM producing **59c** ((rac)(benzyl trans-3-azido-1-(N-(2-((tert-butoxycarbonyl)amino)ethyl)sulfamoyl)-4-(3-(4,4,5,5-tetramethyl-1,3,2-dioxaborolan-2-yl)propyl)pyrrolidine-3-carboxylate)). Compound **59c** was catalytically hydrogenated in a mixture of EtOAc/EtOH giving rise to **59d** ((rac)-trans-3-amino-1-(N-(2-((tert-butoxycarbonyl)amino)ethyl)sulfamoyl)-4-(3-(4,4,5,5-tetramethyl-1,3,2-dioxaborolan-2-yl)propyl)pyrrolidine-3-carboxylic acid). Finally, **59d** was deprotected in HCl at 50° C. This reaction yielded the desired compound, (rac)-3-amino-1-(N-(2-aminoethyl)sulfamoyl)-4-(3-boronopropyl)pyrrolidine-3-carboxylic acid (**59**) that was purified by HPLC and isolated as a 1:2 trifluoroacetic acid salt.

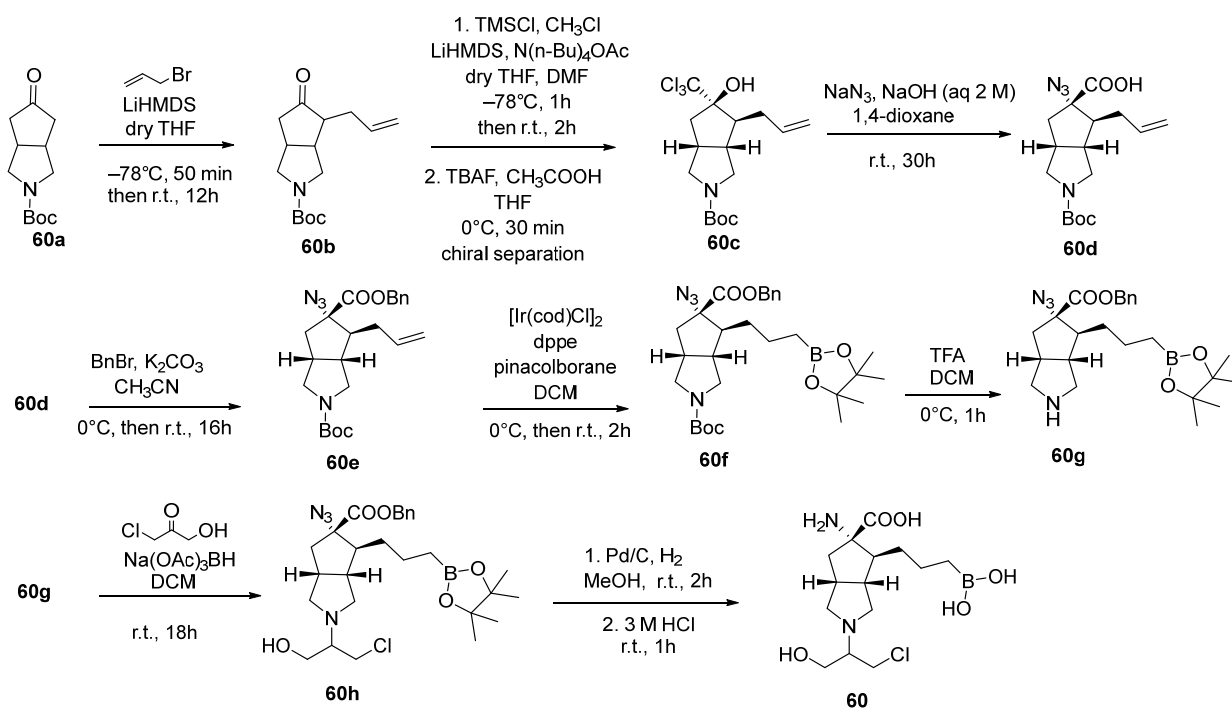


Scheme 21. Synthesis of compound **59**.

The bicyclic inhibitors (3aR,4S,5S,6aR)-5-amino-4-(3-boronopropyl)-2-(1-chloro-3-hydroxypropan-2-yl)octahydrocyclopenta[c]pyrrole-5-carboxylic acid (**60**), (1S,2S,3aR,4S,5S,6aS)-2-amino-1-(3-boronopropyl)-4-fluoro-5-(methylamino)octahydropentalene-2-carboxylic acid (**61**), and (5S,7S,8S)-7-amino-8-(3-boronopropyl)-1-azaspiro[4.4]nonane-7-carboxylic acid (**62**) represent a distinct class of inhibitors, independently developed by Merck Sharp & Dohme Corp. and Arcus Biosciences Inc. These compounds are derivatives of octahydrocyclopenta[c]pyrrole with various nitrogen atom substituents. Foley et al. synthesized a range of bicyclic boronic acid derivatives, with compound **60** proving to be the most promising, showing an $\text{IC}_{50} < 100$ nm against hARG-1. Compound **61** demonstrated an IC_{50} of 6.9 nM against hARG-1 performed by Thioornithine Generating Assay (TOGA). The general synthesis scheme for compound **60** is shown in Scheme 22 [62].

In the first step, tert-butyl-5-oxohexahydrocyclopenta[c]pyrrole-2(1H)-carboxylate (**60a**) was alkylated under the action of allyl bromide and LiHMDS in THF. This produced the allylated compound tert-butyl 4-allyl-5-oxohexahydrocyclopenta[c]pyrrole-2(1H)-carboxylate (**60b**). Subsequently, a reaction of ketone **60b** with CHCl_3 and chlorotrimethylsilane in strongly basic conditions, followed by the deprotection of trimethylsilyl group under the action of acetic acid and tetrabutylammonium fluoride in THF gave rise to the racemic trichloromethyl derivative **60c**. Chiral column chromatography was used to isolate the desired enantiomer. The treatment of **60c** with NaN_3 and NaOH produced the crude carboxylic acid **60d** ((3aR,4S,5S,6aR)-4-allyl-5-azido-2-(tert-butoxycarbonyl)octahydrocyclopenta[c]pyrrole-5-carboxylic acid). The carboxylic group was protected as benzylic ester using benzyl bromide and K_2CO_3 in dry ACN. Next, **60e** was subjected to a hydroboration reaction with $[\text{Ir}(\text{cod})\text{Cl}]_2$, dppe, and pinacolborane in DCM. After purification, the product 5-benzyl 2-(tert-butyl) (3aR,4S,5S,6aR)-5-azido-4-(3-(4,4,5,5-tetramethyl-1,3,2-dioxaborolan-2-yl)propyl)hexahydrocyclopenta[c]pyrrole-2,5(1H)-dicar-

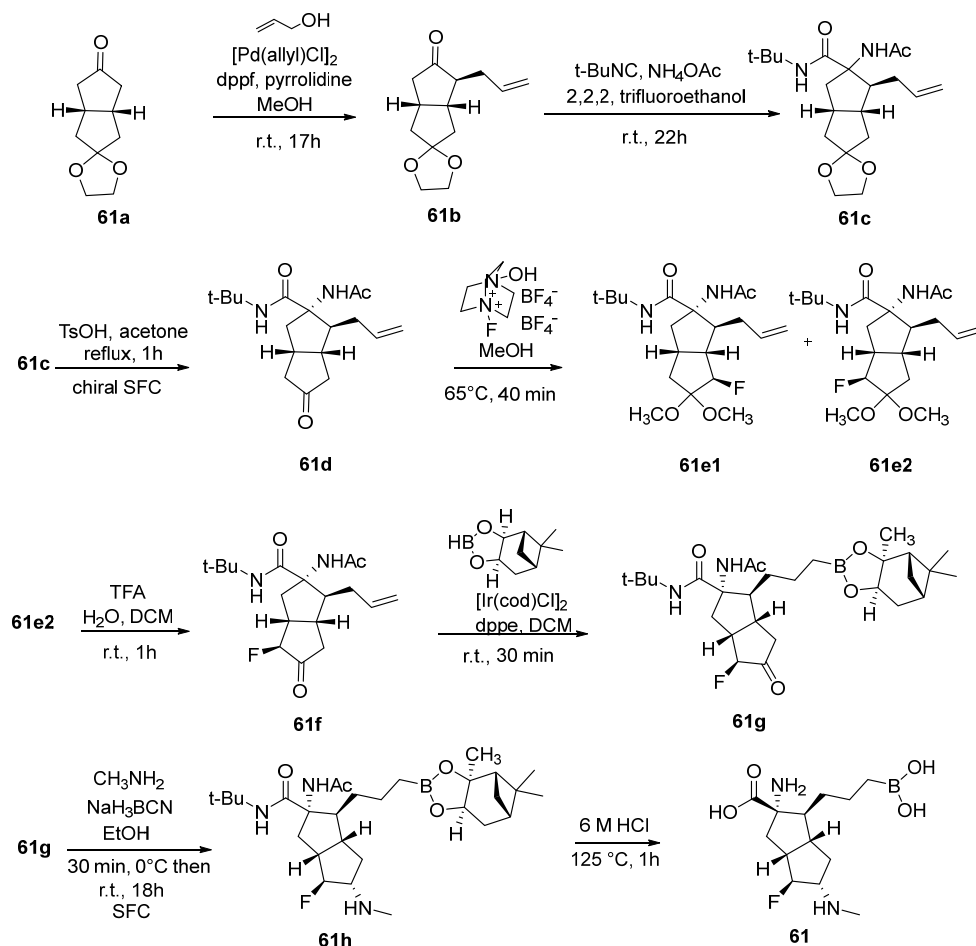
boxylate (**60f**) was obtained. The BOC group was removed by treating **60f** with DCM and TFA, giving the free amine (**60g**) in a 99% yield. Amine (**60g**) in DCM was reacted with 1-chloro-3-hydroxy acetone and $\text{Na}(\text{OAc})_3\text{BH}$, yielding benzyl (3aR,4S,5S,6aR)-5-azido-2-(1-chloro-3-hydroxypropan-2-yl)-4-(3-(4,4,5,5-tetramethyl-1,3,2-dioxaborolan-2-yl)propyl) octahydrocyclopenta[c]pyrrole-5-carboxylate (**60h**), which was used without purification. Finally, **60** was obtained by the hydrogenation of **60h** with 10% Pd/C in MeOH and deprotection with 3M HCl at r.t. for 1 h. Purification by reverse phase C_{18} chromatography yielded the target compound **60** as a white solid.



Scheme 22. Synthesis of compound **60**.

The synthesis of **61** (Scheme 23) began by the introduction of allyl group into the 4-position of (3aR,6aS)-tetrahydro-1H-spiro[pentalene-2,2'-[1,3]dioxolan]-5(3H)-one (**61a**) under the action of allyl alcohol, 1,1'-ferrocenediyl-bis(diphenylphosphine) (dppf), and allylpalladium(II) chloride dimer in MeOH, producing **61b**. To obtain **61c**, an Ugi reaction with (3aR,4S,6aS)-4-allyltetrahydro-1H-spiro[pentalene-2,2'-[1,3]dioxolan]-5(3H)-one (**61b**), NH_4OAc , and tert-butyl isocyanide in 2,2,2-trifluoroethanol was performed. (3aR,4S,6aS)-5-acetamido-4-allyl-N-(tert-butyl)hexahydro-1H-spiro[pentalene-2,2'-[1,3]dioxolane]-5-carboxamide (**61c**) was used without further purification. The deprotection of the dioxolan moiety with p-toluenesulfonic acid in acetone yielded a racemic mixture of epimers (~1:1) resolved using chiral supercritical-fluid chromatography (SFC) to isolate **61d**. For the next step, (1S,2S,3aS,6aR)-2-acetamido-1-allyl-N-(tert-butyl)-5-oxooctahydropentalene-2-carboxamide (**61d**), was reacted with 1-fluoro-4-hydroxy-1,4-diazoniabicyclo[2,2,2]octane bis(tetrafluoroborate) in MeOH at 65 °C for 40 min. This reaction gave two products: (1S,2S,3aS,6R,6aR)-2-acetamido-1-allyl-N-(tert-butyl)-6-fluoro-5,5-dimethoxyoctahydropentalene-2-carboxamide (**61e1**) and (1S,2S,3aR,4S,6aS)-2-acetamido-1-allyl-N-(tert-butyl)-4-fluoro-5,5-dimethoxyoctahydropentalene-2-carboxamide (**61e2**). Treating **61e2** with H_2O and TFA in DCM at 23 °C and stirring for 1 h provided 1S,2S,3aS,6R,6aR)-2-acetamido-1-allyl-N-(tert-butyl)-6-fluoro-5-oxooctahydropentalene-2-carboxamide (**61f**) as a white solid. The hydroboration of **61f** was performed by adding it in DCM to a solution of (+)-pinanediolborane, $[\text{Ir}(\text{cod})\text{Cl}]_2$, and dppe under N_2 at 23 °C. Stir-

ring for 20 min yielded crude (1S,2S,3aS,6R,6aR)-2-acetamido-N-(tert-butyl)-6-fluoro-5-oxo-1-(3-((3aS,4S,6S,7aR)-3a,5,5-trimethylhexahydro-4,6-methanobenzo[d][1,3,2]dioxaborol-2-yl)propyl)octahydropentalene-2-carboxamide (**61g**), used in the next step without further purification. The reaction of **61g** with methylamine in absolute EtOH at 0 °C, followed by sodium cyanoborohydride, produced **61h**. Finally, the deprotection of **61h** using 6 M HCl provided the final product **61** as a white solid [63].

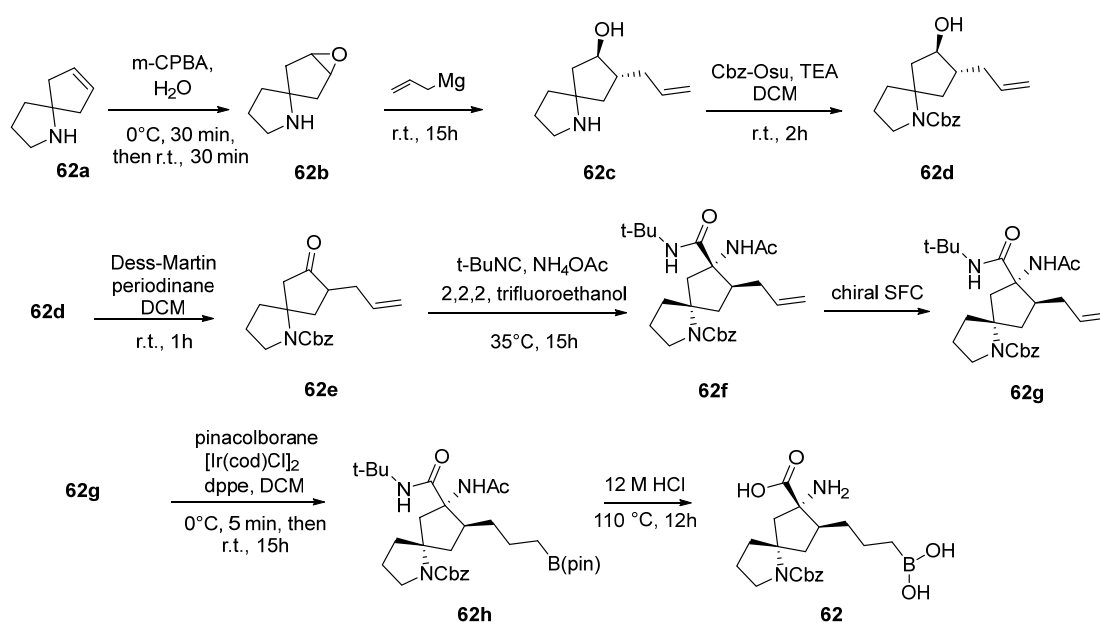


Scheme 23. Synthesis of compound **61**.

Bicyclic systems, like **62**, demonstrated strong activity against both hARG-1 and hARG-2. Compound **62** inhibited hARG-1 with an IC_{50} of 2.1 nM. However, comparing its activity to other compounds is challenging because Merck utilized the (TOGA), while other groups used a colorimetric assay based on ARG-induced urea production.

The synthesis of **62** (Scheme 24), as reported by Mitcheltree et al., started with the oxidation of 1-azaspiro[4.4]non-7-ene (**62a**) to produce crude **62b**, which was used without purification. Reacting 6-oxaspiro[bicyclo[3.1.0]hexane-3,2'-pyrrolidine (**62b**) with allylmagnesium bromide in Et_2O at 0 °C under N_2 gas for 15 h yielded (7R,8R)-8-allyl-1-azaspiro[4.4]nonan-7-ol (**62c**) as a pale-yellow oil. This intermediate was also used directly. Next, TEA and benzyl (2,5-dioxopyrrolidin-1-yl) carbonate (Cbz-OSu) were added to **62c** in DCM, stirred for 2 h at r.t. and yielded (7R,8R)-7-allyl-8-hydroxy-1-azaspiro[4.4]nonane-1-carboxylate (**62d**) as a colourless oil. Oxidizing **62d** with Dess–Martin periodinane provided benzyl 7-allyl-8-oxo-1-azaspiro[4.4]nonane-1-carboxylate (**62e**), also a colourless oil. The subsequent reaction of **62e** with NH_4OAc and tert-butyl isocyanide in 2,2,2-trifluoroethanol at 35 °C for 15 h produced benzyl (5S,7S,8S)-7-acetamido-8-allyl-7-(tert-butylcarbonyl)-1-azaspiro[4.4]nonane-1-carboxylate (**62f**), a racemic mixture.

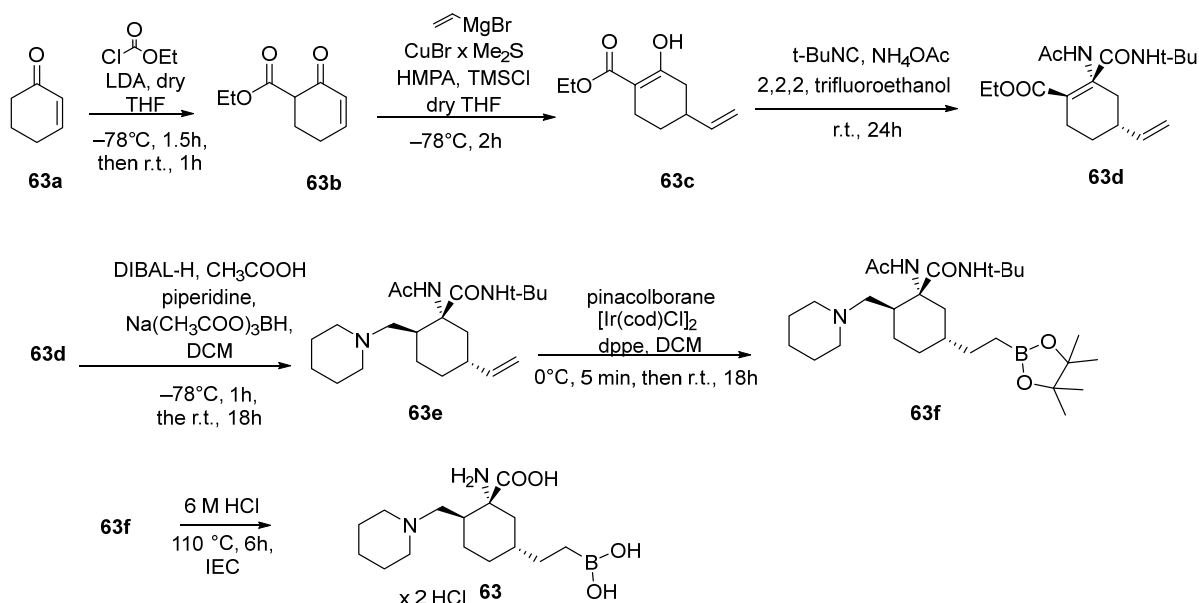
Chiral separation using SFC gave the enantiomer (5*S*,7*S*,8*S*)-7-acetamido-8-allyl-7-(tert-butylcarbamoyl)-1-azaspiro[4.4]nonane-1-carboxylate (**62g**) as a viscous oil. For further modification, **62g** was reacted with dppe, [Ir(cod)Cl]₂, and pinacolborane in DCM under inert conditions, yielding (5*S*,7*S*,8*S*)-7-acetamido-7-(tert-butylcarbamoyl)-8-(3-(4,4,5,5-tetramethyl-1,3,2-dioxaborolan-2-yl)propyl)-1-azaspiro[4.4]nonane-1-carboxylate (**62h**) as a viscous semisolid. Finally, the deprotection of **62h** in 12 M HCl at 110 °C for 12 h produced the target compound (5*S*,7*S*,8*S*)-7-amino-8-(3-boronopropyl)-1-azaspiro[4.4]nonane-7-carboxylic acid (**62**) as a viscous oil [63].



Scheme 24. Synthesis of compound **62**.

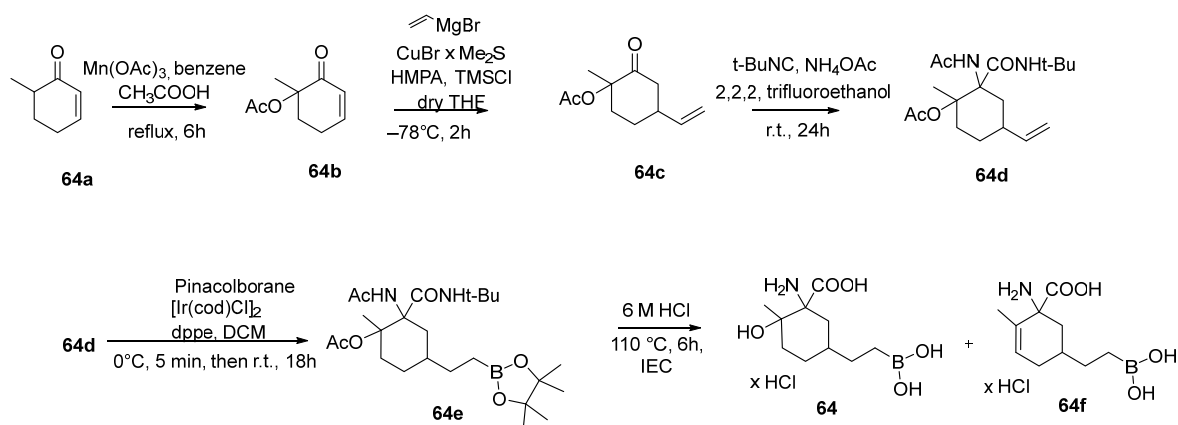
Highly effective inhibitors of ARG activity include 2-substituted alkylamines, such as the compound (1*R*,2*S*,5*R*)-1-acetamido-5-(2-boronoethyl)-2-(piperidin-1-ylmethyl)cyclohexanecarboxylic acid (**63**). This compound exhibited potent inhibitory activity, with IC₅₀ values for hARG-1 and hARG-2, ranging from 1 to 100 nM and 100 to 1000 nM, respectively. In cellular assays, compound **63** demonstrated notable activity with an IC₅₀ of up to 100 nM. Other derivatives, like compound **64** (featuring a hydroxy group at position 2), were less potent than the piperidine analogue **63**. Compound **64** showed intracellular activity between 10 and 100 µM and IC₅₀ < 1000 nM for both ARGs.

The synthesis of **63** is outlined in Scheme 25 and began with the preparation of ethyl 2-oxocyclohex-3-enecarboxylate (**63b**) via the acylation of 2-cyclohexen-1-one (**63a**) with ethyl chloroformate under strongly basic conditions (LDA in THF). Next, ethyl 2-hydroxy-4-vinylcyclohex-1-ene-1-carboxylate (**63c**) was synthesized by reacting **63b** with vinylmagnesium bromide and CuBr × Me₂S in the presence of TMSCl under argon at −78 °C. The treatment of **63c** with NH₄OAc and tert-butyl isocyanide in 2,2,2-trifluoroethanol produced **63d** in a 56% yield. The subsequent reduction of ethyl rac-(1*R*,2*R*,4*R*)-2-acetamido-2-(tert-butylcarbamoyl)-4-vinylcyclohexane-1-carboxylate (**63d**) with diisobutylaluminium hydride (DIBAL-H) at −78 °C, followed by treatment with piperidine and sodium triacetoxyborohydride produced rac-(1*R*,2*S*,5*R*)-1-acetamido-N-tert-butyl-2-(piperidin-1-ylmethyl)-5-vinylcyclohexanecarboxamide (**63e**) as a single diastereoisomer. The boronation of **63e** using pinacolborane, dppe, and [Ir(cod)Cl]₂ in DCM at r.t. formed (1*R*,2*S*,5*R*)-1-acetamido-N-(tert-butyl)-2-(piperidin-1-ylmethyl)-5-(2-(4,4,5,5-tetramethyl-1,3,2-dioxaborolan-2-yl)ethyl)cyclohexanecarboxamide (**63f**). Finally, refluxing **63f** with 6 M HCl for 6 h produced compound **63** as a white solid [64].



Scheme 25. Synthesis of compound 63.

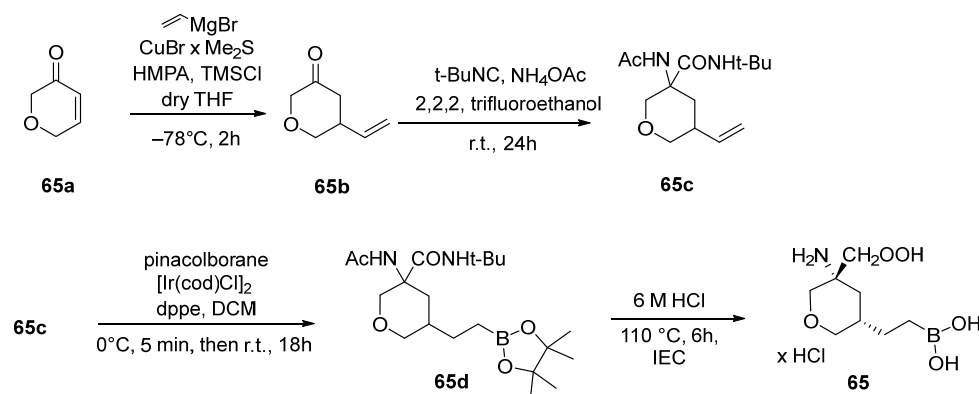
Compound **64** was synthesized similarly to **63**, as shown in Scheme 26. Refluxing a mixture of 6-methyl-2-cyclohexenone (**64a**)⁷ benzene, acetic acid, and manganese(III) acetate dihydrate for 6 h produced **64b**. Subsequently, 1-methyl-2-oxo-4-vinylcyclohexyl acetate (**64c**) was synthesized via the 1,4-addition of vinylmagnesium bromide, catalysed by CuBr x Me₂S in THF. Next, the Ugi reaction of **64c** with NH₄OAc and tert-butyl isocyanide in 2,2,2 trifluoroethanol produced 2-acetamido-2-(tert-butylcarbamoyl)-1-methyl-4-vinylcyclohexyl acetate (**64d**). The hydroboration of **64d** using pinacolborane, dppe, and [Ir(cod)Cl]₂ in DCM at r.t. gave **64e** as a single diastereoisomer. Finally, refluxing **64e** with 6M HCl yielded 1-amino-5-(2-boronoethyl)-2-hydroxy-2-methylcyclohexanecarboxylic acid hydrochloride (**64**) as a single diastereoisomer (white solid). A by-product of **64f** was also obtained as a single diastereoisomer [65].



Scheme 26. Synthesis of compound 64.

Compound **65** was synthesized similarly to compound **64**, but with a different starting material, as illustrated in Scheme 27. The process is not described in detail. After purification via flash chromatography on DOWEX[®] ion exchange resin, the target product, rac-(3R,5R)-3-amino-5-(2-boronoethyl)tetrahydro-2H-pyran-3-carboxylic acid hydrochloride (**65**), was obtained as a single diastereoisomer in a 56% yield (white solid). Com-

pound **65** demonstrated activity against both hARG-1 (IC_{50} = 100–1000 nM) and hARG-2 (IC_{50} = 1–10 mM).



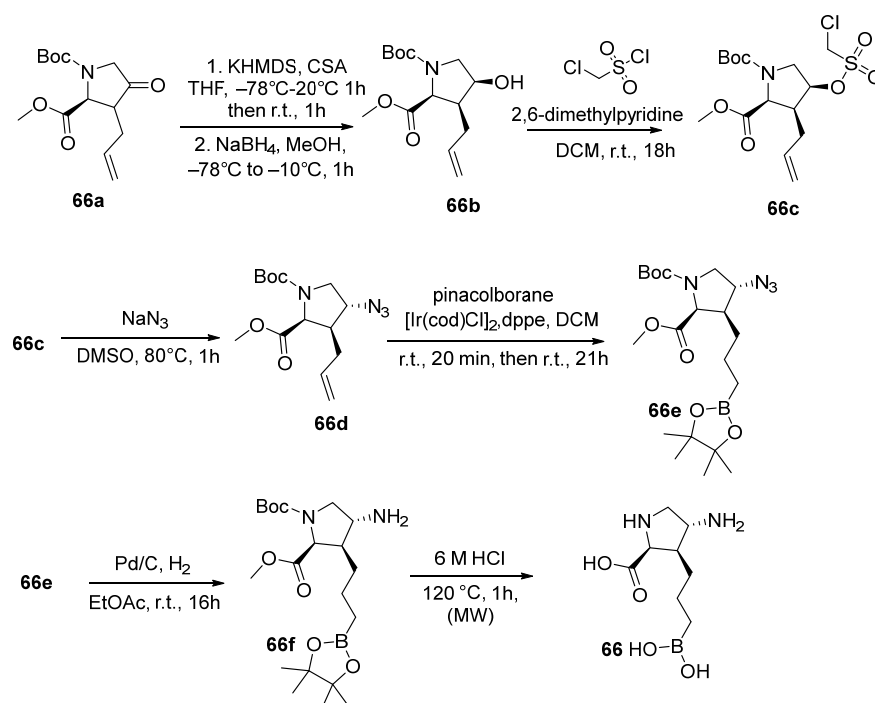
Scheme 27. Synthesis of compound **65**.

A novel class of ARG inhibitors with a proline scaffold was developed by Sichuan Kelun-Biotech Biopharmaceutical, AstraZeneca, and Merck Sharp & Dohme. These inhibitors include proline derivatives with a boronic acid group either in position 1 (alongside a carboxyl group) or at position 2 (as in Merck's compounds). Merck introduced compounds with various substitutions, such as hydroxyl, alkyl, piperidine, pyrrolidine, and aliphatic amino groups. Among these, a standout was the compound (2S,3R,4R)-4-amino-3-(3-boronopropyl)pyrrolidine-2-carboxylic acid (**66**), which had an amino group at position 4. This compound demonstrated significant inhibitory activity with an IC_{50} of 3.2 nM (TOGA) for hARG-1. Another notable compound, (2S,3S,4R)-3-(3-boronopropyl)-4-hydroxypyrrolidine-2-carboxylic acid (**67**), featured a hydroxyl group at position 4, arranged trans to carboxylic acid and the propylboronic acid linker. Its activity against hARG-1 was slightly lower, with an IC_{50} of 6 nM. An azetidine-based derivative, (2S,3S)-3-(aminomethyl)-3-(3-boronopropyl)azetidine-2-carboxylic acid (**68**), was the most effective homolog, showing an IC_{50} of 8 nM for hARG-1. AstraZeneca and Kelun also contributed to this class of inhibitors. AstraZeneca reported derivatives like (2R,4R)-4-amino-2-(4-boronobutyl)pyrrolidine-2-carboxylic acid (**69**), which showed IC_{50} values of 10 nM for hARG-1 and 20 nM for hARG-2. Its methyl analogue, (2R,4R)-2-(4-boronobutyl)-4-(methylamino)pyrrolidine-2-carboxylic acid (**70**), displayed even greater potency, with IC_{50} values of 3 nM for hARG-1 and 10 nM for hARG-2. Kelun's derivatives included proline analogues substituted with hydroxyl or amino groups. Among these, compound **69** showed moderate activity in a standard assay, with an IC_{50} activity of 4.3 μ M for hARG-1. The synthesis of compounds **66**–**70** follows detailed procedures outlined in Schemes 28–32.

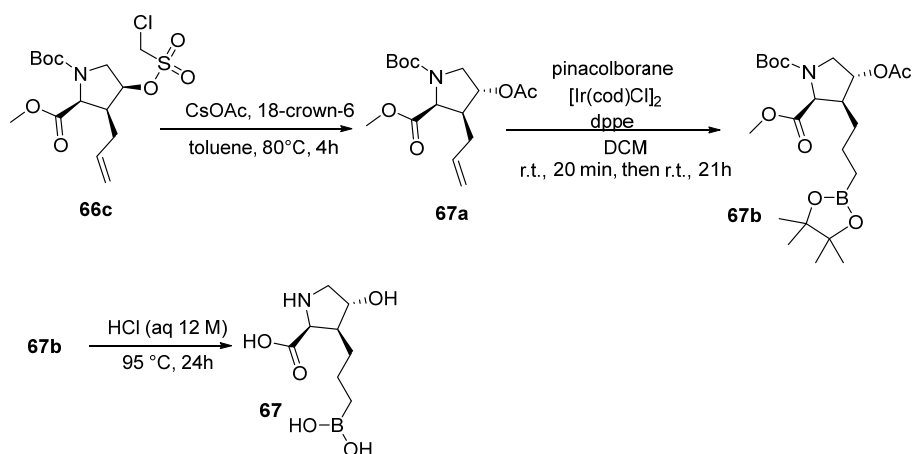
Compound **66** was synthesized as described by Achab et al. (Scheme 28) [66]. The process began with the addition of KHMDS to a solution of 1-(tertbutyl)-2-methyl (2S)-3-allyl-4-oxopyrrolidine-1,2-dicarboxylate (**66a**) in THF at -78 °C under N_2 . After stirring and warming to -20 °C, CSA was added, followed by pre-cooled MeOH and $NaBH_4$ at -78 °C. Purification through silica gel chromatography yielded 1-(tert-butyl)-2-methyl (2S,3S,4S)-3-allyl-4-hydroxypyrrolidine-1,2-dicarboxylate (**66b**) as a black oil. In the next step, **66b** was reacted with 2,6-dimethylpyridine and chloromethanesulfonyl chloride in DCM at 0 °C, producing crude 1-(tert-butyl)-2-methyl (2S,3S,4S)-3-allyl-4-(((chloromethyl)sulfonyl)oxy)pyrrolidine-1,2-dicarboxylate (**66c**). Without further purification, **66c** was treated with sodium azide in DMSO at 80 °C, yielding crude 1-(tert-butyl)-2-methyl (2S,3S,4R)-3-allyl-4-azidopyrrolidine-1,2-dicarboxylate (**66d**). Next, pinacolborane, $[Ir(cod)Cl]_2$ and dppe were used in DCM under argon to convert **66d** into 1-(tert-butyl)-2-methyl (2S,3S,4R)-4-azido-3-(3-(4,4,5,5-tetramethyl-1,3,2-dioxaborolan-2-yl)propyl)pyrrolidine-1,2-dicarboxylate (**66e**).

as a colourless oil. This intermediate underwent azide reduction using Pd/C in EtOAc, forming crude 1-(tert-butyl)-2-methyl (2S,3R,4R)-4-amino-3-(3-(4,4,5,5-tetramethyl-1,3,2-dioxaborolan-2-yl)propyl)pyrrolidine-1,2-dicarboxylate (**66f**). Finally, **66f** was heated with 6 M HCl in a microwave reactor at 120 °C for 1 h to produce (2S,3R,4R)-4-amino-3-(3-boronopropyl)pyrrolidine-2-carboxylic acid (**66**) as a light brown solid. The same study described the synthesis of **67** (Scheme 29) using the intermediate **66c** (Scheme 28).

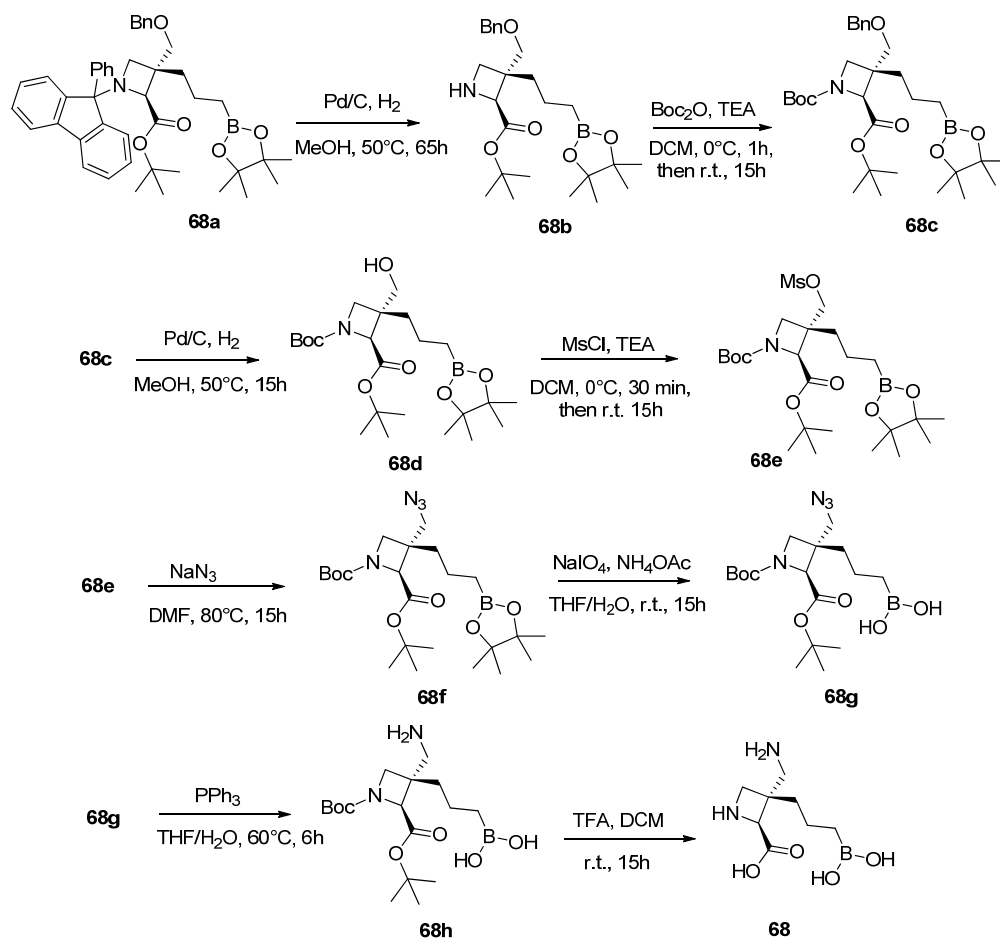
Caesium acetate and 18-crown-6 were added to a solution of intermediate **66c** in toluene stirred under N₂ at r.t. This reaction yielded 1-(tert-butyl)-2-methyl (2S,3S,4R)-4-acetoxy-3-allylpyrrolidine-1,2-dicarboxylate (**67a**) as a colourless oil. In the next step, a mixture of pinacolborane, [Ir(cod)Cl]₂, and dppe in DCM was prepared under N₂ and stirred at r.t. The solution of **67a** was then added, producing 1-(tert-butyl)-2-methyl-(2S,3S,4R)-4-acetoxy-3-(3-(4,4,5,5-tetramethyl-1,3,2-dioxaborolan-2-yl)propyl)pyrrolidine-1,2-dicarboxylate (**67b**). For the final step, **67b** was deprotected by treatment with 12 M HCl in water, resulting in the formation of (2S,3S,4R)-3-(3-boronopropyl)-4-hydroxypyrrolidine-2-carboxylic acid (**67**) as a yellowish solid.



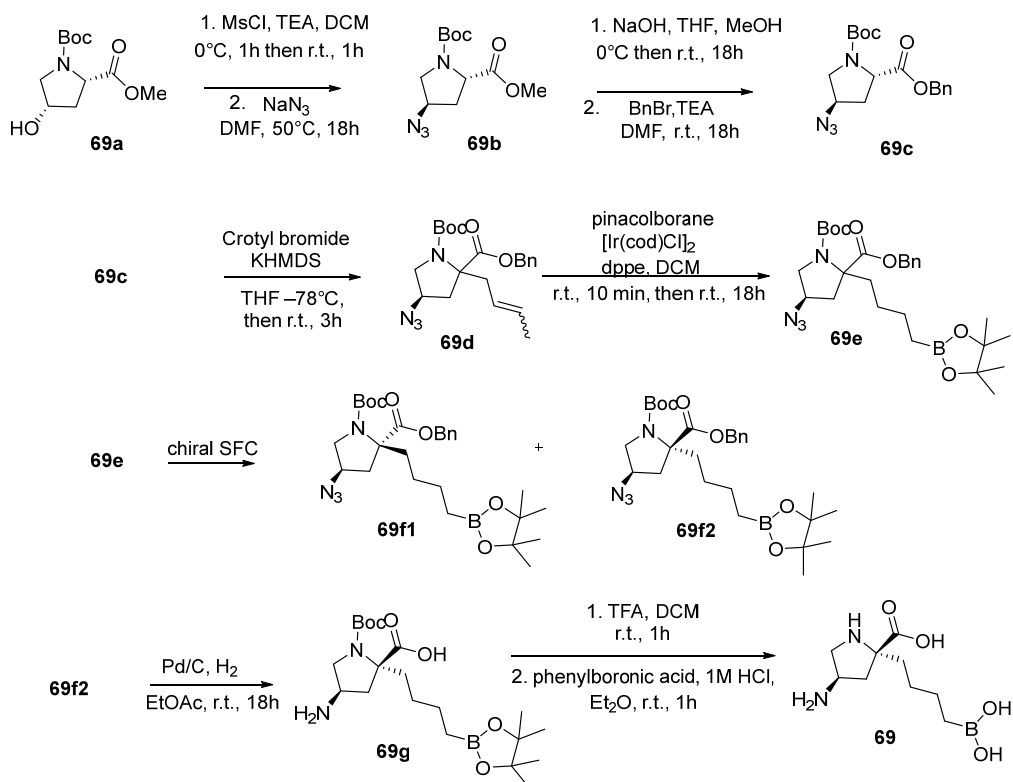
Scheme 28. Synthesis of compound **66**.



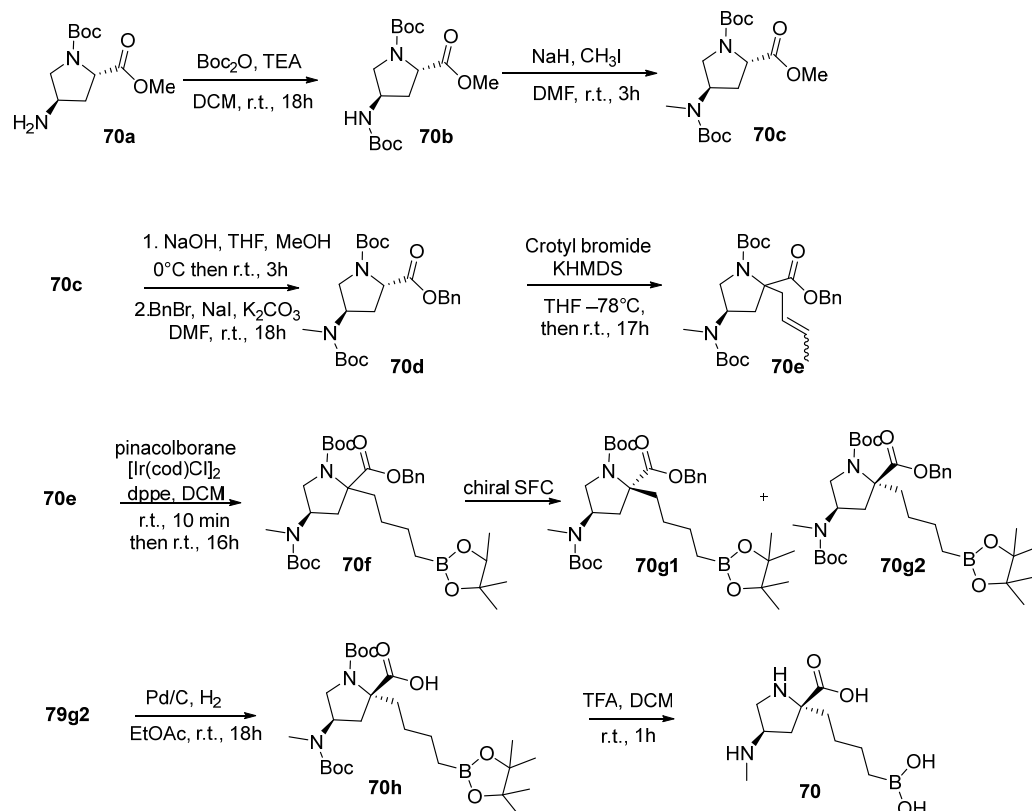
Scheme 29. Synthesis of compound **67**.



Scheme 30. Synthesis of compound 68.



Scheme 31. Synthesis of compound 69.



Scheme 32. Synthesis of compound 70.

The synthesis of **68**, outlined in Scheme 30, began with the intermediate **68a**, prepared following established literature methods. Intermediate (2*S*,3*S*)-tert-butyl 3-((benzyloxy)methyl)-1-(9-phenyl-9*H*-fluoren-9-yl)-3-(3-(4,4,5,5-tetramethyl-1,3,2-dioxaborolan-2-yl)propyl)azetidine-2-carboxylate (**68a**), used in the synthesis of various other compounds, was subjected to catalytic hydrogenation using 10% Pd/C in MeOH, yielding crude (2*S*,3*S*)-tert-butyl 3-(hydroxymethyl)-3-(3-(4,4,5,5-tetramethyl-1,3,2-dioxaborolan-2-yl)propyl)azetidine-2-carboxylate (**68b**). This intermediate was used directly in the next step without further purification. To synthesize **68c**, TEA and BOC-anhydride were added to **68b** at 0 °C, resulting in (2*S*,3*S*)-di-tert-butyl 3-((benzyloxy)methyl)-3-(3-(4,4,5,5-tetramethyl-1,3,2-dioxaborolan-2-yl)propyl)azetidine-1,2-di-carboxylate (**68c**). Subsequent catalytic hydrogenation with 10% Pd/C in MeOH produced (2*S*,3*S*)-di-tert-butyl 3-(hydroxymethyl)-3-(3-(4,4,5,5-tetramethyl-1,3,2-dioxaborolan-2-yl)propyl)azetidine-1,2-dicarboxylate (**68d**), the corresponding hydroxymethyl derivative. Methanesulfonyl chloride and TEA were added to **68d** in DCM at 0 °C to form crude (2*S*,3*S*)-di-tert-butyl 3-(((methylsulfonyl)oxy)methyl)-3-(3-(4,4,5,5-tetramethyl-1,3,2-dioxaborolan-2-yl)propyl)azetidine-1,2-dicarboxylate (**68e**), a methylsulfonyl ester derivative. Without purification, **68e** was reacted with sodium azide in DMF at 80 °C for 15 h yielding (2*S*,3*S*)-di-tert-butyl 3-(azidomethyl)-3-(3-(4,4,5,5-tetramethyl-1,3,2-dioxaborolan-2-yl)propyl)azetidine-1,2-dicarboxylate (**68f**), an azide derivative. The oxidation of **68f** with NH₄OAc and sodium periodate in a THF–H₂O mixture at r.t. for 15 h yielded crude (3-((2*S*,3*S*)-3-(azidomethyl)-1,2-bis(tert-butoxycarbonyl)azetidine-3-yl)propyl)boronic acid (**68g**), a boronic acid derivative. This intermediate underwent reduction with PPh₃ in THF–H₂O at 60 °C under N₂, forming (3-((2*S*,3*S*)-3-(aminomethyl)-1,2-bis(tert-butoxycarbonyl)azetidine-3-yl)propyl)boronic acid (**68h**), an aminomethyl derivative. Finally, TFA was added to **68h** in DCM at 20 °C, deprotecting the BOC groups and yielding (2*S*,3*S*)-3-(aminomethyl)-3-(3-boronopropyl)azetidine-2-carboxylic acid (**68**) as the free base [67].

Mlynarski et al. reported the synthesis of many proline derivatives, including **69** (Scheme 31) and **70** (Scheme 32) [68].

The synthesis of **69** began with (2S, 4S)-1-tert-butyl-2-methyl-4-hydroxypyrrolidine-1,2-dicarboxylate (**69a**), which was treated with methanesulfonyl chloride and TEA in DCM at 0 °C. This yielded 1-(tert-butyl)-2-methyl(2S,4S)-4-((methylsulfonyl)oxy)pyrrolidine-1,2-dicarboxylate, an intermediate used directly in the next step. Reaction with sodium azide in DMF produced **69b** as a mixture of rotamers. A solution of NaOH in H₂O was added to **69b** dissolved in THF/MeOH, generating (2S, 4R)-2-benzyl 1-tert-butyl-4-azidopyrrolidine-1,2-dicarboxylate (**69c**). This compound was treated with crotyl bromide in THF at −78 °C under N₂, followed by KHMDS in toluene. The reaction mixture was warmed to r.t. and stirred for 3 h, yielding **69d** as a mixture of rotamers and E/Z olefins in a 78% yield. Next, **69d** was subjected to hydroboration using pinacolborane, [Ir(cod)Cl]₂ and dppe in DCM under N₂. Stirring overnight yielded **69e**, which was purified by SFC to separate the diastereoisomers. The major diastereoisomer **69f1** was identified as the anti-addition product, while the minor diastereoisomer **69f2** was the syn-addition product. (2R,4R)-2-benzyl 1-tert-butyl 4-azido-2-(4-(4,4,5,5-tetramethyl-1,3,2-dioxaborolan-2-yl)butyl)pyrrolidine-1,2-dicarboxylate (**69f2**) was subjected to catalytic hydrogenation using 10% Pd/C in a mixture of EtOAc and MeOH. This step produced **69g**, which was used without further purification. In the final step, **69g** was first treated with TFA in DCM at r.t. and then with 1 M HCl and phenylboronic acid in Et₂O, obtaining (2R,4R)-4-amino-2-(4-boronobutyl)pyrrolidine-2-carboxylic acid (**69**) as a white solid.

Compound **70**, an analogue of **69** with a methyl amino group at position 4 of the proline ring, was synthesized starting from 1-(tert-butyl)-2-methyl (2S,4R)-4-aminopyrrolidine-1,2-dicarboxylate (**70a**). The primary amino group in **70a** was protected using BOC-anhydride, and then methylated with NaH and CH₃I in DMF to form intermediate **70c**. The synthesis from **70c** followed the same procedures as those for compound **69**, starting from the second step onward. The final product, (2R,4R)-2-(4-boronobutyl)-4-(methylamino)pyrrolidine-2-carboxylic acid (**70**), was obtained as a white solid.

5. Fourth-Generation Inhibitors

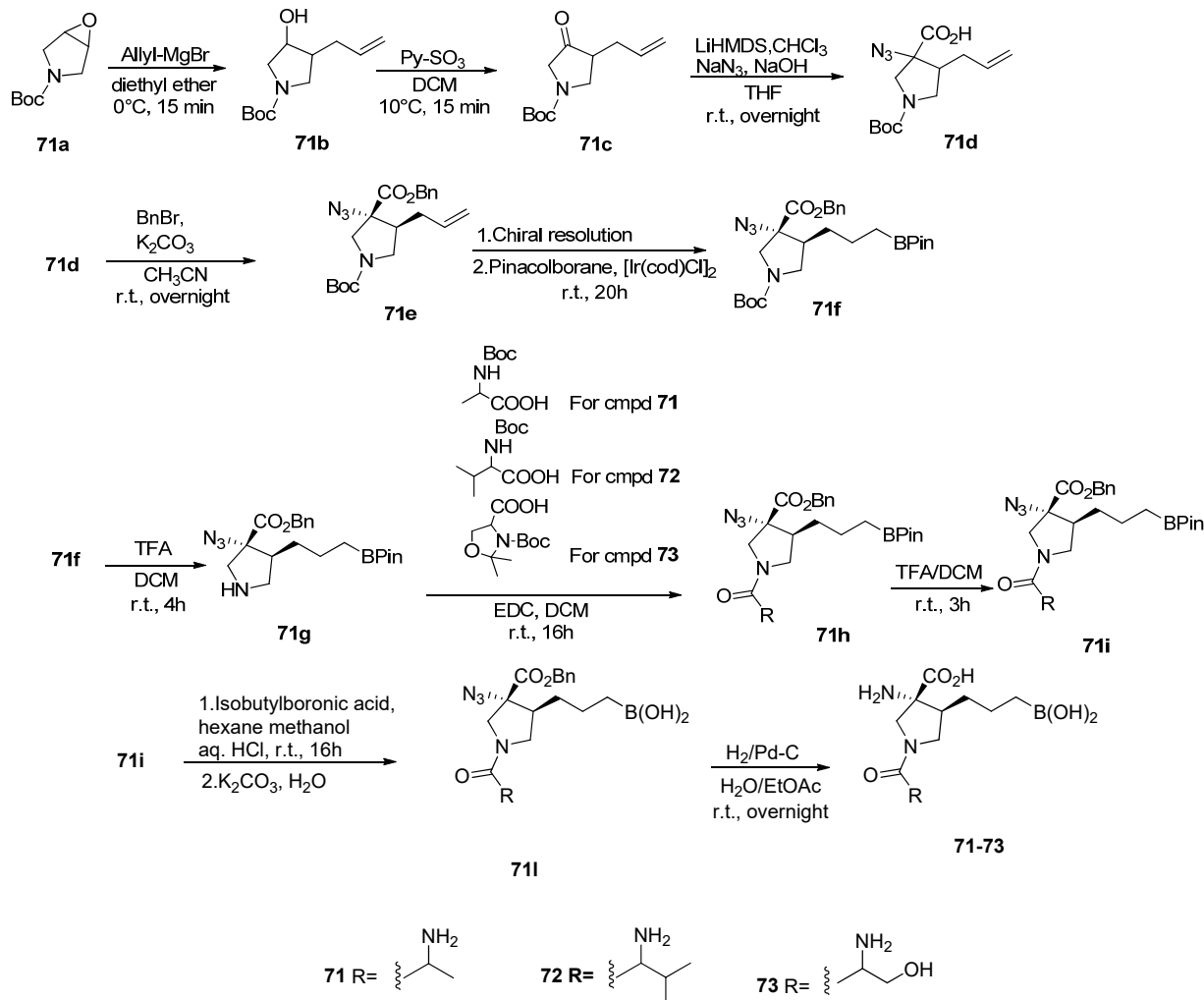
In this section of the review, we introduce a new class of compounds: the fourth-generation ARG inhibitors. These inhibitors are cyclic dipeptides composed of natural and non-natural amino acids, with the amino acids linked to a pyrrolidine or piperidine nitrogen, or an exocyclic amine group in proline residues [22]. The development of this new generation of ARG inhibitors was driven by the limitations of earlier compounds, which exhibited poor pharmacokinetic profiles, including very low oral bioavailability and a highly polar zwitterionic nature.

5.1. Peptide Boronic Acid Derivatives

5.1.1. Peptide Cyclic Inhibitors

The fourth generation of inhibitors includes ABH derivatives, which feature a ring-constrained pyrrolidine that reduces entropy by positioning the quaternary amino acid in an optimal orientation for binding [48,54]. A notable example is numidargistat ((3R,4S)-3-amino-1-((S)-2-aminopropanoyl)-4-(3-boronopropyl)pyrrolidine-3-carboxylic acid (**71**), a potent ARG inhibitor with IC₅₀ values of 86 nM for hARG-1 and 296 nM for hARG-2 [22]. In 2016, it was approved by the Food Drug Administration (FDA) for clinical trials to treat patients with metastatic solid tumours, both as a monotherapy and in combination with chemotherapy and immunotherapy [69]. Compound **71** and its analogues (**72–73**) were synthesized from Sjogren et al., with their synthetic protocols being patent-protected, as shown in Scheme 33 [70]. Specifically, compounds (3R,4S)-3-amino-1-((S)-2-amino-3-

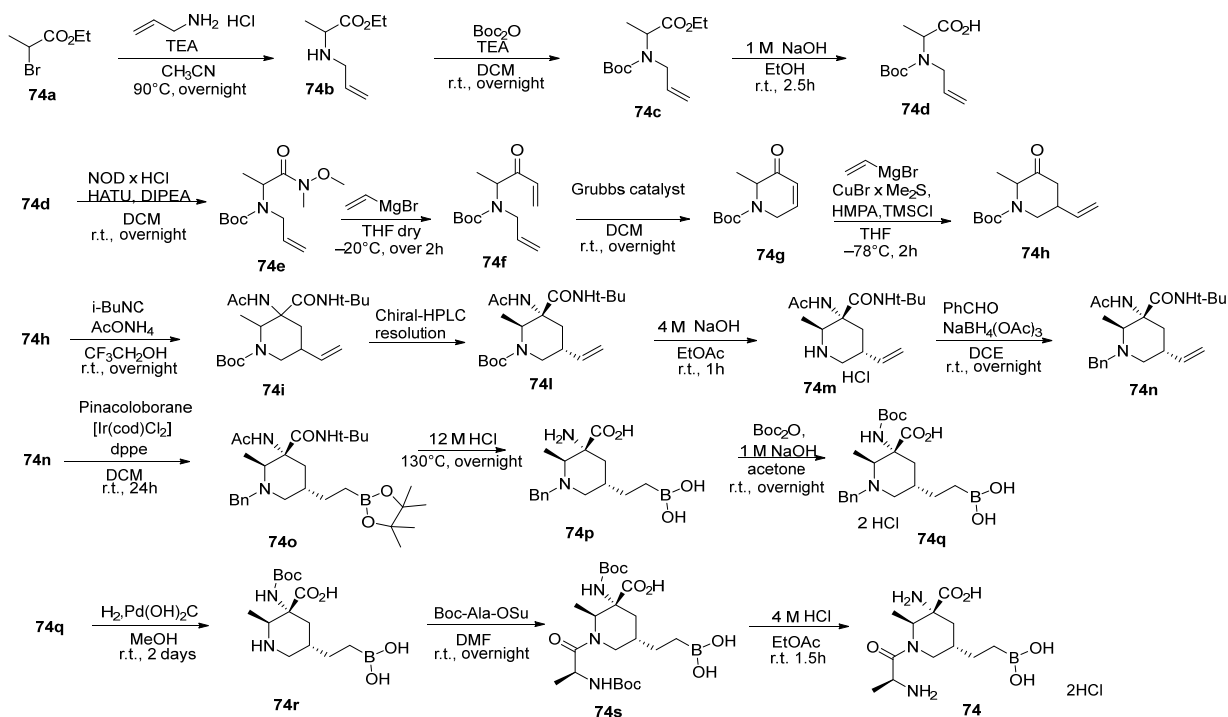
methylbutanoyl)-4-(3-boronopropylpyrrolidine)-3-carboxylic acid (**72**) and (3R,4S)-3-amino-1-((S)-2-amino-3-hydroxypropanoyl)-4-(3-boronopropyl)pyrrolidine-3-carboxylic acid (**73**) were prepared similarly to numidargistat (**71**), with the only difference being the reagents used with intermediate **71g**. For **72**, (tert-butoxycarbonyl)-L-valine was used, while for **73**, (S)-3-(tert-butoxycarbonyl)-2,2-dimethylloxazolidine-4-carboxylic acid was employed.



Scheme 33. Synthesis of compounds **71–73**.

The synthesis started with tert-butyl 6-oxa-3-azabicyclo [3.1.0]hexane-3-carboxylate (**71a**), which was reacted with allyl-MgBr in a Grignard reaction to form compound **71b**. This was then oxidized using a sulphur trioxide pyridine complex (Py-SO₃) to generate the ketone **71c**. Next, tert-butyl 3-allyl-4-oxopyrrolidine-1-carboxylate (**71c**) was treated with CHCl₃ and LiHMDS, followed by NaN₃ and NaOH to yield compound **71d**. The next step involved the protection of compound **71d** with BnBr and K₂CO₃, resulting in ((3R,4S)-3-benzyl 1-tert-butyl-4-allyl-3-azidopyrrolidine-1,3-dicarboxylate (**71e**), which was then subjected to hydroboration with pinacolborane and [Ir(cod)Cl]₂ in DCM to produce compound **71f**. Compound **71f** underwent BOC deprotection with TFA in DCM, yielding **71g**. This was then alkylated with BOC-L-Alanine and EDC in DCM to form **71h**, which was deprotected again with TFA in DCM. In the final steps, compound **71i** was reacted with isobutylboronic acid, hexane, methanol, a solution of HCl, and K₂CO₃ to obtain the boronic derivative **71l**. Finally, hydrogenation with Pd/C resulted in the desired product, (3R,4S)-3-amino-1-((S)-2-aminopropanoyl)-4-(3-boronopropyl)pyrrolidine-3-carboxylic acid (**71**).

An analogue of (2S,3R,5S)-3-amino-1-((S)-2-aminopropanoyl)-5-(2-boronoethyl)-2-methylpiperidine-3-carboxylic acid (**74**), which has a methyl group in position 2 of the piperidine ring, also exhibits activity against hARG-1 and hARG-2 with an IC₅₀ of 249 nM or lower [22]. The full synthesis of this compound is detailed in Scheme 34 and is described briefly here.

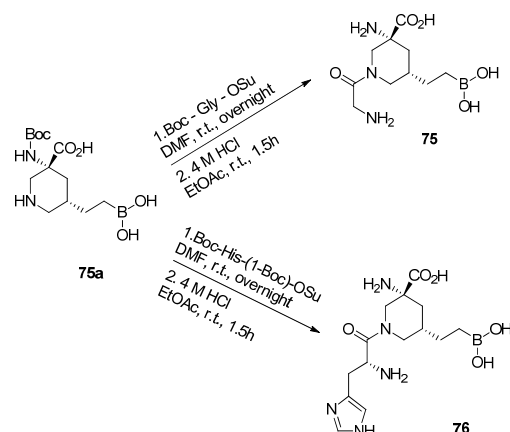


Scheme 34. Synthesis of compound **74**.

The patented synthesis of compound **74** began with a substitution reaction between ethyl 2-bromopropionate (**74a**) and allylamine hydrochloride in the presence of TEA in ACN, yielding compound **74b**. This was followed by amine protection using BOC-anhydride, TEA, and DCM, stirred overnight at r.t., producing compound **74c**. Basic hydrolysis with NaOH and EtOH converted **74c** into N-allyl-N-(tert-butoxycarbonyl)alanine (**74d**). To a solution of **74d** in DCM, N,N-diisopropylethylamine (DIPEA), N,O-dimethylhydroxylamine, and HATU were added, forming the amide **74e** after overnight stirring at r.t. This intermediate underwent alkylation reaction with vinyl magnesium bromide in THF at -20°C , followed by ring-closing metathesis using Grubbs catalyst 2nd generation in DCM, yielding cyclic compound **74g**. A second Grignard reaction with vinylmagnesium bromide and CuBr x Me₂S in THF was performed, followed by the addition of tert-butyl-2-methyl-3-oxo-3,6-dihydropyridin-1(2H)-carboxylate (**74g**) and chlorotrimethyl silane at -78°C , which was then stirred overnight at r.t. to yield tert-butyl-2-methyl-3-oxo-5-vinylpiperidine-1-carboxylate (**74h**). To a solution of **74h** in 2,2,2-trifluoroethanol, NH₄OAc and tert-butylisocyanide were added dropwise, and the mixture was stirred at r. t. overnight. After chiral HPLC resolution, compound **74l** underwent a N-deprotection with HCl / AcOEt, yielding **74m**. This intermediate was protected with benzaldehyde, and sodium triacetoxyborohydride in DCE to obtain **74n** as a white foam. A hydroboration reaction was performed on **74n** using dppe, [Ir(cod)Cl]₂, and pinacolborane in DCM, followed by treatment with 12 M HCl, resulting in the boronic acid derivative **74p**. This was protected using BOC anhydride, a solution 1M NaOH and acetone, producing compound **74q** as a white solid. The next step involved hydrogenation over 20% Pd (OH)₂/C in MeOH, followed by N-alkylation with BOC-L-Ala-Osu in DMF, resulting in **74s**. In the final step, treatment

of **74s** with a solution of 4 M HCl in EtOAc yielded the desired compound (2S,3R,5S)-3-amino-1-((S)-2-aminopropanoyl)-5-(2-boronoethyl)-2-methylpiperidine-3-carboxylic acid (**74**) [71].

The compound (3R,5S)-3-amino-1-(2-aminoacetyl)-5-(2-boronoethyl)piperidine-3-carboxylic acid (**75**) is a glycine derivative with IC₅₀ values ranging from 1 to 249 nM against hARG-1 and 500–999 nM against hARG-2. Its synthesis, outlined in Scheme 35, involves a patented two-step procedure. Starting from (3R, 5S)-5-(2-boronoethyl)-3-((tert-butoxycarbonyl)amino)piperidine-3-carboxylic acid (**75a**), Blaszczyk et al. performed an amidation reaction using BOC-Gly-OSu in DMF, followed by deprotection with 4 M HCl in EtOAc, yielding the final product **75** [22,71].



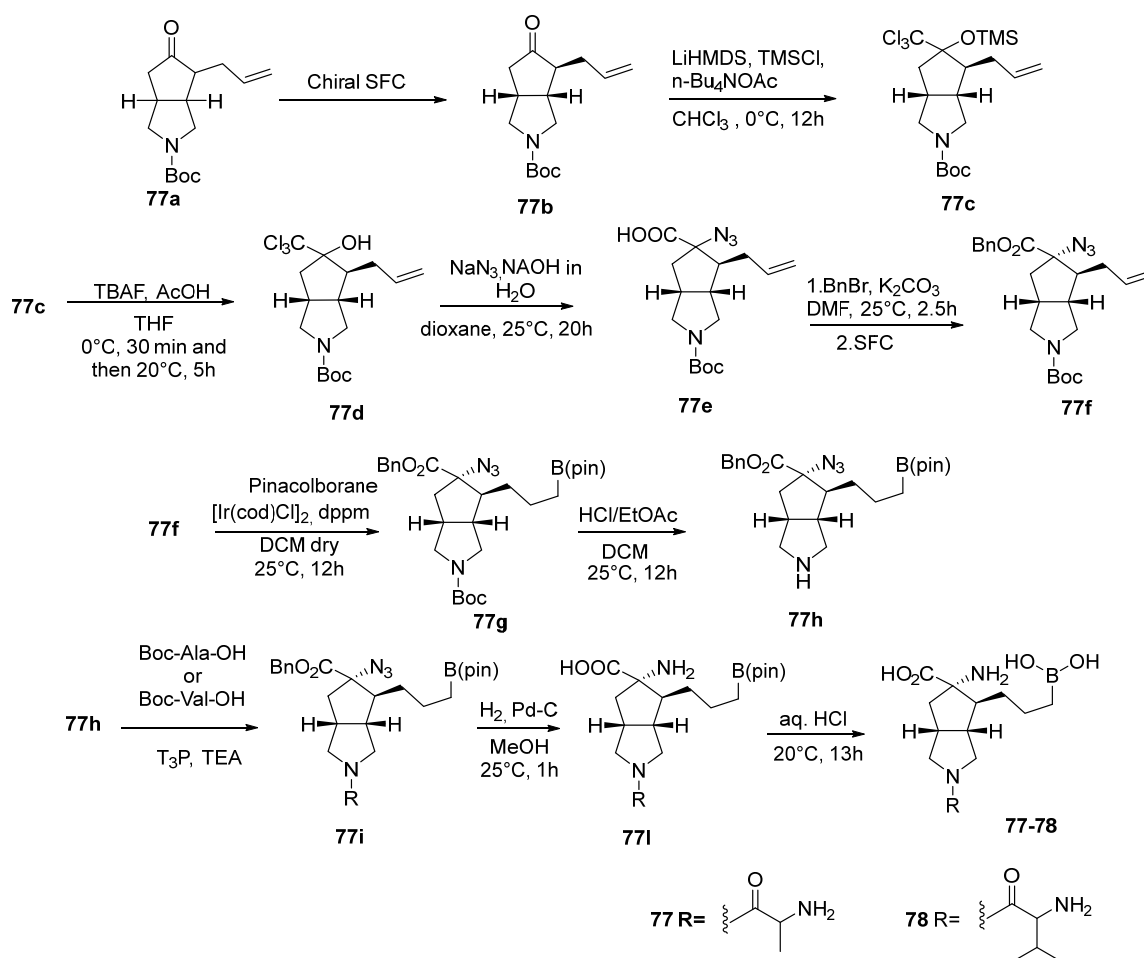
Scheme 35. Synthesis of compounds **75–76**.

Another ARG inhibitor, (3R,5S)-1-(l-histidyl)-3-amino-5-(2-boronoethyl)piperidine-3-carboxylic acid trihydrochloride (**76**) is a histidine derivative with the same IC₅₀ profile as **75** (1–249 nM for hARG-1 and 500–999 nM for hARG-2) [64]. Its synthesis follows the same procedure as **75** but uses BOC-L-His-(1-BOC)-OSu in the first step (Scheme 35).

Among peptide inhibitors, notable examples include (3aR,4S,5S,6aR)-5-amino-2-((S)-2-aminopropanoyl)-4-(3 boronopropyl) octahydrocyclopenta[c] pyrrole-5-carboxylic acid (**77**) with an IC₅₀ of 108 nM against hARG-1 (Merck, TOGA assay), and (3aR,4S,5S,6aR)-5-amino-2-((S)-2-amino-3-methylbutanoyl)-4-(3-boronopropyl)octahydrocyclopenta[c]pyrrole-5-carboxylic acid (**78**), containing a valine moiety and exhibiting an improved IC₅₀ of 52 nM, (TOGA assay) [22]. The synthesis of both compounds follows a patented 10-step protocol outlined in Scheme 36 [62,63]. The processes are identical except for the coupling reagent used in the seventh step: BOC-Ala-OH for **77** and BOC-Val-OH for **78**.

The synthesis of compound **77** began with the resolution of **77a** via SFC, yielding tert-butyl-(3aR,4S,6aR)-4-allyl-5-oxohexahydrocyclopenta[c]pyrrolo-2(1H)-carboxylate (**77b**). In the second step, **77b** was treated with CHCl₃, chlorotrimethylsilane, and LiHMDS (1 M in THF) under N₂ at −78 °C, then warmed to −30 °C and stirred for 1.5 h. Following the addition of tetrabutylammonium acetate in DMF, the mixture was heated to 0 °C and stirred for 12 h, forming tert-butyl-(3aR,4S,6aR)-4-allyl-5-(trichloromethyl)-5-((trimethylsilyl)oxy)hexahydrocyclopenta[c]pyrrole-2(1H)-carboxylate (**77c**). In the third step, the product was treated with acetic acid and tetra-n-butylammonium fluoride in THF, to produce **77d**, which was then reacted with sodium azide and sodium hydroxide in water to give (3aR,4S,6aR)-4-allyl-5-azido-2-(tert-butoxycarbonyl)octahydrocyclopenta[c]pyrrole-5-carboxylic acid (**77e**). The benzylation of **77e** with K₂CO₃ and benzyl bromide yielded 5-benzyl 2-(tert-butyl)(3aR,4S,5S,6aR)-4-allyl-5-azido-2-(tert-butoxycarbonyl)octahydrocyclopenta[c]pyrrole-2,5(1H)-dicarboxylate (**77f**). A hydroboration reaction with [Ir(cod)Cl]₂ and pinacolborane in DMC then produced 5-benzyl 2-(tert-butyl) (3aR,4S,5S,6aR)-5-azido-4-(3-(4,4,5,5-tetramethyl-

1,3,2-dioxaborolan-2-yl)propyl)hexahydro cyclopenta[c]pyrrole-2,5(1H)-dicarboxylate (**77g**), which was deprotected with 4 M HCl in EtOAc, yielding benzyl(3 α R,4S,5S,6 α R)-5-azido-4-(3-(4,4,5,5-tetramethyl-1,3,2-dioxaborolan-2-yl)propyl)octahydrocyclopenta[c]pyrrole-5-carboxylate (**77h**). Compound **77h** was N-alkylated with BOC-Ala-OH or BOC-Val-OH in DMF and in the presence of propanephosphonic acid anydride (T₃P) and TEA to form (3 α R,4S,5S,6 α R)-5-azido-2-((tert-butoxycarbonyl)-L-alanyl)-4-(3-(4,4,5,5-tetramethyl-1,3,2-dioxaborolan-2-yl)propyl)octahydrocyclopenta[c]pyrrole-5-carboxylate or (3 α R,4S,5S,6 α R)-5-azido-2-((tert-butoxycarbonyl)-L-valin)-4-(3-(4,4,5,5-tetramethyl-1,3,2-dioxaborolan-2-yl)propyl)octahydrocyclopenta[c]pyrrole-5-carboxylate (**77i**). Subsequent deprotection with H₂ over Pd-C gave **77l**, which was used directly in the final step. The treatment of **77l** with 6 M HCl at 20 °C for 13 h yielded the final product (3 α R,4S,5S,6 α R)-2-(L-alanyl)-5-amino-4-(3-boronopropyl)octahydrocyclopenta[c]pyrrole-5-carboxylic acid (**77**) and (3 α R,4S,5S,6 α R)-2-(L-valin)-5-amino-4-(3-boronopropyl)octahydrocyclopenta[c]pyrrole-5-carboxylic acid (**78**) as white solids (TFA salt).



Scheme 36. Synthesis of compounds **77–78**.

5.1.2. Proline Cyclic Inhibitors

Other peptide inhibitors of ARG are based on a proline scaffold, where the amino group of the proline core is coupled with various natural amino acids such as valine, leucine, and proline, or unnatural amino acids like cyclopentylglycine, tert-leucine, and indanylglycine. Examples include (2S,3R,4R)-4-((S)-2-amino-3-methylbutanamido)-3-(3-boronopropyl)pyrrolidine-2-carboxylic acid (**79**), (2S,3R,4R)-4-((S)-2-amino-2-cyclopentylacetamido)-3-(3-boronopropyl)pyrrolidine-2-carboxylic acid (**80**), and (2S,3R,4R)-4-((S)-

2-amino-3,3-dimethylbutanamido)-3-(3-boronopropyl)pyrrolidine-2-carboxylic acid (**81**). These compounds, reported in Figure 5, exhibit improved inhibitory properties.

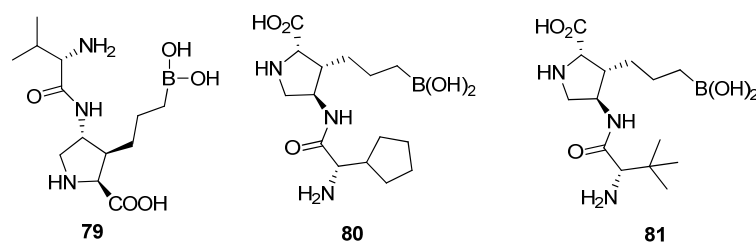
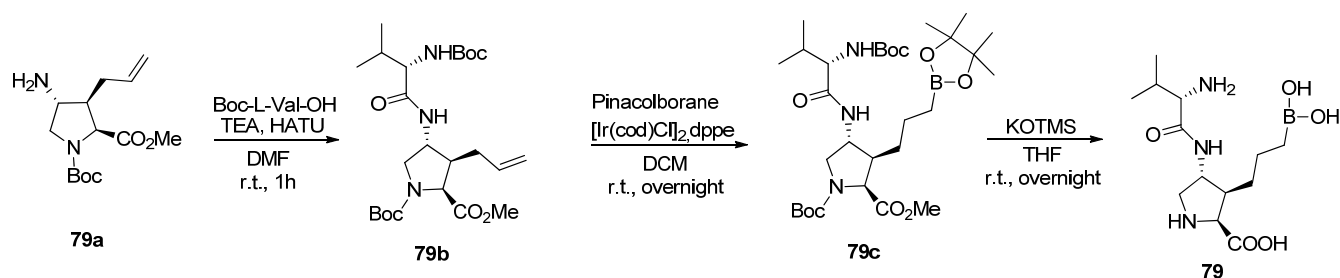


Figure 5. Chemical structures of compounds 79–81.

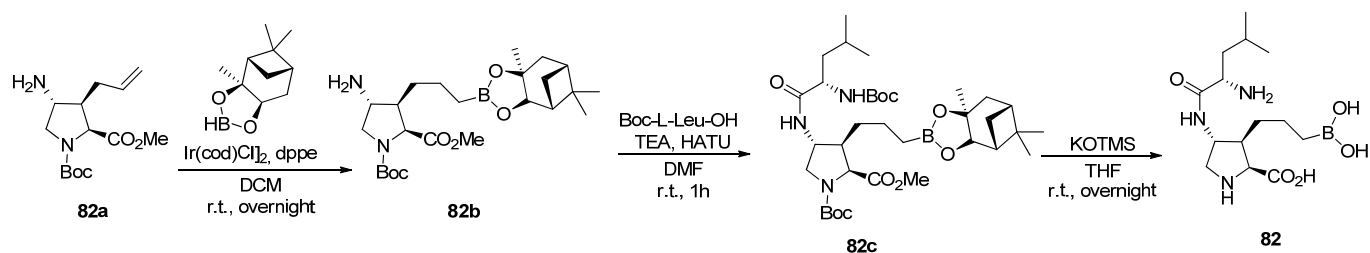
Compound **79**, featuring an isopropyl group as a substituent, inhibits hARG-1 with an $IC_{50} = 320$ nM and hARG-2 with $IC_{50} = 330$ nM (TOGA assay). In contrast, compounds **80** and **81**, containing cyclopentylglycine and tert-leucine as unnatural amino acids linked to the proline scaffold, are significantly more potent, inhibiting hARG-1 with an $IC_{50} = 0.8$ nM (TOGA assay) [22]. Compounds **80** and **81** were synthesized following the same method as compound **79** (Scheme 37) but using appropriate starting materials [72].



Scheme 37. Synthesis of compound 79.

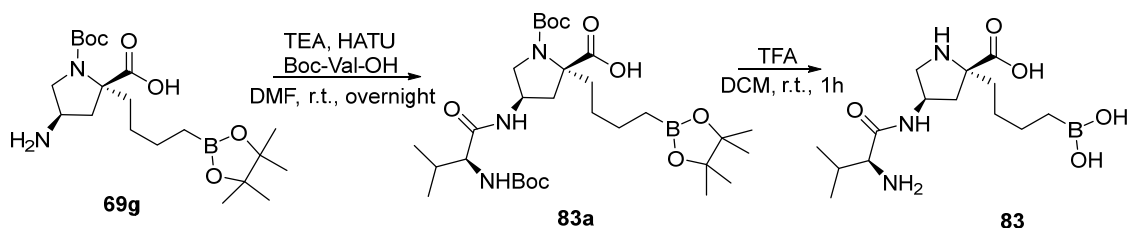
The patented synthesis of compound **79**, described by Achab AA et al., involves three steps [72]. Starting with (2S,3R,4R)-1-tert-butyl 2-methyl 3-allyl-4-aminopyrrolidine-1,2-dicarboxylate (**79a**), the compound undergoes N-alkylation using BOC-L-Val-OH, TEA, and HATU, yielding intermediate **79b**. This is followed by a hydroboration reaction with pinacolborane, $[Ir(cod)Cl]_2$, and dppe to produce compound **79c**. In the final step, the intermediate is treated with potassium trimethylsilanolate, then with 6 M HCl, to obtain the target compound (2S,3R,4R)-4-((S)-2-amino-3-methylbutanamido)-3-(3-boronopropyl)pyrrolidine-2-carboxylic acid (**79**).

Another ARG inhibitor is (2S,3R,4R)-4-((S)-2-amino-4-methylpentanamido)-3-(3-boronopropyl)pyrrolidine-2-carboxylic acid (**82**), which incorporates leucine and the natural amino acid attached to the amine group of the proline scaffold. This compound inhibits hARG-1 with an $IC_{50} = 1.6$ nM (TOGA) and is synthesized in three steps, as outlined in Scheme 38 [22,72]. Starting with 1-(tert-butyl)-2-methyl(2S,3R,4R)-3-allyl-4-aminopyrrolidine-1,2-dicarboxylate (**82a**), a hydroboration reaction with a pinanediolborane derivative, (3aR,4R,6R,7aS)-3a,5,5-trimethylhexahydro-4,6-methanobenzo[d][1,3,2]dioxaborole, $[Ir(cod)Cl]_2$, and dppe yields compound **82b**. This intermediate is then N-alkylated using BOC-L-Leu-OH, TEA, and HATU to produce compound **82c**. In the final step, compound **82c** reacts with potassium trimethylsilanolate, followed by treatment with 6 M HCl, resulting in the desired compound, (2S,3R,4R)-4-((S)-2-amino-4-methylpentanamido)-3-(3-boronopropyl)pyrrolidine-2-carboxylic acid (**82**).



Scheme 38. Synthesis of compound 82.

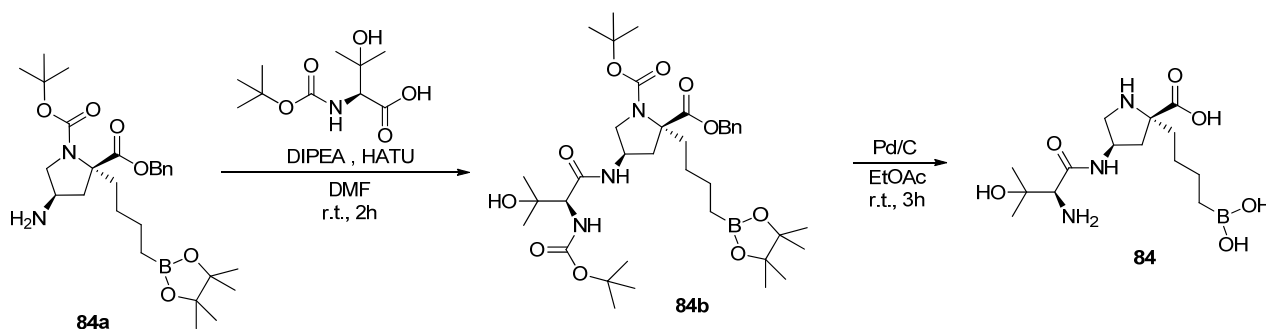
The compound (2R,4R)-4-((S)-2-amino-3-methylbutanamido)-2-(4-boronobutyl)pyrrolidine-2-carboxylic acid (**AZD0011**, **83**), a valine analogue, exhibited IC_{50} values of 320 nM against hARG-1 and 330 nM against hARG-2, as determined by the TOGA assay. Furthermore, pharmacological tests using the mouse xenograft model revealed that **83** acted as prodrug, releasing the parent compound **69** in vivo [73]. The synthesis of **83**, outlined in Scheme 39 [62], involved two steps starting from (2R,4R)-4-amino-1-(tert-butoxycarbonyl)-2-(4-(4,4,5,5-tetramethyl-1,3,2-dioxaborolan-2-yl)butyl)pyrrolidine-2-carboxylic acid (**69g**). In the first step, **69g** underwent N-alkylation with BOC-Val-OH, TEA, and HATU yielding intermediate **83a**. The second step involved deprotection using TFA, Et_2O , a solution 1 M HCl, and phenylboronic acid, producing the final compound (2R,4R)-4-((S)-2-amino-3-methylbutanamido)-2-(4-boronobutyl)pyrrolidine-2-carboxylic acid (**83**).



Scheme 39. Synthesis of compound 83.

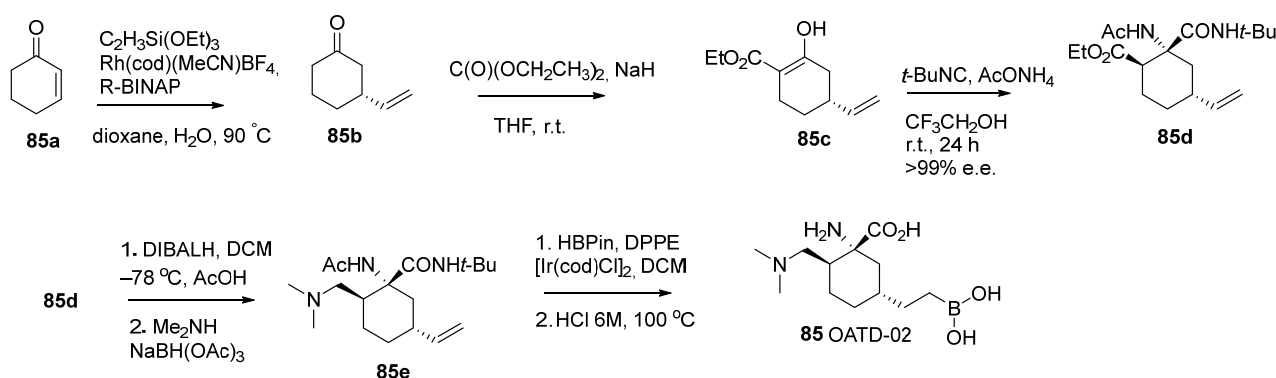
The compound (2R,4R)-4-((S)-2-amino-3-hydroxy-3-methylbutanamido)-2-(4-boronobutyl)pyrrolidine-2-carboxylic acid (**84**), a hydroxyvaline analogue, displayed IC_{50} values of 340 nM and 520 nM against hARG-1 and hARG-2, respectively, as determined by the TOGA assay [22]. Its synthesis outlined in Scheme 40, involved two steps starting with (2R,4R)-2-benzyl-1-tert-butyl 4-amino-2-(4-(4,4,5,5-tetramethyl-1,3,2-dioxaborolan-2-yl)butyl)pyrrolidine-1,2-dicarboxylate (**84a**). The first step was N-alkylation with (S)-N- α -tert-butoxycarbonyl-3,3-dimethyl-serine, DIPEA, and HATU, yielding intermediate **84b**. In the second step, deprotection was achieved using Pd/C in $EtOAc$, followed by treatment with TFA, Et_2O , a solution 1 M HCl, and phenylboronic acid, producing the final compound (2R,4R)-4-((S)-2-amino-3-hydroxy-3-methylbutanamido)-2-(4-boronobutyl)pyrrolidine-2-carboxylic acid (**84**) [68].

As observed in the structures of the fourth-generation ARG inhibitors presented thus far, the nitrogen atom is linked to an amino acid of a varying nature through a peptide bond. In some cases, the design of these compounds has resulted in improvements in both activity and pharmacokinetic profiles, fulfilling the objectives for which this generation was developed. However, in other instances, these inhibitors exhibited lower inhibitory activity compared to the non-peptide derivatives of the third generation and could only be considered prodrugs in specific cases. For example, it has been demonstrated that peptide derivatives, such as compound **83**, were rapidly metabolized in vivo through the hydrolysis of the peptide bond, releasing the non-peptide derivative **69**, which exhibited superior activity.



Scheme 40. Synthesis of compound 84.

OATD-02 (85), developed by OncoArendi Therapeutics (now Molecule), is a boronic acid derivative and an intracellular dual inhibitor of ARG-1 and ARG-2, with potent IC_{50} values of 20 nM and 48 nM for hARG-1 and -2, respectively [22]. Currently in preclinical development [74], its synthesis involves five steps, as detailed in Scheme 41 [28,75]. Starting from 2-cyclohexen-1-one (**85a**), the reaction with triethoxyvinylsilane under the catalysis of $Rh(cod)(MeCN)_2BF_4$ and R-BINAP in dioxane produced intermediate **85b**. Further processing with sodium hydride and diethyl carbonate yielded **85c**, which was converted to **85d** by reaction with NH_4OAc in 2,2,2-trifluoroethanol and tert-butyl isocyanide. The subsequent reduction of (1R,2R,4R)-2-acetamido-2-(tert-butylcarbamoyl)-4-vinylcyclohexane-1-carboxylate (**85d**) with a solution 1 M DIBAL-H in DCM at $-78^\circ C$, followed by the addition of dimethylamine in THF and sodium triacetoxyborohydride, led to the formation of (1R,2S,5R)-1-acetamido-N-(tert-butyl)-2-((dimethylamino)methyl)-5-vinylcyclohexanecarboxamide (**85e**). Reacting **85e** with pinacolborane in the presence of dppe and $[Ir(cod)Cl]_2$, followed by reflux in 6 M HCl, yielded the crude product. Purification through chromatography on the silica gel C-18 (isocratic elution, H_2O), and, next, flash chromatography on the DOWEX[®] 50WX8 ion exchange resin (eluent 0.1 M ammonia in water) produced the final compound (OATD-02) **85**.



Scheme 41. Synthesis of compound 85.

6. Side Chain β -Substituted ABH Analogues

Recently, Shields and colleagues developed novel ARG inhibitors by exploring the previously little-studied β -position of the compound ABH (**9**) [76]. Specifically, they synthesized promising inhibitors by alkylating the β -position of ABH with various functionalized alkyl chains to increase potency. Until now, companies and research groups had focused primarily on substitution at the α -position or the simultaneous substitution of both the α - and β -positions through cyclization. Through their chemical modifications, Shields et al. have extensively occupied the channel leading to the active site by targeting the β -position, without relying on cyclization. Among the twenty compounds synthesized, the most potent

inhibitors able to inhibit ARG-1 with an IC_{50} value lower than that ABH (i.e., lower than the 470 nM obtained from the biochemical assays performed by the same authors) were compounds **86–88**, shown in Figure 6. Notably, compounds **87** and **88** shared the same chemical structure but differed in spatial arrangement: **87** was the anti derivative, and **88** was the syn derivative. The anti arrangement (**87**) exhibited higher potency. The X-ray crystallography of the **87** and **88**-ARG-2 complexes prompted the authors to add an amino acid residue to **87** and **88**, forming a peptide bond to further improve potency. Various amino acid residues were tested, and the most promising inhibitors were derivatives **89** and **90** (Figure 6). For the syn compound, alanine was added while valine was added to the anti compound. Interestingly, the syn compound (**88**) became more potent after alanine was added (**89**), surpassing both **87** and its corresponding derivative, **90**. Moreover, pharmacological tests confirmed that **89** and **90** acted as prodrugs, releasing the respective parent compounds in vivo [76].

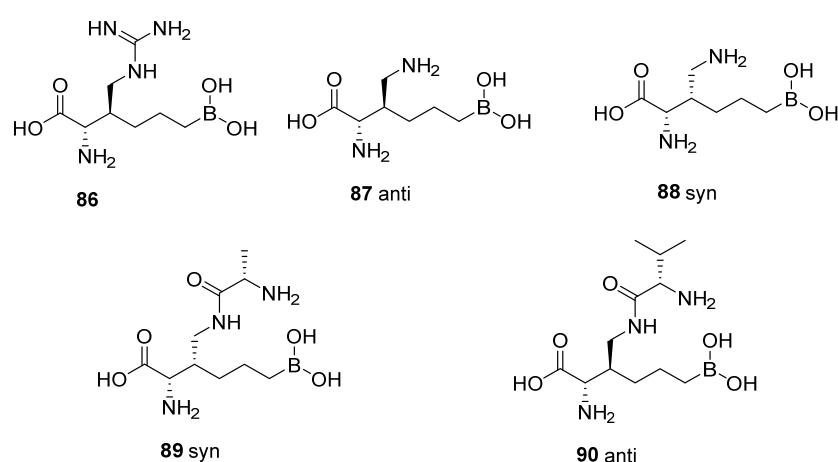
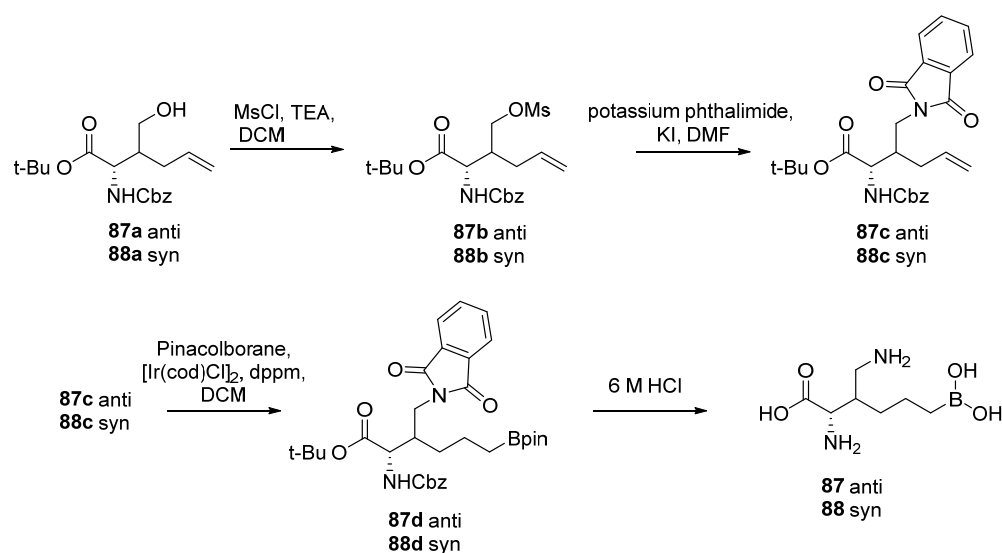


Figure 6. Chemical structures of compounds **86–90**.

The synthetic procedure of compounds **87** and **88** is shown in Scheme 42.



Scheme 42. Synthesis of compounds **87–88**.

The synthesis began with the mesylation of *tert*-butyl (2*S*,3*S*)-2-(((benzyloxy)carbonyl)amino)-3-(hydroxymethyl)hex-5-enoate (**87a**) and *tert*-butyl (2*S*,3*R*)-2-(((benzyloxy)carbonyl)amino)-3-(hydroxymethyl)hex-5-enoate (**88a**) and the subsequent protection of the amino

function using potassium phthalimide to give the corresponding protected amines *tert*-butyl (2S,3R)-2-(((benzyloxy)carbonyl)amino)-3-((1,3-dioxoisindolin-2-yl)methyl)hex-5-enoate (**87c**) and *tert*-butyl (2S,3S)-2-(((benzyloxy)carbonyl)amino)-3-((1,3-dioxoisindolin-2-yl)methyl)hex-5-enoate (**88c**). Subsequently, the hydroboration reaction of **87c** and **88c** was performed in the presence of [Ir(cod)Cl]₂, dppm and pinacolborane yielding **87d** and **88d**, respectively. In the last step, a global deprotection in acidic medium was performed to remove the benzyl carbamate, *tert*-butyl ester, and the pinacol-protecting groups, revealing the final compounds (2S,3R)-2-amino-3-(aminomethyl)-6-boronohexanoic acid dihydrochloride (**87**) and (2S,3S)-2-amino-3-(aminomethyl)-6-boronohexanoic acid dihydrochloride (**88**) as hydrochloride salts. These salts were freebased by passage through an ion exchange column and then freeze-dried.

7. Natural Compounds as ARG Inhibitors

Plant-derived compounds, often inspired by traditional medicine, offer a promising avenue for discovery ARG inhibitors. Natural and semi-synthetic compounds not only enhance molecular diversity but also hold the potential to reduce toxicity [34,77].

Among natural ARG inhibitors, polyphenols stand out for their bioactivity and safety. This class includes flavonoids, phenolic acids, and tannins, which have demonstrated significant ARG inhibitory activity and could serve as valuable lead compounds. On the semi-synthetic side, cinnamide derivatives, derived from cinnamic acid, show great potential. These compounds can be chemically modified to improve their potency and selectivity. By combining natural and semi-synthetic approaches, researchers can create a robust platform for developing new ARG inhibitors, benefiting from molecular diversity, reduced toxicity, and structure–activity relationship (SAR) insights.

7.1. Polyphenols

Polyphenols are among the most prominent natural compounds identified as ARG inhibitors. These secondary plant metabolites, abundant in fruits, vegetables, and medicinal plants, offer a wide array of health benefits. Key classes of polyphenols include flavonoids, phenolic acids, stilbenes, and lignans, many of which have demonstrated ARG-inhibitory activity, partly linked to their influence on NO production.

Notable examples (Table 2) include chlorogenic acid (**91**) (a phenolic acid), picetannol (**92**) and resveratrol (**93**) (stilbens), and taxifolin (**94**) (flavanoid). These compounds showed IC₅₀ values of 10.6 µM, 12.1 µM, 18.2 µM, and 23.2 µM, respectively, against ARG-1 in assays using mammalian bovine liver [78]. Piceatannol-3'-O-β-D-glucopyranoside (**95**), a stilbene glycoside, inhibited both ARG-1 and ARG-2 in a dose-dependent manner with IC₅₀ values of 11.2 µM and 11.0 µM, measured in rat liver and kidney lysates, respectively [79]. Studies by Arraki et al. [80] highlighted several polyphenols, including ellagic acid (**96**), various luteolin derivatives extracted from the leaves of *Morus alba*, like luteolin-7-diglucoside (**97**), luteolin-7-glucoside (**98**), and luteolin (**99**), as well as stilbenes like scirpusin B (**100**), ε-viniferin (**101**), cyperusphenol B (**102**), carexinol A (**103**), and the newly identified virgatanol (**104**) stilbenes and polyphenols isolated from various species of *Cyperus* and *Carex*, from the Cyperaceae family—which showed inhibitory effects on purified bovine liver (Table 2). Additionally, Sauchinone (**105**), isolated from *Saurus chinensis* extract, showed an IC₅₀ of 61.4 µM against ARG-2 in murine kidney lysates [81]. Methanolic extracts of *Scutellaria indica* also showed promise, with compounds (2S)-5,7-dihydroxy-8,20-dimethoxyflavanone (**106**) and (2S)-5,20,50-trihydroxy-7, 8-dimethoxyflavanone (**107**) displaying IC₅₀ values of 25.1 µM and 11.6 µM, respectively, against ARG-2 [82]. However, comparing these findings is challenging due to the variability in assay conditions. Despite this limitation, structural analyses suggest that features like the caffeoyl (3,4-dioxybenzoyl) group and

catechol functionality are crucial for ARG inhibition. Although the identified natural compounds mostly exhibit micromolar-range activity, these insights provide a foundation for designing more potent ARG inhibitors and expanding the chemical space of natural product-derived therapeutics.

Table 2. Structures and IC₅₀ values of natural and semi-synthetic compounds.

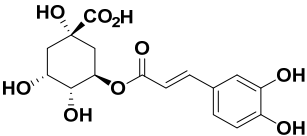
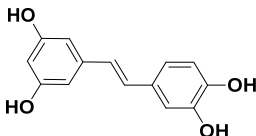
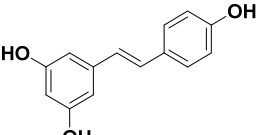
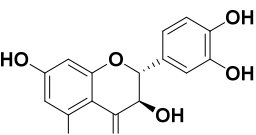
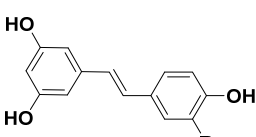
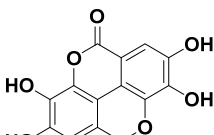
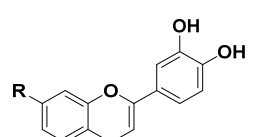
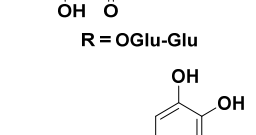
Compound	Structure	ARG-1 Activity	ARG-2 Activity
91 Chlorogenic acid		IC ₅₀ = 10.6 μM ^a	
92 Picetannol		IC ₅₀ = 12.1 μM ^a	
93 Resveratrol		IC ₅₀ = 18.2 μM ^a	
94 Taxifolin		IC ₅₀ = 23.2 μM ^a	
95 Piceatannol-3'-O-β-D-glucopyranoside	 R = OGlu	IC ₅₀ = 11.22 μM ^b	IC ₅₀ = 11.06 μM ^c
96 Ellagic acid		IC ₅₀ = 78.9 μM ^a	
97 Luteolin-7-diglucoside	 R = OGlu-Glu	IC ₅₀ = 152.4 μM ^a	
98 Luteolin-7-glucoside	 R = OGlu	IC ₅₀ = 99.4 μM ^a	

Table 2. Cont.

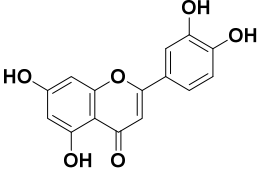
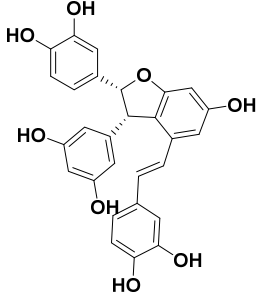
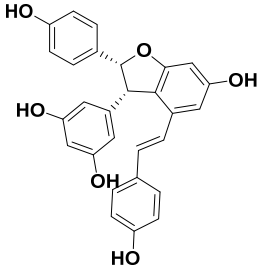
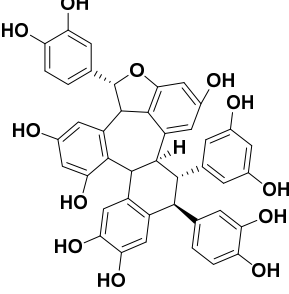
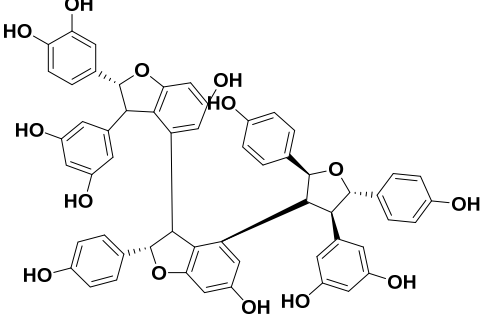
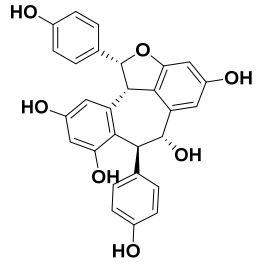
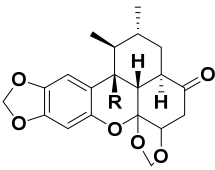
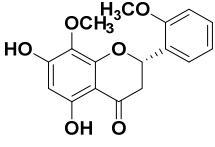
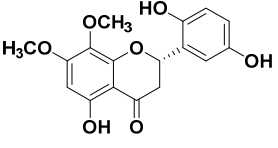
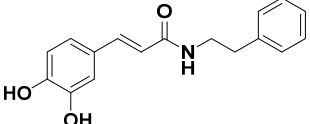
Compound	Structure	ARG-1 Activity	ARG-2 Activity
99 Luteolin		IC ₅₀ = 95.3 μM ^a	
100 Scirpusin B		IC ₅₀ = 22.6 μM ^a	
101 ε-Viniferin		IC ₅₀ = 27.8 μM ^a	
102 Cyperusphenol B		IC ₅₀ = 12.2 μM ^a	
103 Carexinol A		IC ₅₀ = 25.3 μM ^a	
104 Virgatanol		IC ₅₀ = 182.1 μM ^a	

Table 2. Cont.

Compound	Structure	ARG-1 Activity	ARG-2 Activity
105 Sauchinone			IC ₅₀ = 61.4 µM ^d
106 (2S)-5,7-dihydroxy-8,20-dimethoxyflavanone			IC ₅₀ = 25.1 µM ^c
107 (2S)-5,20,50-trihydroxy-7,8-dimethoxyflavanone			IC ₅₀ = 11.6 µM ^c
108 Caffeic acid phenylamide (CAPA)		IC ₅₀ = 6.9 µM ^a IC ₅₀ = 60.3 µM ^e	

^a bovine liver ARG; ^b rat liver ARG; ^c rat kidney ARG; ^d murine kidney ARG; ^e human ARG.

7.2. Cinnamide Derivatives

Pham et al. simplified the structure of chlorogenic acid—an ester of caffeic and quinic acid—to create compound (108) (Table 2), also known as caffeic acid phenylamide (CAPA). In tests using a micro-assay on purified bovine liver arginase (bARG-1), CAPA showed slightly better activity than chlorogenic acid, with IC₅₀ values of 6.9 µM and 10.6 µM, respectively. However, when tested on recombinant human arginase (hARG-1), CAPA's activity decreased significantly, with an IC₅₀ of 60.3 µM.

This study highlights the value of using bARG-1, a cost-effective alternative, for initial screening of potential mammalian ARG inhibitors. However, it also emphasizes the importance of testing promising compounds on hARG-1 to ensure their relevance before advancing to further studies. The research identified the cinnamoyl group and catechol moiety as essential structural features for inhibitory activity. Despite CAPA's relatively high IC₅₀ against hARG-1, its structure points to cinnamide derivatives as promising lead compounds for developing therapeutically effective ARG inhibitors [83].

8. Conclusions and Future Perspectives

In conclusion, ARG, the enzyme responsible for the metabolism of the amino acid L-arginine, plays a key role in numerous pathophysiological processes, making it a significant target for researchers aiming to combat various disorders. Although the enzyme was discovered many years ago, recent advancements have spurred renewed research into ARG and its inhibitors, leading to the development of new molecules designed to target this enzyme. This review traces the evolution of ARG inhibitors, categorizing them into different generations and classes based on structure variations, including recently developed molecules and those derived from natural or semi-synthetic sources. For the first time, in this review the structures and syntheses of ARG inhibitors described in patent applications have been reported.

As emphasized throughout the review, various pathologies are characterized by the uncontrolled expression of one of the two ARG isoforms, underscoring the need for

selective inhibitors targeting either ARG-1 or ARG-2. Despite numerous studies and clinical trials demonstrating the potential of ARG as a biomarker and diagnostic tool for cancer progression, there is still a need for standardized clinical definitions of ARG activity and for the consistent measurement of ARG-1 and ARG-2 expression levels in blood or tissues for cancer diagnosis. To address this challenge, an artificial intelligence-based prediction model could be developed, leveraging deep learning of clinical data, including cancer types, ARG activity values, expression levels, and patient information, to assess cancer progression.

Despite significant progress, a fully selective inhibitor remains elusive due to the structural similarities between the two isoforms. Notable examples include numidargistat and OATD-02, although neither shows significant selectivity for one isoform over the other. However, OATD-02 offers a unique advantage as the first potent dual ARG-1/ARG-2 inhibitor in its class. Its enhanced antitumor activity *in vivo* has been attributed to its complex mechanism of action, targeting both intracellular and extracellular ARGs. Consequently, OATD-02 stands out as the only pharmacological tool capable of effectively harnessing the benefits of inhibiting both isoenzymes, while also regulating also CD8⁺ and Treg cell activity in contrast to numidargistat.

Both numidargistat and OATD-02 have advanced to the clinical phase, ref. [84] with OATD-02 still in the recruitment phase. Numidargistat has been evaluated in five separate phase I studies for advanced or metastatic solid tumours, primarily in combination with other immunotherapies or conventional chemotherapies. However, the literature suggests that immunochemotherapy has shown superior efficacy compared to immunotherapy alone [85]. While numidargistat has a manageable safety profile, characterized primarily by inhibition of the urea cycle, immune-related adverse events, and a pharmacodynamic increase in plasma arginine levels [86,87], it has not yet advanced beyond phase I due to a response below expectations in terms of overall response rate and disease control rate. Another ARG inhibitor in clinical trials, CB-280 (structure undisclosed), is being tested for cystic fibrosis [88]. This compound has shown good tolerability, with no dose-limiting toxicities or severe grade adverse reactions [89]. In addition to small molecule inhibitors, a peptide vaccine targeting ARG-1 has been tested in clinical studies demonstrating a good safety profile, with no severe adverse reactions and with 90% of patients showing a measurable immune response to the peptide, though the clinical antitumor response has been modest [90]. Further details on the clinical studies have been published in Failla et al. [31].

The challenge of developing selective inhibitors for the ARG isoforms remains highly relevant. Structural modifications, such as incorporating boronic acid in place of the guanidine group and side chain derivatizations, have led to significant improvements, though an ideal compound has yet to be achieved. High-throughput screening offers a promising solution, especially when the target structure is not fully defined, and it can be used alongside computational strategies.

Moreover, improving the pharmacokinetic profile of these molecules presents another challenge. A promising approach involves leveraging medicinal chemistry techniques to achieve the desired selectivity for one of the two isoforms while simultaneously enhancing pharmacokinetic properties, as discussed in our previous perspective [31]. Strategies such as the prodrug approach, utilizing small molecules or polymers as carriers, could improve drug targeting [91]. Alternatively, molecular hybridization techniques hold potential for improving pharmacokinetic profile of ARG inhibitors, thereby boosting their pharmacological activity [92–94]. Furthermore, since ARG inhibitors have shown promise as probes for molecular imaging, improving their selectivity and biopharmaceutical properties could pave the way for both therapeutic and diagnostic applications.

Author Contributions: Conceptualization, F.S.; methodology, M.C.M.; validation, M.F.; investigation, C.B.; data curation, M.G.R.; writing—original draft preparation, M.C.M., C.B., M.E.S. and K.C.; writing—review and editing, K.C. and L.L.; supervision, F.S.; project administration, F.S.; funding acquisition, F.S. All authors have read and agreed to the published version of the manuscript.

Funding: This research was funded AIRC SIS 2022 (ID 28705, P.I. Federica Sodano).

Conflicts of Interest: The authors declare no conflicts of interest.

References

1. Caldwell, R.B.; Toque, H.A.; Narayanan, S.P.; Caldwell, R.W. Arginase: An Old Enzyme with New Tricks. *Trends Pharmacol. Sci.* **2015**, *36*, 395–405. [\[CrossRef\]](#)
2. Wu, G.; Morris, S.M. Arginine Metabolism: Nitric Oxide and Beyond. *Biochem. J.* **1998**, *336*, 1–17. [\[CrossRef\]](#)
3. Morris, S.M. Recent Advances in Arginine Metabolism: Roles and Regulation of the Arginases. *Br. J. Pharmacol.* **2009**, *157*, 922–930. [\[CrossRef\]](#)
4. Ostrand-Rosenberg, S.; Sinha, P. Myeloid-derived suppressor cells: Linking inflammation and cancer. *J. Immunol.* **2009**, *182*, 4499–4506. [\[CrossRef\]](#)
5. Kumar, V.; Patel, S.; Tcyganov, E.; Gabrilovich, D.I. The nature of myeloid-derived suppressor cells in the tumor microenvironment. *Trends Immunol.* **2016**, *37*, 208–220. [\[CrossRef\]](#)
6. Canè, S.; Geiger, R.; Bronte, V. The roles of arginases and arginine in immunity. *Nat. Rev. Immunol.* **2024**; *Epub ahead of print*. [\[CrossRef\]](#) [\[PubMed\]](#)
7. Lowe, M.M.; Boothby, I.; Clancy, S.; Ahn, R.S.; Liao, W.; Nguyen, D.N.; Schumann, K.; Marson, A.; Mahuron, K.M.; Kingsbury, G.A.; et al. Regulatory T Cells Use Arginase 2 to Enhance Their Metabolic Fitness in Tissues. *JCI Insight* **2019**, *4*, 129756. [\[CrossRef\]](#)
8. Munder, M. Arginase: An Emerging Key Player in the Mammalian Immune System. *Br. J. Pharmacol.* **2009**, *158*, 638–651. [\[CrossRef\]](#)
9. Durante, W. Role of Arginase in Vessel Wall Remodeling. *Front. Immunol.* **2013**, *4*, 111. [\[CrossRef\]](#)
10. Wiesinger, H. Arginine Metabolism and the Synthesis of Nitric Oxide in the Nervous System. *Prog. Neurobiol.* **2001**, *64*, 365–391. [\[CrossRef\]](#)
11. Wink, D.A.; Hines, H.B.; Cheng, R.Y.S.; Switzer, C.H.; Flores-Santana, W.; Vitek, M.P.; Ridnour, L.A.; Colton, C.A. Nitric Oxide and Redox Mechanisms in the Immune Response. *J. Leukoc. Biol.* **2011**, *89*, 873–891. [\[CrossRef\]](#)
12. Gotoh, T.; Mori, M. Arginase II Downregulates Nitric Oxide (NO) Production and Prevents NO-Mediated Apoptosis in Murine Macrophage-Derived RAW 264.7 Cells. *J. Cell Biol.* **1999**, *144*, 427–434. [\[CrossRef\]](#)
13. Choudry, M.; Tang, X.; Santorian, T.; Wasnik, S.; Xiao, J.; Xing, W.; Lau, K.H.W.; Mohan, S.; Baylink, D.J.; Qin, X. Deficient Arginase II Expression without Alteration in Arginase I Expression Attenuated Experimental Autoimmune Encephalomyelitis in Mice. *Immunology* **2018**, *155*, 85–98. [\[CrossRef\]](#)
14. Bhatta, A.; Yao, L.; Xu, Z.; Toque, H.A.; Chen, J.; Atawia, R.T.; Fouda, A.Y.; Bagi, Z.; Lucas, R.; Caldwell, R.B.; et al. Obesity-Induced Vascular Dysfunction and Arterial Stiffening Requires Endothelial Cell Arginase 1. *Cardiovasc. Res.* **2017**, *113*, 1664–1676. [\[CrossRef\]](#)
15. Berkowitz, D.E.; White, R.; Li, D.; Minhas, K.M.; Cernetich, A.; Kim, S.; Burke, S.; Shoukas, A.A.; Nyhan, D.; Champion, H.C.; et al. Arginase Reciprocally Regulates Nitric Oxide Synthase Activity and Contributes to Endothelial Dysfunction in Aging Blood Vessels. *Circulation* **2003**, *108*, 2000–2006. [\[CrossRef\]](#)
16. Clemente, G.S.; van Waarde, A.; Antunes, I.F.; Dömling, A.; Elsinga, P.H. Arginase as a Potential Biomarker of Disease Progression: A Molecular Imaging Perspective. *Int. J. Mol. Sci.* **2020**, *21*, 5291. [\[CrossRef\]](#)
17. Erdely, A.; Kepka-Lenhart, D.; Salmen-Muniz, R.; Chapman, R.; Hulderman, T.; Kashon, M.; Simeonova, P.P.; Morris, S.M., Jr. Arginase activities and global arginine bioavailability in wild-type and ApoE-deficient mice: Responses to high fat and high cholesterol diets. *PLoS ONE* **2010**, *5*, e15253. [\[CrossRef\]](#)
18. Zhang, Y.; Higgins, C.B.; Fortune, H.M.; Chen, P.; Stothard, A.I.; Mayer, A.L.; Swarts, B.M.; DeBosch, B.J. Hepatic arginase 2 (Arg2) is sufficient to convey the therapeutic metabolic effects of fasting. *Nat. Commun.* **2019**, *10*, 1587. [\[CrossRef\]](#)
19. Lange, P.S.; Langley, B.; Lu, P.; Ratan, R.R. Arginine Metabolism: Enzymology, Nutrition, and Clinical Significance Novel Roles for Arginase in Cell Survival, Regeneration, and Translation in the Central Nervous System. *J. Nutr.* **2004**, *134*, 2812S–2817S. [\[CrossRef\]](#)
20. Polis, B.; Srikanth, K.D.; Gurevich, V.; Bloch, N.; Gil-Henn, H.; Samson, A.O. Arginase Inhibition Supports Survival and Differentiation of Neuronal Precursors in Adult Alzheimer’s Disease Mice. *Int. J. Mol. Sci.* **2020**, *21*, 1133. [\[CrossRef\]](#)
21. Liu, P.; Fleete, M.S.; Jing, Y.; Collie, N.D.; Curtis, M.A.; Waldvogel, H.J.; Faull, R.L.M.; Abraham, W.C.; Zhang, H. Altered arginine metabolism in Alzheimer’s disease brains. *Neurobiol. Aging* **2014**, *35*, 1992. [\[CrossRef\]](#)

22. Borek, B.; Gajda, T.; Golebiowski, A.; Blaszczyk, R. Boronic Acid-Based Arginase Inhibitors in Cancer Immunotherapy. *Bioorganic Med. Chem.* **2020**, *28*, 115658. [\[CrossRef\]](#)
23. Muller, J.; Cardey, B.; Zedet, A.; Desingle, C.; Grzybowski, M.; Pomper, P.; Foley, S.; Harakat, D.; Ramseyer, C.; Girard, C.; et al. Synthesis, Evaluation and Molecular Modelling of Piceatannol Analogues as Arginase Inhibitors. *RSC Med. Chem.* **2020**, *11*, 559–568. [\[CrossRef\]](#)
24. Van Zandt, M.C.; Whitehouse, D.L.; Golebiowski, A.; Ji, M.K.; Zhang, M.; Beckett, R.P.; Jagdmann, G.E.; Ryder, T.R.; Sheeler, R.; Andreoli, M.; et al. Discovery of (R)-2-Amino-6-Borono-2-(2-(Piperidin-1-Yl)Ethyl)Hexanoic Acid and Congeners as Highly Potent Inhibitors of Human Arginases i and II for Treatment of Myocardial Reperfusion Injury. *J. Med. Chem.* **2013**, *56*, 2568–2580. [\[CrossRef\]](#)
25. Blaszczyk, R.; Brzezinska, J.; Dymek, B.; Stanczak, P.S.; Mazurkiewicz, M.; Olczak, J.; Nowicka, J.; Dzwonek, K.; Zagodzdzon, A.; Golab, J.; et al. Discovery and Pharmacokinetics of Sulfamides and Guanidines as Potent Human Arginase 1 Inhibitors. *ACS Med. Chem. Lett.* **2020**, *11*, 433–438. [\[CrossRef\]](#)
26. Golebiowski, A.; Whitehouse, D.; Beckett, R.P.; Van Zandt, M.; Ji, M.K.; Ryder, T.R.; Jagdmann, E.; Andreoli, M.; Lee, Y.; Sheeler, R.; et al. Synthesis of Quaternary α -Amino Acid-Based Arginase Inhibitors via the Ugi Reaction. *Bioorganic Med. Chem. Lett.* **2013**, *23*, 4837–4841. [\[CrossRef\]](#)
27. Steggerda, S.M.; Bennett, M.K.; Chen, J.; Emberley, E.; Huang, T.; Janes, J.R.; Li, W.; MacKinnon, A.L.; Makkouk, A.; Marguier, G.; et al. Inhibition of Arginase by CB-1158 Blocks Myeloid Cell-Mediated Immune Suppression in the Tumor Microenvironment. *J. Immunother. Cancer* **2017**, *5*, 101. [\[CrossRef\]](#)
28. Blaszczyk, R.; Nowicka, J.; Borek, B.; Brzezinska, J.; Gzik, A.; Dziegielewski, M.; Golebiowski, A.; Jedrzejczak, K.; Matyszewski, K.; Olczak, J. Arginase Inhibitors and Their Therapeutic Applications. World Intellectual Property Organization. WO2017191130A2, 9 November 2017.
29. Grzybowski, M.M.; Stańczak, P.S.; Pomper, P.; Blaszczyk, R.; Borek, B.; Gzik, A.; Nowicka, J.; Jedrzejczak, K.; Brzezińska, J.; Rejczak, T.; et al. OATD-02 Validates the Benefits of Pharmacological Inhibition of Arginase 1 and 2 in Cancer. *Cancers* **2022**, *14*, 3967. [\[CrossRef\]](#)
30. Niu, F.; Yu, Y.; Li, Z.; Ren, Y.; Li, Z.; Ye, Q.; Liu, P.; Ji, C.; Qian, L.; Xiong, Y. Arginase: An Emerging and Promising Therapeutic Target for Cancer Treatment. *Biomed. Pharmacother.* **2022**, *149*, 112840. [\[CrossRef\]](#)
31. Failla, M.; Molaro, M.C.; Schiano, M.E.; Serafini, M.; Tiburtini, G.A.; Gianquinto, E.; Scoccia, R.; Battisegola, C.; Rimoli, M.G.; Chegaev, K.; et al. Opportunities and Challenges of Arginase Inhibitors in Cancer: A Medicinal Chemistry Perspective. *J. Med. Chem.* **2024**, *67*, 19988–20021. [\[CrossRef\]](#)
32. Christianson, D.W. Arginase: Structure, Mechanism, and Physiological Role in Male and Female Sexual Arousal. *Acc. Chem. Res.* **2005**, *38*, 191–201. [\[CrossRef\]](#)
33. Tommasi, S.; Elliot, D.J.; Da Boit, M.; Gray, S.R.; Lewis, B.C.; Mangoni, A.A. Homoarginine and Inhibition of Human Arginase Activity: Kinetic Characterization and Biological Relevance. *Sci. Rep.* **2018**, *8*, 3697. [\[CrossRef\]](#) [\[PubMed\]](#)
34. Pudlo, M.; Demougeot, C.; Girard-Thernier, C. Arginase Inhibitors: A Rational Approach Over One Century. *Med. Res. Rev.* **2017**, *37*, 475–513. [\[CrossRef\]](#) [\[PubMed\]](#)
35. Boucher, J.L.; Custot, J.; Vadon, S.; Delaforge, M.; Lepoivre, M.; Tenu, J.P.; Yapo, A.; Mansuy, D. N Omega-Hydroxyl-L-Arginine, an Intermediate in the L-Arginine to Nitric Oxide Pathway, Is a Strong Inhibitor of Liver and Macrophage Arginase. *Biochem. Biophys. Res. Commun.* **1994**, *203*, 1614–1621. [\[CrossRef\]](#)
36. Di Costanzo, L.; Ilies, M.; Thorn, K.J.; Christianson, D.W. Inhibition of Human Arginase I by Substrate and Product Analogues. *Arch. Biochem. Biophys.* **2010**, *496*, 101–108. [\[CrossRef\]](#)
37. Colleluori, D.M.; Ash, D.E. Classical and Slow-Binding Inhibitors of Human Type II Arginase. *Biochemistry* **2001**, *40*, 9356–9362. [\[CrossRef\]](#)
38. Wallace, G.C.; Fukuto, J.M. Synthesis and Bioactivity of N Omega-Hydroxyarginine: A Possible Intermediate in the Biosynthesis of Nitric Oxide from Arginine. *J. Med. Chem.* **1991**, *34*, 1746–1748. [\[CrossRef\]](#)
39. Bodanszky, M.; Bodanszky, A. In *The Practice of Peptide Synthesis*, 1st ed.; Springer: New York, NY, USA, 1984.
40. Bailey, D.M.; Degrazia, C.G.; Lape, H.E.; Frering, R.; Fort, D.; Skulan, T. Hydroxyguanidines. A New Class of Antihypertensive Agents. *J. Med. Chem.* **1973**, *16*, 151–156. [\[CrossRef\]](#)
41. Moali, C.; Brollo, M.; Custot, J.; Sari, M.A.; Boucher, J.L.; Stuehr, D.J.; Mansuy, D. Recognition of α -Amino Acids Bearing Various C=NOH Functions by Nitric Oxide Synthase and Arginase Involves Very Different Structural Determinants. *Biochemistry* **2000**, *39*, 8208–8218. [\[CrossRef\]](#)
42. Teng, H.B. Synthesis of N ω -Hydroxy-nor-L-Arginine. *Chin. J. Appl. Chem.* **2010**, *27*, 1111–1113.
43. Custot, J.; Moali, C.; Brollo, M.; Boucher, J.L.; Delaforge, M.; Mansuy, D.; Tenu, J.P.; Zimmermann, J.L. N ω -Hydroxy-nor-L-Arginine: A High-Affinity Inhibitor of Arginase Well Adapted To Bind to Its Manganese Cluster. *J. Am. Chem. Soc.* **1997**, *119*, 4086–4087. [\[CrossRef\]](#)

44. Vadon, S.; Custot, J.; Boucher, J.L.; Mansuy, D. Synthesis and Effects on Arginase and Nitric Oxide Synthase of Two Novel Analogues of N"-Hydroxyarginine, Nu-Hydroxyindospicine and p-h y Drox y Amidinophen y Lalanine. *J. Chem. Soc.* **1996**, *1*, 645–648.
45. Metcalf, B.W.; Bey, P.; Danzin, C.; Jung, M.J.; Casara, P.; Vevert, J.P. Catalytic Irreversible Inhibition of Mammalian Ornithine Decarboxylase (E.C.4.1.1.17) by Substrate and Product Analogs. *J. Am. Chem. Soc.* **1978**, *100*, 2551–2553. [[CrossRef](#)]
46. Selamnia, M.; Mayeur, C.; Robert, V.; Blachier, F. Difluoromethylornithine (DFMO) as a Potent Arginase Activity Inhibitor in Human Colon Carcinoma Cells. *Biochem. Pharmacol.* **1998**, *55*, 1241–1245. [[CrossRef](#)]
47. Zhu, J.; Chadwick, S.T.; Price, B.A.; Zhao, S.X.; Costello, C.A.; Vemishetti, P. Processes for the Production of Alpha-Difluoromethyl Ornithine (DFMO). WO2003020209A2, 4 May 2004.
48. Baggio, R.; Elbaum, D.; Kanyo, Z.F.; Carroll, P.J.; Christopher Cavalli, R.; Ash, D.E.; Christianson, D.W. Inhibition of Mn²⁺-Arginase by Borate Leads to the Design of a Transition State Analogue Inhibitor, 2(S)-Amino-6-Boronohexanoic Acid. *J. Am. Chem. Soc.* **1932**, *119*, 8107–8108. [[CrossRef](#)]
49. Preite, M.D.; Manriquez Mujica, J.M.; Correa Vargas, J.M.; Iturriaga Aguera, R.M.; Casanello Toledo, P.C.; Krause Leyton, B.J. Method for the Enantioselective Synthesis of 2(s)-Amino-6-Boronohexanoic Acid (ABH) and Purification Thereof. WO2016037298A1, 17 May 2016.
50. Matteson, D.S.; Soloway, A.H.; Tomlinson, D.W.; Campbell, J.D.; Nixon, G.A. Synthesis and Biological Evaluation of Water-Soluble 2-Boronoethylthio Compounds. *J. Med. Chem.* **1964**, *7*, 640–643. [[CrossRef](#)]
51. Van Zandt, M.C.; Golebiowski, A.; Ji, M.K.; Whitehouse, D.; Ryder, T.; Beckett, P. Inhibitor Arginase and Their Therapeutic Application. US20120083469A1, 5 April 2012.
52. Clemente, G.S.; Antunes, I.F.; Kurhade, S.; Van Den Berg, M.P.M.; Sijbesma, J.W.A.; Van Waarde, A.; Buijsman, R.C.; Willemsen-Seegers, N.; Gosens, R.; Meurs, H.; et al. Mapping Arginase Expression with ¹⁸F-Fluorinated Late-Generation Arginase Inhibitors Derived from Quaternary α -Amino Acids. *J. Nucl. Med.* **2021**, *62*, 1163–1170. [[CrossRef](#)]
53. Moretto, J.; Pudlo, M.; Demougeot, C. Human-Based Evidence for the Therapeutic Potential of Arginase Inhibitors in Cardiovascular Diseases. *Drug Discov. Today* **2021**, *26*, 138–147. [[CrossRef](#)]
54. Ilies, M.; Di Costanzo, L.; Dowling, D.P.; Thorn, K.J.; Christianson, D.W. Binding of α,α -Disubstituted Amino Acids to Arginase Suggests New Avenues for Inhibitor Design. *J. Med. Chem.* **2011**, *54*, 5432–5443. [[CrossRef](#)]
55. Van Zandt, M.; Golebiowski, A.; Koo Ji, M.; Whitehouse, D.; Ryder, T.; Beckett, R.P. Inhibitor Arginase and Their Therapeutic Application. WO 2013/059437A1, 25 April 2013.
56. Tomczuk, B.E.; Olson, G.L.; Pottorf, R.S.; Wang, J.; Nallaganchu, B.R. Arginase Inhibitors and Methods of Use Thereof. WO2012091757A1, 5 July 2012.
57. Błaszczyk, R.; Brzezinska, J.; Golebiowski, A.; Olczak, J. Arginase Inhibitors and Their Therapeutic Applications. WO2016108707A1, 7 July 2016.
58. Golebiowski, A.; Paul Beckett, R.; Van Zandt, M.; Ji, M.K.; Whitehouse, D.; Ryder, T.R.; Jagdmann, E.; Andreoli, M.; Mazur, A.; Padmanilayam, M.; et al. 2-Substituted-2-Amino-6-Boronohexanoic Acids as Arginase Inhibitors. *Bioorganic Med. Chem. Lett.* **2013**, *23*, 2027–2030. [[CrossRef](#)]
59. Van Zandt, M.; Jagdmann, G.E., Jr. Boronates as Arginase Inhibitors. WO2012058065A1, 3 March 2012.
60. Van Zandt, M.C.; Jagdmann, G.E.; Whitehouse, D.L.; Ji, M.; Savoy, J.; Potapova, O.; Cousido-Siah, A.; Mitschler, A.; Howard, E.I.; Pyle, A.M.; et al. Discovery of N-Substituted 3-Amino-4-(3-Boronopropyl)Pyrrolidine-3-Carboxylic Acids as Highly Potent Third-Generation Inhibitors of Human Arginase i and II. *J. Med. Chem.* **2019**, *62*, 8164–8177. [[CrossRef](#)]
61. Wang, Z.; Li, N.; Ma, J.; Shao, Y. Heterocyclic Compounds as Arginase Inhibitors. WO2019120296A1, 27 June 2019.
62. Foley, C.N.; Grange, R.L.; Guney, T.; Kalisiak, J.; Newcomb, E.T.; Tran, A.T. Arginase Inhibitors. WO2019173188A1, 19 September 2019.
63. Mitcheltree, M.J.; Li, D.; Achab, A.; Beard, A.; Chakravarthy, K.; Cheng, M.; Cho, H.; Eangoor, P.; Fan, P.; Gathiaka, S.; et al. Discovery and Optimization of Rationally Designed Bicyclic Inhibitors of Human Arginase to Enhance Cancer Immunotherapy. *ACS Med. Chem. Lett.* **2020**, *11*, 582–588. [[CrossRef](#)] [[PubMed](#)]
64. Błaszczyk, R.; Brzezinska, J.; Gzik, A.; Golebiowski, A.; Nowicka, J.; Borek, B.; Dziegielewska, M.; Jedrzejczak, K.; Matyszewski, K.; Olczak, J. Arginase Inhibitors and Their Therapeutic Applications. US 10391077, 27 August 2019.
65. Marques, F.A.; Lenz, C.A.; Simonelli, F.; Noronha Sales Maia, B.H.L.; Vellasco, A.P.; Eberlin, M.N. Structure Confirmation of a Bioactive Lactone Isolated from Otoba Parvifolia through the Synthesis of a Model Compound. *J. Nat. Prod.* **2004**, *67*, 1939–1941. [[CrossRef](#)] [[PubMed](#)]
66. Lu, M.; Zhang, H.; Li, D.; Childers, M.; Pu, Q.; Palte, R.L.; Gathiaka, S.; Lyons, T.W.; Palani, A.; Fan, P.W.; et al. Structure-Based Discovery of Proline-Derived Arginase Inhibitors with Improved Oral Bioavailability for Immuno-Oncology. *ACS Med. Chem. Lett.* **2021**, *12*, 1380–1388. [[CrossRef](#)] [[PubMed](#)]
67. Achab, A.A.; Childers, M.L.; Cumming, J.N.; Fischer, C.A.; Gathiaka, S.; Gunadyn, H.; Lesburg, C.A.; Li, D.; Lu, M.; Palani, A.; et al. Arginase Inhibitors and Methods of Use. US20210040127A1, 11 February 2021.

68. Mlynarski, S.N.; Grebe, T.; Kawatkar, S.; Verschoyle Finley, M.R.; Simpson, I.; Wang, J.; Cook, S. Arginase Inhibitors and Methods of Use Thereof. WO2019159120A1, 22 August 2019.
69. Gross, M.; Chen, J.; Emberley, E.; Janes, J.; Li, W.; Mackinnon, A.; Pan, A.; Parlati, F.; Rodriguez, M.; Steggerda, S.; et al. Abstract A195: CB-1158 Inhibits the Immuno-Oncology Target Arginase and Causes an Immune Mediated Anti-Tumor Response. *Mol. Cancer Ther.* **2015**, *14*, A195. [\[CrossRef\]](#)
70. Sjogren, E.B.; Li, J.; Van Zandt, M.; Whitehouse, D. Compositions and Methods for Inhibiting Arginase Activity. WO2017075363A1, 4 May 2017.
71. Blaszczyk, R.; Gzik, A.; Borek, B.; Dziegielewski, M.; Jedrzejczak, K.; Nowicka, J.; Chrzanowski, J.; Brzezinska, J.; Golebiowski, A.; Olczak, J.; et al. Dipeptide Piperidine Derivatives. US20190300525A1, 3 October 2019.
72. Achab, A.A.; Childers, M.L.; Cumming, J.N.; Fischer, C.; Gathiaka, S.; Gunaydin, H.; Lesburg, C.A.; Li, D.; Lu, M.; Palani, A.; et al. Arginase Inhibitors and Methods of Use. WO2019177873A1, 19 September 2019.
73. Mlynarski, S.N.; Aquila, B.M.; Cantin, S.; Cook, S.; Doshi, A.; Finlay, M.R.V.; Gangl, E.T.; Grebe, T.; Gu, C.; Kawatkar, S.P.; et al. Discovery of (2R,4R)-4-((S)-2-Amino-3-methylbutanamido)-2-(4-boronobutyl)pyrrolidine-2-carboxylic Acid (AZD0011), an Actively Transported Prodrug of a Potent Arginase Inhibitor to Treat Cancer. *J. Med. Chem.* **2024**, *67*, 20827–20841. [\[CrossRef\]](#)
74. Grzybowski, M.M.; Stańczak, P.S.; Pęczkowicz-Szyska, J.; Wolska, P.; Zdziarska, A.M.; Mazurkiewicz, M.; Brzezińska, J.; Blaszczyk, R.; Gołębiowski, A.; Dobrzański, P.; et al. Abstract P71: Novel Dual Arginase 1/2 Inhibitor OATD-02 (OAT-1746) Improves the Efficacy of Immune Checkpoint Inhibitors. *Ann. Oncol.* **2017**, *28*, xi20–xi21. [\[CrossRef\]](#)
75. Borek, B.; Nowicka, J.; Gzik, A.; Dziegielewski, M.; Jedrzejczak, K.; Brzezinska, J.; Grzybowski, M.; Stanczak, P.; Pomper, P.; Zagodzón, A.; et al. Arginase 1/2 Inhibitor OATD-02: From Discovery to First-in-Man Setup in Cancer Immunotherapy. *Mol. Cancer Ther.* **2023**, *22*, 807–817. [\[CrossRef\]](#)
76. Shields, J.D.; Aquila, B.M.; Emmons, D.; Finlay, M.R.V.; Gangl, E.T.; Gu, C.; Mlynarski, S.N.; Petersen, J.; Pop-Damkov, P.; Sha, L.; et al. Design and Synthesis of Acyclic Boronic Acid Arginase Inhibitors. *J. Med. Chem.* **2024**, *67*, 20799–20826. [\[CrossRef\]](#)
77. Girard-Thernier, C.; Pham, T.N.; Demougeot, C. The Promise of Plant-Derived Substances as Inhibitors of Arginase. *Mini Rev. Med. Chem.* **2015**, *15*, 798–808. [\[CrossRef\]](#)
78. Bordage, S.; Pham, T.N.; Zedet, A.; Gugglielmetti, A.S.; Nappey, M.; Demougeot, C.; Girard-Thernier, C. Investigation of Mammal Arginase Inhibitory Properties of Natural Ubiquitous Polyphenols by Using an Optimized Colorimetric Microplate Assay. *Planta Med.* **2017**, *83*, 647–653. [\[CrossRef\]](#)
79. Woo, A.; Min, B.; Ryoo, S. Piceatannol-3'-O-β-D-Glucopyranoside as an Active Component of Rhubarb Activates Endothelial Nitric Oxide Synthase through Inhibition of Arginase Activity. *Exp. Mol. Med.* **2010**, *42*, 524–532. [\[CrossRef\]](#) [\[PubMed\]](#)
80. Arraki, K.; Totoston, P.; Attia, R.; Zedet, A.; Pudlo, M.; Messaoud, C.; Demougeot, C.; Girard, C. Arginase Inhibitory Properties of Flavonoid Compounds from the Leaves of Mulberry (*Morus Alba*, Moraceae). *J. Pharm. Pharmacol.* **2020**, *72*, 1269–1277. [\[CrossRef\]](#) [\[PubMed\]](#)
81. Lim, C.J.; Cuong, T.D.; Hung, T.M.; Ryoo, S.; Lee, J.H.; Kim, E.H.; Woo, M.H.; Choi, J.S.; Min, B.S. Arginase II Inhibitory Activity of Phenolic Compounds from *Saururus Chinensis*. *Bull. Korean Chem. Soc.* **2012**, *33*, 3079–3082. [\[CrossRef\]](#)
82. Kim, S.W.; Cuong, T.D.; Hung, T.M.; Ryoo, S.; Lee, J.H.; Min, B.S. Arginase II Inhibitory Activity of Flavonoid Compounds from *Scutellaria Indica*. *Arch. Pharm. Res.* **2013**, *36*, 922–926. [\[CrossRef\]](#)
83. Pham, T.N.; Bordage, S.; Pudlo, M.; Demougeot, C.; Thai, K.M.; Girard-Thernier, C. Cinnamide Derivatives as Mammalian Arginase Inhibitors: Synthesis, Biological Evaluation and Molecular Docking. *Int. J. Mol. Sci.* **2016**, *17*, 1656. [\[CrossRef\]](#)
84. ClinicalTrials.gov. National Library of Medicine. 2024. Available online: <https://clinicaltrials.gov> (accessed on 7 January 2025).
85. Gandhi, L.; Rodríguez-Abreu, D.; Gadgeel, S.; Esteban, E.; Felip, E.; De Angelis, F.; Domine, M.; Clingan, P.; Hochmair, M.J.; Powell, S.F.; et al. Pembrolizumab plus Chemotherapy in Metastatic Non-Small-Cell Lung Cancer. *N. Engl. J. Med.* **2018**, *378*, 2078–2092.
86. Naing, A.; Bauer, T.; Papadopoulos, K.P.; Rahma, O.; Tsai, F.; Garralda, E.; Naidoo, J.; Pai, S.; Gibson, M.K.; Rybkin, I.; et al. Phase I study of the arginase inhibitor INCB001158 (1158) alone and in combination with pembrolizumab (PEM) in patients (Pts) with advanced/metastatic (adv/met) solid tumours. *Ann. Oncol.* **2019**, *30*, v160.
87. Naing, A.; Papadopoulos, K.P.; Pishvaian, M.; Rahma, O.; Hanna, G.J.; Garralda, E.; Saavedra, O.; Gogov, S.; Kallender, H.; Cheng, L.; et al. First-in-human phase 1 study of the arginase inhibitor INCB001158 alone or combined with pembrolizumab in patients with advanced or metastatic solid tumours. *BMJ Oncol.* **2024**, *3*, e000249. [\[CrossRef\]](#)
88. National Library of Medicine, Study to Evaluate the Safety of CB-280 in Patients with Cystic Fibrosis-NCT04279769. Available online: <https://clinicaltrials.gov/study/NCT04279769> (accessed on 17 June 2024).
89. Boas, S.; Donaldson, S.; McBennett, K.; Liou, T.; Howrylak, J.; Johnson, L.; Teneback, C.; Dozor, A.; Sawicki, G.; Dumlaio, J.; et al. 529: A phase 1b, randomized, double-blind, placebo-controlled, dose-escalation trial of CB-280, an arginase inhibitor, in patients with cystic fibrosis. *J. Cyst. Fibros.* **2021**, *20*, S250. [\[CrossRef\]](#)

90. Lorentzen, C.L.; Martinenaite, E.; Kjeldsen, J.W.; Holmstroem, R.B.; Mørk, S.K.; Pedersen, A.W.; Ehrnrooth, E.; Andersen, M.H.; Svane, I.M. Arginase-1 targeting peptide vaccine in patients with metastatic solid tumors—A phase I trial. *Front. Immunol.* **2022**, *13*, 1023023. [[CrossRef](#)]
91. Sodano, F.; Cristiano, C.; Rolando, B.; Marini, E.; Lazzarato, L.; Cuozzo, M.; Albrizio, S.; Russo, R.; Rimoli, M.G. Galactosylated Prodrugs: A Strategy to Improve the Profile of Nonsteroidal Anti-Inflammatory Drugs. *Pharmaceutics* **2022**, *15*, 552. [[CrossRef](#)] [[PubMed](#)]
92. Sodano, F.; Gazzano, E.; Fraix, A.; Rolando, B.; Lazzarato, L.; Russo, M.; Blangetti, M.; Riganti, C.; Fruttero, R.; Gasco, A.; et al. A Molecular Hybrid for Mitochondria-Targeted NO Photodelivery. *ChemMedChem* **2018**, *13*, 87–96. [[CrossRef](#)] [[PubMed](#)]
93. Sodano, F.; Rolando, B.; Spyraakis, F.; Failla, M.; Lazzarato, L.; Gazzano, E.; Riganti, C.; Fruttero, R.; Gasco, A.; Sortino, S. Tuning the Hydrophobicity of a Mitochondria-Targeted NO Photodonor. *ChemMedChem* **2018**, *13*, 1238–1245. [[CrossRef](#)] [[PubMed](#)]
94. Sodano, F.; Gazzano, E.; Rolando, B.; Marini, E.; Lazzarato, L.; Fruttero, R.; Riganti, C.; Gasco, A. Tuning NO release of organelle-targeted furoxan derivatives and their cytotoxicity against lung cancer cells. *Bioorg Chem.* **2021**, *111*, 104911. [[CrossRef](#)] [[PubMed](#)]

Disclaimer/Publisher’s Note: The statements, opinions and data contained in all publications are solely those of the individual author(s) and contributor(s) and not of MDPI and/or the editor(s). MDPI and/or the editor(s) disclaim responsibility for any injury to people or property resulting from any ideas, methods, instructions or products referred to in the content.